Aus dem Institut für Medizinische Mikrobiologie
und Krankenhaushygiene
Direktor: Prof. Dr. Michael Lohoff

des Fachbereichs Medizin der Philipps-Universität Marburg

Dietary cellulose attenuates intestinal inflammation by promoting microbiota maturation and gut barrier function

Inaugural-Dissertation

zur Erlangung des Doktorgrades der
Naturwissenschaften

dem Fachbereich Medizin der Philipps-Universität Marburg
vorgelegt von

Florence Fischer
aus Schlema

Marburg, 2020

Angenommen vom Fachbereich Medizin der Philipps-Universität Marburg am:
28. September 2020

Gedruckt mit Genehmigung des Fachbereichs.

Dekan:	Prof. Dr. Helmut Schäfer
Referent:	Prof. Dr. Ulrich Steinhoff
1. Korreferent:	Jun-Prof. Dr. Leon Schulte

Für meine Eltern

Ina und Sven Fischer

Table of contents

List of figures

Abbreviations

1-10	
3-dehydroCA	3-dehydrocholic acid
A	
A. finegoldii	*Alistipes finegoldii*
AHR	aryl hydrocarbon receptor
αMCA	α-muricholic acid
αTMCA	α-tauromuricholic acid
B	
BHI	brain-heart-infusion
βMCA	β-muricholic acid
β-ME	β-Mercaptoethanol
BSA	bovine serum albumin
BSS	balanced salt solution
βTMCA	β-tauromuricholic acid
C	
CA	cholic acid
CD	control diet
Cldn	claudin
D	
DCA	deoxycholic acid
DSS	dextran sulphate sodium
DTT	dithiothreitol
E	
E. coli	*Escherichia coli*
EDTA	ethylenediaminetetra-acetic acid
ELISA	enzyme-linked immunosorbent assay
F	
FCS	foetal calf serum
FFD	fibre free diet
FISH	fluorescence-in-situ-hybridisation
FITC	fluorescein isothiocyanate
FOXP3	forkhead-box-protein 3
G	
GapDH	glycerinaldehyd-3-phosphat-dehydrogenase
GF	germ-free
H	
HBSS	Hank's balances salt solution
HCA	hyocholic acid
HDCA	hyodeoxycholic acid
HEPES	4- (2-Hydroxyethyl) piperazine-1-ethanesulfonic acid
HI	heat inactivated
HRP	horseradish-peroxidase
I	
IBD	inflammatory bowel disease
IEC(s)	intestinal epithelial cell(s)
IL	interleukin
ILC(s)	innate lymphoid cell(s)
K/L	
Ki67	proliferation marker protein Ki-67
LB	Luria-Bertani medium
LCA	lithocholic acid

M

MAMP	microbe-associated molecular pattern
MDCA	murideoxycholic acid
$MgCl_2$	magnesium chloride
mod.	modified
MS	mass spectrometer
Muc	mucin

N

NaCl	sodium chloride
NfE	nitrogen-free extractives
NLR	nucleotide binding and oligomerization domain-like receptor
ns	non-significant

O

Ocln	occludin
OMM^{12}	Oligo-Mouse-Microbiota 12
OTU	operational taxonomic unit

P

PAMP	pathogen-associated molecular pattern
PBS	phosphate-buffered saline
PCR	polymerase chain reaction
PMA	phorbol-12-myristat-13-acetate
PRR	pattern recognition receptor

R

Reg3γ	regenerating islet-derived protein 3γ
RORγt	retinoic acid receptor-related orphan receptor γt
RPMI-cm	Roswell Park Memorial Institute-complete medium
RT	room temperature
RT-qPCR	real-time quantitative polymerase chain reaction

S

SA-PE	streptavidin-phycoerythrin
SCFA(s)	short chain fatty acid(s)
SD	standard deviation
SDS	sodium dodecyl sulphate
sIgA	secretory immunoglobulin A
SPF	specific pathogen free
STAT3	signal transducer and activator of transcription 3

T

TCA	taurocholic acid
TCDCA	taurochenodeoxycholic acid
TFF3	trefoil factor 3
TH cell(s)	T helper cell(s)
Tjp	tight junction protein
TLR	Toll-like receptors
TMB	3,3', 5,5'-tetramethylbenzidine
TNFα	tumour necrosis factor α
T_{reg} cell(s)	regulatory T cell(s)
TUDCA	tauroursodeoxycholic acid

U/W

UDCA	ursodeoxycholic acid
(w)	with
(w/o)	without
ωMCA	ω-muricholic acid

1 Introduction

1.1 Dietary fibres

Although it is generally accepted that dietary fibres exert health-promoting effects, their intake in most westernised societies is critically low (Stephen et al. 2017). And this is not the only 'fibre gap': While epidemiological studies clearly demonstrated a relation between fibres and non-communicable diseases, the cellular and molecular mechanisms are not yet sufficiently understood (Jones 2014). Filling this gap of knowledge will provide a basis for specific recommendations on fibre consumption to further improve public health nutrition (Jones 2014).

1.1.1 Definition and classification of dietary fibres

Due to their heterogeneity, defining dietary fibres has been a matter of many discussions and has evolved over the years (Jones 2014; Stephen et al. 2017). One of the most common definitions describes dietary fibres as carbohydrate polymers consisting of ten or more (three or more, according to local jurisdiction) monomeric units, which are not degraded by endogenous enzymes in the human intestinal tract and belong to either (1) edible, naturally occurring carbohydrate polymers, (2) carbohydrate polymers which are isolated from food raw material and which have been shown to have a beneficial health effect or (3) synthetic carbohydrate polymers with a proven beneficial health effect (FAO/WHO codex alimentarius commission 2009).

This definition comprises a highly heterogeneous group of substances. Hence fibres can be classified according to several characteristics including main sources, chemical structure as well as physicochemical and physiological properties (Stephen et al. 2017). Classifications frequently used distinguish between (1) non-starch polysaccharides as cellulose, hemicellulose, pectin and hydrocolloids, (2) resistant oligosaccharides such as inulin, galacto- and fructo-oligosaccharides, (3) resistant starch and (4) natural occurring lignin or between water-soluble and -insoluble fibres (European Food Safety Authority 2010). Of note, the latter classification demands caution as solubility is sometimes paralleled with the physiological effect,

i.e. microbial utilisation, which is not always correct (European Food Safety Authority 2010; Brotherton 2015).

1.1.2 Nutritional situation

Geography and culture must always be considered when it comes to examination of the human nutrition. In the last hundred years, industrialised western societies developed some common dietary habits (Cordain et al. 2005). The so-called 'westernised diet' is generally characterised by the intake of processed food, which is accompanied by a high energy density, saturated fats, simple carbohydrates and low amounts of dietary fibre (Statovci et al. 2017).

In particular, the nutritional situation regarding fibre is alarming. The German Society of Nutrition recommends an intake of 30 g dietary fibre per day for adults (DGE, ÖGE, SGE 2019). However, approximately only 32 % of men and 25 % of women meet this recommendation (Max Rubner-Institut & Bundesinstitut für Ernährung und Lebensmittel 2008), which reflects the situation of fibre consumption in most westernised societies (Jones 2014; Stephen et al. 2017). By contrast, fibre intake of rural-living, agricultural societies exceeds that of western societies to a considerable degree due to the high consumption of whole grain cereals, legumes, vegetables and fruit, all rich in dietary fibre (Filippo et al. 2017).

Denis Burkitt (Figure 1) was the first who described the 'fibre hypothesis' based on his research studies in rural Africa and work of colleagues, including Cleave, Walker, Campbell, Trowell, Painter and Cummings (Cummings and Engineer 2018). Burkitt's hypothesis proposed an association between a diet low in fibre and a heightened incidence of non-communicable 'civilization diseases', such as coronary heart disease, diabetes and certain gastrointestinal disorders (Burkitt 1975; Burkitt and Trowell 1977). It was a shift in paradigm to designate diet as a common

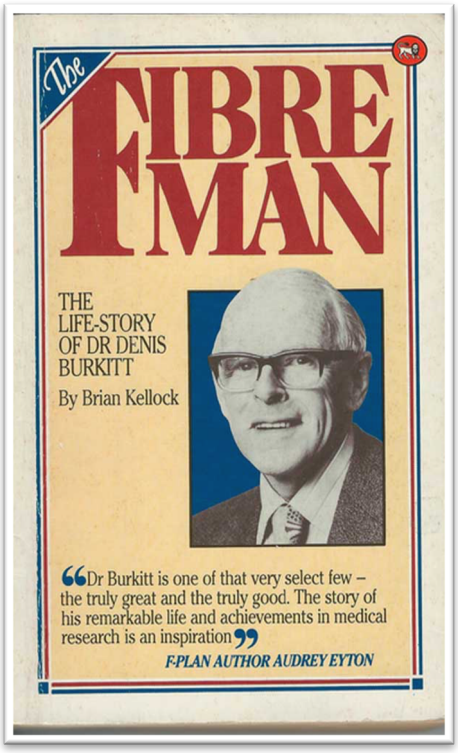

Figure 1. 'The Fibre Man'.
by Brian Kellock (1985)

cause for this group of diseases, but nowadays numerous epidemiological studies have confirmed this hypothesis (Cummings and Engineer 2018; O'Keefe 2019).

1.1.3 General health benefits of dietary fibre

Due to their heterogeneity, not all fibres fulfil all functions, which means that some physiological effects are shared by various types of fibre and others are unique (Jones 2014). The specific mechanism of action is dependent on their physicochemical properties, such as solubility, viscosity and organic acid absorption, and mainly related to colonic functions, blood cholesterol and glucose homeostasis (Guillon and Champ 2000; Stephen et al. 2017).

Many fibres form gels and increase the chymus viscosity, thereby promoting saturation and delay of gastric emptying. Consequently, the postprandial glucose level increases much slower than in the absence of dietary fibre. Due to their bulking effect, fibres also regulate the transit time in the lower gastrointestinal tract, thus preventing diarrhea and constipation. Their influence on blood cholesterol is among others based on the binding of primary bile acids, which are consequently not reabsorbed in the ileum (FAO/WHO 1998; Anderson et al. 2009).

Since dietary fibres are neither digested nor absorbed by the host, they reach lower regions of the intestine, where they are metabolically accessible for intestinal microbes. Many fibres fulfil the qualifications of prebiotics, i.e. food ingredients that selectively promote the growth and/or activity of beneficial microbes thereby improving health (Gibson and Roberfroid 1995). In this function, dietary fibres prevent dysbiotic compositional alterations, such as the loss of overall diversity or individual beneficial bacteria and the preponderance of potential harmful pathobionts (Petersen and Round 2014; Sonnenburg and Sonnenburg 2014).

Additionally, fermentation of dietary fibres not only fuels the microbial diversity, but also leads to the production of various bioactive metabolites (Nicholson et al. 2012). A major group of fermentation products are short-chain-fatty acids (SCFA), including acetate, propionate and butyrate, which serve as energy sources of colonocytes, but also as signalling molecules (Koh et al. 2016). Especially butyrate has been shown to impact on several physiological pathways involved in cell proliferation, apoptosis and immune responses (Daly and Shirazi-Beechey 2006; Furusawa et al. 2013; Arpaia et al. 2013).

1.1.4 Dietary cellulose – simple raw material of life

Cellulose is the most abundant organic substance on earth (Hon 1994). All plant cell walls are mainly composed of this macromolecule, which exclusively consists of unbranched β-1,4-linked glucose monomers. Depending on the botanical source, 500-15,000 molecules build up to such glucose chains, eighteen of which are organised as semi-crystalline elementary microfibrils. These microfibrils are embedded in a gel-matrix of hemicellulose, pectin, lignin and some proteins, which together provide the strong structure and toughness of plant cell walls (O'Sullivan 1997; Höfte and Voxeur 2017).

Dietary cellulose belongs to the class of insoluble fibre, which accounts for the majority of total fibre intake (Lairon et al. 2005; Dong et al. 2019). Main sources are cereals and legumes, but also vegetables, fruit and nuts. Cellulose and modified cellulose analogues are also used by the food industry, for instance as additive in instant and dairy products (Stephen et al. 2017).

Cellulose is a very stable molecule and its final degradation to glucose is largely dependent on microorganisms that produce cellulose-degrading enzymes (Weimer 1992). These so-called cellulases are glycoside hydrolases, which cleave the β-1,4-glycosidic bonds of cellulose (Figure 2). They can be further classified into (1) endo-β-(1,4)-glucanases (EC 3.2.1.4), (2) exo-β-(1,4)-glucanases (EC 3.2.1.91), (3) exo-β-(1,4)-glucosidase (EC 3.2.1.74) and β-glucosidase (EC 3.2.1.21) (Ezeilo et al. 2017). Moreover, cellobiose phosphorylases (EC 2.4.1.20) contribute to the final degradation of cellobiose by a phosphorolytic cleavage into α-D-glucose 1-phosphate and D-glucose (Alexander 1968). The forestomach (rumen) of ruminants harbours various cellulase-producing bacteria, such as *Ruminococcus albus*, *Ruminococcus flavefaciens* and *Fibrobacter succinogenes* (Hungate 1966; Russell et al. 2009). This symbiosis facilitates the conversion of low-quality plant material into energy-supplying metabolites (Cammack et al. 2018). Thus, by the domestication of animals, ruminal cellulose digestion has become the 'world's largest commercial fermentation process' in that it provides meat and milk for human nutrition (Weimer 1992).

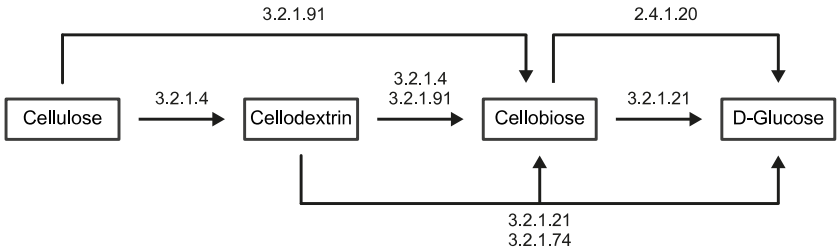

Figure 2. Enzymatic cellulose degradation.

The scheme of cellulose degrading pathways including enzymes (EC numbers) and intermediates.

In contrast to ruminants, the upper intestine of mono-gastric mammals is entirely devoid of cellulolytic bacteria. Thus, cellulose reaches lower parts of the gut and is utilised by the resident bacteria to a certain degree (Wolin 1981). However, the observed fermentability by the intestinal microbiota in men varies widely and contributes very little to short chain fatty acid production (Slavin et al. 1981; Kelleher et al. 1984; Cummings 1984; Vince et al. 1990; Chassard et al. 2012). Therefore, cellulose is often considered as bulking material, improving gastrointestinal transit and postprandial glucose homeostasis, rather than a substrate for microbial metabolism (Sonnenburg and Sonnenburg 2014).

Besides, recent research revealed that cellulose also has an impact on intestinal homeostasis by shaping the microbiota and influencing the course of certain diseases (Nagy-Szakal et al. 2013; Berer et al. 2018). Very little is known about the mechanisms of these effects at cellular and molecular levels. Consequently, there is no health claim or recommendation specifically concerning dietary cellulose (Stephen et al. 2017).

1.2 The intestinal homeostasis

The surface of the intestine is about 32 m^2, a large surface exposing our self to a tremendous number of foreign dietary and microbial antigens (Helander and Fändriks 2014). In addition to the digestion and absorption of nutrients, the intestine must distinguish between tolerance of harmless antigens and defence against pathogens to maintain homeostasis. Cellular key players that fulfil this demanding task are intestinal epithelial and immune cells, but also the symbiotic gut microbiota (Kayama and Takeda 2012).

1.2.1 Intestinal epithelial cells (IECs)

The intestinal epithelium consists of a single layer of various cell types, which are organised in invaginations called Lieberkühn crypts and additionally in the small intestine in villi that protrude into the lumen to increase the absorptive surface (Haber et al. 2017; Allaire et al. 2018). As adaption to the harsh environment in the gut, the epithelium renews every 3-7 days, which is driven by stem cells protected at the bottom of the crypts (Barker 2014).

1.2.1.1 Absorptive enterocytes

The majority of IEC are absorptive enterocytes or colonocytes (Cheng and Leblond 1974; Haber et al. 2017). The apical membrane of these cells is organised in microvilli and contains transmembrane mucins, such as mucin 3 (Khatri et al. 2001). This so-called brush border provides a microenvironment for efficient nutrient degradation and uptake, whilst preventing harmful contact to bacteria, fungi and viruses (Snoeck et al. 2005). In order to seal the paracellular space, IEC are connected by specialised intercellular junctions consisting of desmosomes, adherence and tight junctions. The most apical tight junctions selectively permit the transport of some soluble molecules, but prevent the invasion of large molecules and microorganisms (Zihni et al. 2016). Tight junctions are composed of several cytoplasmatic and transmembrane proteins, including claudins, occludin and zonula occludens (Stevenson et al. 1986; Furuse et al. 1993; 1998).

1.2.1.2 Secretory intestinal epithelial cells

Apart from absorptive enterocytes, the epithelium harbours various specialised secretory IECs which play an important role in protecting barrier integrity (Allaire et al. 2018). Goblet cells produce secretory O-glycosylated proteins, so-called mucins, with mucin 2 (Muc2) most abundantly produced in the gut (Johansson and Hansson 2016). Mucins bind water and form a viscous gel, the mucus, which provides a physical segregation of the epithelium and intestinal microbes (Johansson et al. 2008). Additionally, goblet cells secrete trefoil factor 3 (TFF3), which is essential for epithelial restitution after injury (Suemori et al. 1991; Mashimo et al. 1996). Paneth cells in small intestinal crypts secrete a broad range of antimicrobial substances, including α-defensins (cryptdins in mice), lysozyme and

the regenerating islet-derived protein (REG) 3α (REG3γ in mice) (Bevins and Salzman 2011). The latter, a C-type lectin, directly binds microbial peptidoglycan and disturbs the cell wall integrity of gram-positive bacteria, which significantly limits their attachment to the epithelium (Cash 2006; Vaishnava et al. 2011). Moreover, it has also been shown to protect from infections with gram-negative bacteria (Loonen et al. 2014). Together, absorptive IECs, secretory goblet and Paneth cells provide a strong physical and biochemical barrier which prevents adverse contact between host and microbe. Finally, it should be noted that despite specialisation some functions are shared by several IEC types. For instance, REG3γ is produced by enterocytes, Paneth cells as well as goblet cells (Burger-van Paassen et al. 2012).

In addition to the cell types mentioned above, other specialised secretory cell types are the enteroendocrine cells which secrete several hormones such as cholecystokinin and serotonin, and tuft cells which are enriched in markers related to taste-transduction (Isomäki 1973; Sjölund et al. 1983). Although their abundance is only about 1 % of all IEC, both cell types play important roles in the mediation between luminal stimuli and the host's immune, nervous and endocrine system (Gerbe et al. 2012; Worthington et al. 2018; Haber et al. 2017). Finally, microfold cells (M cells) are IEC specialised in the sampling of luminal antigens (Mabbott et al. 2013). They are situated in the epithelium overlying lymph follicles, so-called Peyer's Patches, which are unique to the small intestine (Owen and Jones 1974). Peyer's Patches are part of the gut-associated lymphoid tissue (GALT), an organised lymphoid structure of the gastrointestinal tract, and provide an environment in which M cells can efficiently transmit luminal signals to nearby professional antigen-presenting cells (Mowat 2003). Taken together, the epithelium is not only a physical barrier, but also a sensor of the intestinal environment (Allaire et al. 2018).

1.2.2 Intestinal immune system

The intestinal immune system is the largest immune compartment of the body and comprises many cell types: Luminal antigens sampled by IEC and professional antigen-presenting cells in the epithelium are presented to adaptive immune cells, especially $CD4^+$ (cluster of differentiation 4^+) T cells and B cells in draining lymph nodes and the GALT. Thereby, their differentiation and function are modulated depending on the specific stimulus (Mowat 2003).

1.2.2.1 Innate immune system

Despite the potent intestinal barrier provided by IECs, some pathogens and opportunistically invasive commensals or bacterial constituents can reach the mucosal surface (Allaire et al. 2018). IECs are able to sense pathogen- and microbe-associated molecular patterns (PAMPs/MAMPs) via cellular pattern recognition receptors (PRRs), such as Toll-like receptors (TLR) and nucleotide binding and oligomerization domain-like receptors (NLRs) (Parlato and Yeretssian 2014; Abreu 2010). According to their polarised structure, IECs are equipped with different, spatial segregated PRRs (Lee et al. 2008). Whereas the binding of antigens to apical receptors provokes anti-inflammatory mechanisms, for example the expression of antimicrobial peptides (Lee et al. 2006), the stimulation of basolateral or intracellular PRRs elicits pro-inflammatory responses via activation of NF-κB and subsequent production of cytokines (Gewirtz et al. 2001; Barnich et al. 2005).

IECs are in close interaction with professional antigen-presenting cells, such as macrophages and dendritic cells which are also endowed with PRRs. Macrophages are highly phagocytic effector cells that engulf dead cells but also invading microorganisms, thus playing an important role in the first line of defence (Wang et al. 2019b). Intestinal macrophages are hyporesponsive to TLR stimulation and produce a lot of IL-10 under homeostatic conditions, which serves as an anti-inflammatory mediator by promoting local regulatory T (T_{reg}) cells (Denning et al. 2007; Ueda et al. 2010). Furthermore, dendritic cells also sample antigens via several mechanisms, for example, by trans-epithelial dendrites or via Peyer's Patches' M cells and are specialised in presenting them to lymphocytes, which can induce either a tolerogenic or an inflammatory immune reaction (Kayama and Takeda 2012; Rescigno et al. 2001).

1.2.2.2 Adaptive immune system

Adaptive immune cells exist in the epithelium and the underlying lamina propria. Whereas lymphocytes found in the epithelium are mainly $CD8^+$ intraepithelial T cells, the underlying lamina propria harbours $CD4^+$ and $CD8^+$ T cells at a ratio of about 2/1 (Mowat and Agace 2014). Moreover, the intestinal lamina propria comprises the majority of plasma cells in the body of which around 80 % produce sIgA (secretory IgA) (Brandtzaeg 2010). SIgA plays a critical role in the symbiotic

relationship between host and microbe, for instance by blocking the attachment of bacteria and bacterial products to IEC through binding and steric hindrance (Mantis et al. 2011).

Apart from a certain plasticity, following activation naive $CD4^+$ TH cells (T helper cells) differentiate into functional distinct effector subsets, including TH1, TH2 and TH17 and T-regulatory (T_{reg}) cells (Brucklacher-Waldert et al. 2014). TH1 cells differentiate in response to viruses and intracellular bacteria and secrete IFN-γ, while IL-4 producing TH2 cells are important in the humoral immunity against extracellular parasites, such as helminths. As parasites are usually absent in healthy human and laboratory animals, the intestine is largely devoid of TH2 cells (Maynard and Weaver 2009). TH17 cells are highly abundant in the intestinal lamina propria and play an important role in both protection of mucosal surfaces against extracellular bacteria and fungi as well as maintaining homeostasis (Curtis and Way 2009; Omenetti and Pizarro 2015). Their differentiation is dependent on the transcription factor RORγt and is homeostatically induced by certain members of the microbiota, especially SFB (segmented filamentous bacteria) (Ivanov et al. 2006; 2008; 2009). TH17 cells secrete IL-17 and IL-22 (Park et al. 2005; Liang et al. 2006). Whereas IL-17 rather has a pro-inflammatory character, IL-22 improves the epithelial barrier integrity by promoting the antimicrobial host response, tissue repair and wound healing (Eyerich et al. 2017).

Another $CD4^+$ subset is the FOXP3-expressing regulatory T cell which secretes the anti-inflammatory cytokine IL-10. The colon harbours the highest frequency of these cells of which one fraction is derived from the thymus (tT_{reg} cells) and another fraction is differentiated in the periphery (pT_{reg} cells) (Tanoue et al. 2016). Beside TH17 cells, also some T_{reg} cells express RORγt following induction by the microbiota or inflammatory stimuli (Sefik et al. 2015; Yang et al. 2018; Ohnmacht et al. 2015). The function of these $T_{reg}17$ cells ($ROR\gamma t^+$ $FOXP3^+$ $CD4^+$ T cells) is still under debate. Recently it was shown that they exert anti-inflammatory functions during colitis, nevertheless, they are able to secrete IL-17 (Sefik et al. 2015; Yang et al. 2016).

1.2.2.3 Non-classical lymphocytes

There is another rather recently recognized group of innate immune cells, which should be shortly mentioned. Innate lymphoid cells (ILCs) mimic the phenotype of

$CD4^+$ TH cells, including the expression transcription factors, surface markers and effector cytokines (Eberl et al. 2015). However, they are not endowed with specific antigen receptors and they do not undergo clonal selection and expansion after stimulation as classical lymphocytes do (Eberl et al. 2015). ILCs provide an immune response adapted to the infection or injury prior to the action of the adaptive immune cells, but also play an important role for tissue homeostasis (Klose and Artis 2016). For instance, ILC3 express the transcription factor RORγt and secrete IL-17 and IL-22 dependent on the stimulus as their TH17 T cells counterpart (Buonocore et al. 2010; Castleman et al. 2019).

1.2.3 Intestinal microbiota

Microorganisms, including bacteria, fungi and protozoans, colonise all epithelial barrier sites of the mammalian body (Coates et al. 2019). However, within the adult intestinal microbiota, bacteria are the most abundant and diverse microorganisms (Rajilić-Stojanović and Vos 2014).

1.2.3.1 Development of the intestinal microbiota

Apart from the prenatal exposure to bacterial-derived substances, the foetus has no contact to bacteria during pregnancy (Mesa et al. 2020). The colonisation with diverse bacteria starts during birth. In vaginally delivered new-borns, the first bacteria of the intestinal microbiota originate from the maternal vaginal tract, such as *Streptococcus* in mice and *Lactobacillus* and *Prevotella* in human (Dominguez-Bello et al. 2010; Pantoja-Feliciano et al. 2013). During breastfeeding, the microbiota is dominated by Firmicutes species, especially of the *Lactobacillaceae* and *Streptococcaceae* family in human and mice (Yatsunenko et al. 2012; Pantoja-Feliciano et al. 2013). In addition, *Bifidobacterium* species are highly abundant in suckling infants, but not in mice (Stewart et al. 2018; Levi Mortera et al. 2019).

Some studies suggest that the intestinal microbiota stabilises within the first three to four years of life (Stewart et al. 2018; Yatsunenko et al. 2012). Indeed, the overall diversity of the microbiota increases consecutively to weaning and the intake of solid food (Koenig et al. 2011; Pantoja-Feliciano et al. 2013). At the taxonomic level, the abundance of *Lachnospiraceae* and *Ruminococcaceae* increases, whereas *Enterobacteriaceae*, *Bifidobacteriaceae* and *Clostridiaceae* decrease (Yassour et al.

2016). Only a few studies examined the microbiota in childhood beyond three years (Derrien et al. 2019). These studies revealed functional and taxonomical differences between the infant and adult microbiota suggesting that the maturation of the microbiota takes longer than previously thought (Hollister et al. 2015; Odamaki et al. 2016; Derrien et al. 2019).

The adult microbiota is stable over a long period of time (Faith et al. 2013). The dominant phyla are Bacteroidetes and Firmicutes as well as Verrucomicrobia, Actinobacteria and Proteobacteria at lower abundances (Human Microbiome Project Consortium 2012; Martinez-Guryn et al. 2019). A peak in the ratio of Firmicutes to Bacteroidetes is characteristic for maturation of the microbiota in adulthood (Mariat et al. 2009). Although the intestinal microbiota of adults is highly individual at strain level, there is more similarity from a functional point of perspective (Human Microbiome Project Consortium 2012).

The microbiota changes again during aging, which is reflected by a decrease of the Firmicutes/Bacteroidetes ratio and an increasing abundance of the genus *Alistipes* in men and mice (Mariat et al. 2009; Claesson et al. 2011; Langille et al. 2014; Bischoff 2016; Fransen et al. 2017). However, due to a broad range of cofounding factors, it is difficult to dissect these changes in human studies (An et al. 2018). It is still under debate, whether the overall diversity is impaired and which phyla are dominant in the aging human microbiota (An et al. 2018).

1.2.3.2 Anatomy and physiology of the intestinal microbiota

There is a high regional specialisation of structural and functional properties of the intestinal epithelium and immune system (Mowat and Agace 2014). According to this, the intestine offers diverse ecological niches, which also result in regional differences of the intestinal microbiota (Martinez-Guryn et al. 2019). The most important factors defining these niches are the partial oxygen pressure, bile acids, dietary and immune factors (Maslowski and Mackay 2011; Ridlon et al. 2014; Friedman et al. 2018).

Starting from the mouth, the diversity and bacterial load increases from the proximal to the distal gastrointestinal tract (Martinez-Guryn et al. 2019). The small intestinal microbiota has a high abundance of aerotolerant *Lactobacillaceae* (Firmicutes) and bacterial species of the Proteobacteria and Actinobacteria phyla (Gu et al. 2013;

Friedman et al. 2018). By contrast, obligate anaerobe bacteria, such as *Lachnospiraceae* and *Ruminococcaceae* (Firmicutes), as well as *Prevotellaceae* and *Rikenellaceae* (Bacteroidetes) peak in the caecum and colon (Nava et al. 2011; Gu et al. 2013). Remarkably, in addition to this horizontal distribution from proximal to distal, there is also a distinct distribution between the crypts, mucus and gut lumen (Pédron et al. 2012; Li et al. 2017).

The intestinal microbiota, sometimes referred to as the 'forgotten organ', has important physiological impact on the host (O'Hara and Shanahan 2006). The early hygiene hypothesis proposed that children who are more frequently exposed to infections are at a lower risk of developing allergies (Strachan 1989). This hypothesis was further expanded for autoimmune diseases and the observation that not only pathogens but also commensals exert protective immunomodulatory effects (Bach 2018). Today, it is well known that the gut microbiota is critically involved in the physiological maturation, i.e. imprinting, of the mucosal immune system (Al Nabhani and Eberl 2020). The absence or impairment of early imprinting increases the susceptibility for allergy or intestinal inflammation later in life (Kronman et al. 2012; Al Nabhani et al. 2019; Metzler et al. 2019). Not only direct interactions but also bacteria-derived metabolites contribute to this crosstalk between host and microbe (McDermott and Huffnagle 2014; Kayama and Takeda 2020).

Along the gastrointestinal tract, the caecum and colon are the major sites for bacterial fermentation of undigested carbohydrates and other metabolic processes. Especially Bacteroidales and Clostridiales species are able to degrade dietary fibre and produce SCFAs, which have various physiological functions (Koh et al. 2016, as mentioned above). Another group of bacterial-derived metabolites are secondary bile acids which are generated from primary bile acids. Primary bile acids are cholic acid (CA) and chenodeoxycholic acid (CDCA) (in rodents also muricholic acids, MCAs). They are synthesised in the liver of the host from cholesterol and are conjugated to glycine or taurine prior to secretion into the duodenum (Wahlström et al. 2016). A small proportion of primary bile acids which is not reabsorbed in the ileum reaches the caecum and colon, where it undergoes bacterial conversion – mainly deconjugation, oxidation and dehydroxylation – into secondary bile acids (Ridlon et al. 2006). Bile acids are not only emulsifiers supporting digestion and

absorption of dietary fats and fat-soluble vitamins, but also function as signalling molecules with several functions, for instance in epithelial proliferation and host's metabolism (Aguiar Vallim et al. 2013; Barrasa et al. 2013). However, high concentration of bile acids has been shown to induce DNA damage and promote tumour growth (Barrasa et al. 2013). Further, bile acids are in a complex, mutually relation with the intestinal microbiota in that bacteria shape the pool of bile acid in terms of composition and size and, in turn, bile acids influence the growth of bacteria (Wahlström et al. 2016). Thus, besides the competition for limited nutrients and space, secondary bile acids are a mechanism of how the gut microbiota provide resistance against colonisation of pathogens and expansion of pathobionts (Pickard et al. 2017). Of note, SCFAs and secondary bile acids are only a few representatives of the numerous substances produced by intestinal microbes. There are many more potentially bioactive metabolites, including vitamins, lipids and indoles (Nicholson et al. 2012).

1.2.4 Disorder of the intestinal homeostasis

Perturbation of the commensal relationship between host and microbe may have adverse consequences, such as intestinal inflammation (Maloy and Powrie 2011). Acute colitis induced by pathogens, diet or stress affects almost everyone at least once in life. The disease is characterised by abdominal pain and diarrhea, however, in many cases it is self-limiting or easy to treat (Vargas-Robles et al. 2019). By contrast, chronic inflammatory bowel diseases (IBD) including Crohn's disease and ulcerative colitis are more severe forms of colitis. The highest prevalence of IBD was reported in Europe and America (Ng et al. 2017). There is no curative therapy for these pathologies that are associated with serious long-term consequences, such as malnutrition and colorectal cancer (Guan 2019).

The pathology of these diseases is not yet clearly understood, but is considered to be multi-dimensional (Guan 2019). On the host's site, genetic abnormalities in around 240 loci are known to increase the risk for IBD (Lange et al. 2017). Many of these genes encode proteins of the antimicrobial host defence or immune system, as shown for defects of Mucin 2 and IL-10 (Kühn et al. 1993; Glocker et al. 2009; van der Sluis et al. 2006). Furthermore, an adverse and harmful immune reaction may also be induced upon intestinal dysbiosis (Petersen and Round 2014; Belkaid and

Harrison 2017). It has indeed been shown that the gut microbiota of IBD patients differ in various ways from that of a healthy subject, including alterations of the diversity, the taxonomical composition, transcriptional and metabolic profiles (Lloyd-Price et al. 2019). However, it is still not clear, whether dysbiosis is cause or consequence of IBD, since chronic inflammation can also shape the microbiota (Ni et al. 2017). Additionally, environmental factors, including nutrition, stress or smoking, play a role in the pathogenesis of IBD. In particular, a diet low in fibre is associated with an increased risk for IBD as well as colorectal cancer (Bingham et al. 2003; Gonzalez and Riboli 2010; Hou et al. 2011; Ananthakrishnan et al. 2013). Possible mechanistical links are, among others, the binding of potentially harmful substances, such as secondary bile acids, the promotion of beneficial microbes and their fermentation to SCFAs (Zeng et al. 2019). Despite consensus about their role in prevention, in the nutritional therapy of IBD, fibre are still a matter of debate, since a high fibre intake might increase the risk to develop an ileus in the inflamed intestine (Wedlake et al. 2014).

1.3 Objective

Industrialisation did not only change economy and technology, but also social life style, including nutrition. Whereas raw plant-based food predominated the preindustrial diet, the modern 'westernised diet' is characterised by processed groceries that often have a high energy density and low fibre content (Cordain et al. 2005). Today, there is a substantial 'fibre gap' between recommendations and the actual consumption (Jones 2014). However, a diet low in fibre has been shown to be associated with many civilization diseases, such as inflammatory bowel disease (O'Keefe 2019). The mechanisms of such health-promoting effects are still not entirely understood, especially with respect to insoluble fibres, such as cellulose.

The purpose of the present study was to investigate comprehensive cellular and molecular effects of dietary cellulose on the intestinal homeostasis, including microbiota, immune system and epithelium, in health and disease. Furthermore, this study should shed light on a selected host-microbe interaction, which might be causally related to the mechanism of health-promoting effects of cellulose.

2 Material and methods

2.1 Material

2.1.1 Mice and experimental diets

2.1.1.1 Mice strains

Strain	Hygiene status	Origin	Maintenance
C57BL/6	SFP	Charles River Laboratories	Institute for Medical Microbiology and Hospital Hygiene, University Marburg
C57BL/6	gnotobiotic, OMM[12]	Institute for Laboratory Animal Science and Central Animal Facility, Hannover Medical School	Institute for Medical Microbiology and Hospital Hygiene, University Marburg
C57BL/6	germ-free	Institute for Medical Microbiology and Hospital Hygiene, University Marburg	Institute for Medical Microbiology and Hospital Hygiene, University Marburg

2.1.1.2 Experimental diets

Diet	Product identification	Company
control diet, CD	S7242-E014	sniff Spezialdiäten GmbH
fibre free diet, FFD	S7242-E018	sniff Spezialdiäten GmbH
conventional chow	LASQCdiet® Rod16-R	LASvendi

2.1.1.3 Ingredients and composition of purified diets

	Control diet	Fibre free diet
Ingredients (%)		
Sucrose	44.1	46.1
Corn starch	20.0	25.0
Amino acid mixture	17.5	17.5
Cellulose	7.0	0.0
Corn oil	5.0	5.0
Additives	6.4	6.4
Composition (%)		
NfE	66.9	73.9
Crude protein	15.2	15.2
Crude fibre	7.0	0.0
Crude fat	5.0	5.0
Crude ash	4.0	4.0
Water	1.9	1.9

2.1.2 Bacteria

Strain	Origin
Alistipes finegoldii 17242	DSMZ, Braunschweig
Escherichia coli DH5α	Institute of Medical Microbiology and Hygiene, Marburg

2.1.3 Enzymes

Enzyme	Origin
BamHI	Fermentas, Vilnius, Litauen
HindIII	Fermentas, Vilnius, Litauen
Lysozyme, chicken egg white	Merck, Sigma-Aldrich, Darmstadt
MfeI	Fermentas, Vilnius, Litauen
NcolI	Fermentas, Vilnius, Litauen
NotI	Fermentas, Vilnius, Litauen
Ribonuclease	VWR Funding, Amresco, West Chester, USA

2.1.4 Consumables and equipment

Consumables, equipment	Type	Company
Anaerobic culture system	Anaerocult® A anaerobic jar	Merck, Millipore, Darmstadt
	GasPak™ EZ anaerobe container system	BD, Heidelberg
Capillary Electrophoresis (CE) system	Agilent 1600A	Agilent Technologies, Santa Clara, USA
	Fused CE silica capillary (ID 50µM, 100 cm)	Agilent Technologies, Santa Clara, USA
Cell counter	Cell counting slides	BioRad, Hercules, USA
	TC20™ Automated Cell Counter	BioRad, Hercules, USA
Cell homogenisators and dissociaters	Bead Beater	MP Biomedicals, Eschwege
	GentleMACS™ Octo dissociator	Miltenyi Biotec, Bergisch Gladbach
	Glass beads, 0.1 mm	Carl Roth, Karlsruhe
	NucleoSpin® bead tubes	Macherey-Nagel, Düren
	Precellys® Evolution homogenizer	Bertin Instruments, Montigny-le-Bretonneux, France
	Ultra-Turrax® T10 basic	IKA, Staufen im Breisgau
Cell strainers	Easystrainer™, 100 µm	Greiner, Kremsmünster, Austria
	Pre-separation cell strainer, 30 µm	Miltenyi Biotec, Bergisch Gladbach
Centrifuges	Megafuge™	Heraeus, Hanau
	Microstar 17R, Ministar	Avantor, VWR, Pennsylvania, USA
Flow cytometer	Attune™ NxT	Thermo Fisher Scientific, Waltham, USA
Gel documentation system		Herolab, Wiesloch

Consumables, equipment	Type	Company
Heater and shaker	IKA KS260	IKA, Staufen
	Thermomixer comfort	Eppendorf, Hamburg
	Unitexer 1	LCG Labware, Meckenheim
Incubator	HERAcell™ 240i	Heraeus, Hanau
Inoculation loop	10 µl	Sarstedt, Nümbrecht
Mass spectrometer (MS)	Agilent 6120 single quadrupole MS	Agilent Technologies, Santa Clara, USA
	amaZon ETD ion trap	Bruker Daltonics, Billerica, USA
	LTQ FT Ultra MS	Thermo Fisher Scientific, Waltham, USA
	maXis™	Bruker Daltonics, Billerica, USA
Microplate reader	FLUOstar omega®	BMG Labtech, Ortenberg
Microscope	Leica DM 5500 wide field microscope	Leica Mikrosystems, Wetzlar
NanoDrop system	1000	Thermo Fisher Scientific, Waltham, USA
Digital pH meter	inoLab® pH Level 2	Xylem, WTW, Weilheim
Pipettes	Eppendorf Research® plus	Eppendorf, Hamburg
	TipOne® filter tips	Starlab, Hamburg
Power supply	Standard Power Pack P25	Biometra, Göttingen
(RT-) PCR systems	LightCycler® 480 Instrument II	Roche Molecular Systems, Basel, Switzerland
	Thermal Cycler C1000 Touch™	BioRad, Hercules, USA
	StepOnePlus™ Real-time PCR System	Thermo Fisher Scientific, Applied Biosystems, Waltham, USA
Scales	Adventurer® Analytical AV812M, Explorer® Analytical EP114CM	Ohaus, Nänikon, Switzerland

Consumables, equipment	Type	Company
Sequencing system	MiSeq sequencing system	Illumina, San Diego, USA
Sterile filters	Filtropur BT50 filters, 0.22 µm	Sarstedt, Nümbrecht
	Syringe filters, 0.2 µm	Thermo Fisher Scientific, Waltham, USA
Syringes and needles	Syringe, 1.0 ml	B. Braun, Melsungen
	Gavage needle	Thermo Fisher Scientific, Waltham, USA
Tubes and dishes	Biosphere® plus SafeSeal tube, 1.5 ml, 2.0 ml	Sarstedt, Nümbrecht
	Centrifuge tube, 15 ml, 50 ml	Sarstedt, Nümbrecht
	Cell culture dishes, 24 wells	Sarstedt, Nümbrecht
	C tubes	Miltenyi Biotec, Bergisch Gladbach
	DNA LoBind tubes, 1.5 ml	Eppendorf, Hamburg
	Microplates, polystyrene	Greiner, Kremsmünster, Austria
	Microplates, polypropylene	Greiner, Kremsmünster, Austria
	Reaction tubes, 0.5 ml, 1.5 ml, 2.0 ml	Eppendorf, Hamburg
	Petri dishes	Greiner, Kremsmünster, Austria
(Ultra) High Performance Liquid Chromatography ((U)HPLC) system	Acquity™ UPLC	Waters, Milford, USA
	Acquity™ UPLC BEH™ C8 column	Waters, Milford, USA
	Agilent 1100 HPLC system	Agilent Technologies, Santa Clara, USA
	NUCLEODUR® 125/2 C18ec HPLC column	Macherey-Nagel, Düren

Consumables, equipment	Type	Company
Water purification system	Milli-Q® Integral and Synthesis	Merck, Millipore, Darmstadt

2.1.5 Chemicals and reagents

Chemical, reagent	Company
1 kb Plus DNA ladder	Thermo Fisher Scientific, Waltham, USA
4-(2-Hydroxyethyl)piperazine-1-ethanesulfonic acid (HEPES)	Roth, Karlsruhe
Acetic acid, 0.1 %, pH 4.2	Biosolve, Valkenswaard, Netherlands
Acetonitrile (LC-MS CHROMASOLV®)	FLUKA, Sigma Aldrich, St Louis, USA
Agarose	Biozym, Hessisch Oldendorf
Ammonium acetate	Merck, Sigma-Aldrich, Darmstadt
Ammonium chloride (NH_4Cl_2)	Merck, Sigma-Aldrich, Darmstadt
Ampicillin	Merck, Sigma-Aldrich, Darmstadt
Attune™ Bleach, Focussing Fluid, Performance Tracking Beads, Shutdown Solution, Wash Solution	Thermo Fisher Scientific, Waltham, USA
β-Mercaptoethanol (β-ME)	Merck, Sigma-Aldrich, Darmstadt
Brain-Heart-Infusion (BHI) broth	Thermo Fisher Scientific, Waltham, USA
Brefeldin A	BioLegend
Bovine serum albumin (BSA)	Merck, Sigma-Aldrich, Darmstadt
Butyric acid-4,4,4-d3, 98 atom % D	Merck, Sigma-Aldrich, Darmstadt
Carmine powder	Merck, Sigma-Aldrich, Darmstadt
Cellotetraose	Biozol, Toronto Research Chemicals
Chloroform, 99 %	Alfa Aesar
Columbia agar plate, 5 % sheep blood	BD, Heidelberg
CompBead Anti-Mouse Ig, κ/Negative Control Compensation Particles Set	BD, Heidelberg

Chemical, reagent	Company
CompBead Anti-Rat and Anti-Hamster Ig κ /Negative Control Compensation Particles Set	BD, Heidelberg
Deuterated bile acids	Merck, Sigma-Aldrich, Darmstadt
Dextran sulphate sodium salt (DSS), colitis grade 36,000-50,000	MP Biomedicals, Eschwege
Dithiothreitol (DTT)	Enzo life science, Lörrach
DNA stabilization buffer	Stratec Biomedical, Birkenfeld
Ethanol, absolute	Carl Roth, Karlsruhe
Ethidium bromide solution, 1 %	Carl Roth, Karlsruhe
Ethylenediaminetetraacetic acid (EDTA), 0.5 M, pH 8.0	Promega, Madison, USA
Extrazol	Biolab Innovative Research Technologies, Gdańsk, Poland
Foetal calf serum (FCS)	Thermo Fisher Scientific, Gibco, Waltham, USA
Formaldehyde solution, 36.5-38.0 %	Merck, Sigma-Aldrich, Darmstadt
Glacial acetic acid	Merck, Darmstadt
HALT™ Protease Inhibitor Cocktail, 100 x	Thermo Fisher Scientific, Waltham, USA
Hank's Salt	Biochrom, Berlin
Hank's balances salt solution (HBSS), w/o: Ca^{2+} and Mg^{2+}, w/o: Phenol red, w: 0.35 g/L $NaHCO_3$	Pan Biotech, Aidenbach
HBSS, (10x) w: Ca and Mg, w/o: Phenol red, w/o: $NaHCO_3$	Pan Biotech, Aidenbach
Ionomycin	Merck, Sigma-Aldrich, Darmstadt
Isopropanol (2-propanol)	Merck, Sigma-Aldrich, Darmstadt
Luria-Bertani (LB) agar powder	Thermo Fisher Scientific, Gibco, Waltham, USA
LB broth	Thermo Fisher Scientific, Gibco, Waltham, USA
L-Glutamine, 200 mM	Biochrom, Berlin

Chemical, reagent	Company
Mayer's Hämalaun	Carl Roth, Karlsruhe
MEM non-essential amino acids (NEAS), 100 x	Merck, Sigma-Aldrich, Darmstadt
Methanol	Carl Roth, Karlsruhe
Milk powder	Carl Roth, Karlsruhe
Sodium azide	Merck, Sigma-Aldrich, Darmstadt
Sodium chloride ($NaCl_2$)	Merck, Sigma-Aldrich, Darmstadt
Sodium chloride, 0.9 %-solution	Braun, Melsungen
Sodium bicarbonate ($NaHCO_3$)	Merck, Sigma-Aldrich, Darmstadt
Paraffine	Carl Roth, Karlsruhe
Penicillin-streptomycin solution	AppliChem, Darmstadt
Periodic acid solution, 0.5 %	Merck, Millipore, Darmstadt
Phenol:Chloroform:Isoamyl Alcohol, 25:24:1, [v/v]	Merck, Sigma-Aldrich, Darmstadt
PhiX standard library	Illumina, San Diego, USA
Phorbol-12-myristat-13-acetate (PMA)	Merck, Sigma-Aldrich, Darmstadt
Phosphate-buffered saline (PBS) w/o Ca^{2+} and Mg^{2+}	Bio&SELL, Nürnberg
ProLong™ Gold Antifade Mountant with DAPI	Thermo Fisher Scientific, Molecular BioProducts Waltham, USA
RNase Away Surface Docontaminant	Thermo Fisher Scientific, Molecular BioProducts, Waltham, USA
Roswell Park Memorial Institute 1640 (RPMI) medium	Merck, Sigma-Aldrich, Darmstadt
ROTI®histol	Carl Roth, Karlsruhe
Saponin	Merck, Sigma-Aldrich, Darmstadt
SCFA standards (acetic, propionic, butyric acid)	Merck, Sigma-Aldrich, Darmstadt
Schiff's reagent	Merck, Millipore, Darmstadt
Schaedler agar plate, 5 % sheep blood	BD, Heidelberg
Sodium dodecyl sulphate (SDS)	Merck, Sigma-Aldrich, Darmstadt
Sulfuric acid (H_2SO_4)	Fluka, Munich

Chemical, reagent	Company
TMB Substrate Reagent Set (RUO)	BD, Heidelberg
Triethlyamine	Merck, Sigma-Aldrich, Darmstadt
Tris-base	Carl Roth, Karlsruhe
Tris-HCl	Carl Roth, Karlsruhe
Triton X-100	Merck, Sigma-Aldrich, Darmstadt
Trypan blue	BioRad, Hercules, USA
t-RNA from baker's yeast	Roche, Basel, Switzerland
Tween-20	Merck, Sigma-Aldrich, Darmstadt
Water, sterile and pyrogen-free (Ampuwa)	Fresnius Kabi, Bad Homburg vor der Höhe
Water, PCR-grade	B. Braun, Melsungen
Xylene	Merck, Darmstadt

2.1.6 Buffers and media

Buffer, media	Composition
Ammonium chloride solution	9.1 g/L NH_4Cl_2, 20 mM HEPES, H_2O dest.
Balanced salt solution (BSS)	9.9 g/l Hank's Salt, 1.425 g/l $NaHCO_3$, 10 mM HEPES, H_20 dest. (pH 7.2)
Cellotetraose standard	400 µg/ml, protein isolation buffer
Digestion Solution	5 % [v/v] FCS, HBSS (w)
Enzyme-linked immunosorbent assay (ELISA) capture antibody solution	α-mouse lipocalin-2 or α-mouse IL-18 antibody in 1 x PBS; α-mouse IgA antibody in ELISA coating buffer
ELISA coating buffer	7.13 g/l $NaHCO_3$, 1.59 g/l Na_2CO_3, H_2O dest., pH 8.2
ELISA detection antibody solution	α-mouse lipocalin-2 biotin-conjugated or α-mouse IgA peroxidase-conjugated antibody in ELISA reagent diluent; α-mouse IL-18 HRP-conjugated antibody in 0.5 % [w/v] BSA/ELISA wash buffer
ELISA enzyme solution	1:200 streptavidin-HRP in ELISA reagent diluent

Buffer, media	Composition
ELISA isolation buffer	0.01 % [w/v] sodium azide, 1 % [v/n] 100 x HALT™ Protease Inhibitor Cocktail, 2 % [w/v] milk powder, 1 x PBS
ELISA reagent diluent	1 % [w/v] BSA, 1 x PBS (lipocalin-2); 2 % [w/v] BSA, ELISA wash buffer (IL-18); 10 % [v/v] FCS, 1 x PBS (sIgA)
ELISA stop solution	2 N H_2SO_4
ELISA substrate solution	1:1 mixture of Color Reagent A (H_2O_2) and Color Reagent B (3,3', 5,5'-tetramethylbenzidine)
ELISA top standard	1000 pg/ml lipocalin-2 standard; 1500 pg/ml IL-18 standard; 1 µg/ml sIgA standard
ELISA wash buffer	0.05 % [v/v] Tween-20, 1 x PBS (lipocalin-2, sIgA); 0.05 % [v/v] Tween-20, 20 mM Tris, 150 mM NaCl (pH 7.2-7.4; IL-18)
Ethanol, 75 %	75 % [v/v] ethanol absolute, PCR-grade water
Foetal calf serum	heat inactivated (30 min, 56°C)
FISH hybridisation buffer	0.9 M $NaCl_2$, 20 mM Tris-HCl (pH 7.4), 0.05 % [w/v] SDS, aqua dest.
FISH hybridisation solution	0.5 pmol/µl FISH probe in FISH hybridisation buffer
FISH wash buffer	0.9 M $NaCl_2$, 20 mM Tris-HCl (pH 7.4), 0.006 % [w/v] SDS, aqua dest.
Formaldehyde, 2 %	2 % [v/v] formaldehyde, 1 x PBS
HBSS (w)	10 mM HEPES, HBSS w Ca^{2+} and Mg^{2+}
HBSS (w/o)	10 mM HEPES, HBSS w/o Ca^{2+} and Mg^{2+}
LB agar	15 g/l LB agar powder, H_20 dest.
LB broth	20 g/l LB broth powder, H_20 dest.
Legendplex™ bead mix	1:13 dilution of individual beads in Legendplex™ assay buffer
Legendplex™ wash buffer	5 % [v/v] 20 x Legendplex™ wash buffer, H_2O dest.

Buffer, media	Composition
Lysozyme solution	20 mM Tris-HCl [pH 7.4], 2 mM EDTA, 1.2 % [v/v] Triton X-100, H_2O dest.
Methacarn solution	60 % [v/v] methanol, 30 % [v/v] chloroform,10 % [v/v] glacial acetic acid
PBS, 10 x	PBS powder w/o Ca^{2+} and Mg^{2+}, H_2O dest.
PBS, 1 x	10 % [v/v] 10 x PBS, H_2O dest.
PBS/1 % FCS	1 % [v/v] FCS, 1 x PBS
PB buffer	0.5 % [v/v] FCS, 1 x PBS
Predigestion solution	5 mM EDTA, 5 % [v/v] FCS, 1 mM DTT, HBSS (w/o)
Protein isolation buffer	1 % [v/v] 100 x HALT™ Protease Inhibitor Cocktail, 1 x PBS
RPMI-complete medium (RPMI-cm)	10 % [v/v] FCS, 50 µM β-ME, 60 mg/ml penicillin, 100 mg/ml streptomycin, 1 % [v/v] NEAS, 40 mM L-glutamine, RPMI
Restimulation medium	50 ng/ml PMA, 750 ng/ml ionomycin, 5 µg/ml brefeldin A, RPMI-cm
Saponin buffer	0.3 % [w/v] saponin, 2 % [v/v] FCS, 1 x PBS

2.1.7 Kits

Kit	Company
AMP + Mass Spectrometry Kit	Cayman Chemical, Ann Arbor, MI, USA
AMPure XD for PCR Purification	Beckmann Coulter, Brea, USA
eBioscience™ Foxp3/Transcription Factor fixation/permeabilization concentrate and diluent	Thermo Fisher Scientific, Waltham, Massachusetts, USA
CloneJET PCR Cloning Kit	Thermo Fisher Scientific, Waltham, Massachusetts, USA
Haemoccult®	Beckmann Coulter, Brea, USA
Mouse IL-18 ELISA Pair Set	Sino Biologicals
KOD Hot Start Polymerase Kit	Novagen, Merck, Darmstadt

Kit	Company
Lamina Propria Dissociation Kit, mouse	Miltenyi Biotec Germany, Bergisch Gladbach
LightCycler® 480 Probes Master	Roche Molecular Systems, Baser, Switzerland
Lipocalin-2/NGAL DuoSet ELISA, mouse	R&D Systems, Minneapolis, Minnesota, USA
Legendplex™ TH17 panel (8-plex), mouse	BioLegend, San Diego, USA
NucleoSpin Gel and PCR Clean-up Kit	Macherey-Nagel, Düren
NucleoSpin gDNA Clean-up Kit	Macherey-Nagel, Düren
NucleoSpin Plasmid Kit	Macherey-Nagel, Düren
QIAmp DNA stool mini kit	Quiagen GmbH, Hilden
qPCR Core kit for SYBR® Green I	Eurogentec, Lüttich, Belgium
RevertAid First Strand cDNA Synthesis Kit	Thermo Fisher Scientific, Waltham, Massachusetts, USA
TURBO DNA-free™ Kit, invitrogen	Thermo Fisher Scientific, Waltham, Massachusetts, USA
Zombie NIR™ Fixable Viability Kit	BioLegend, San Diego, USA

2.1.8 Antibodies

2.1.8.1 Antibodies for ELISA

Antibody	Conjugate	Clone	Working Concentration	Company
rabbit α-mouse IgA		polyclonal	1 µg/ml	Rockland, # 610-4106
rabbit α-mouse IgA	HRP	polyclonal	50 ng/ml	Rockland, # 610-4306
rabbit α-mouse IL-18		monoclonal	2 µg/ml	Sino Biologicals, # 50073-R169
rabbit α-mouse IL-18	HRP	monoclonal	250 ng/ml	Sino Biologicals, # 50073-R167

Antibody	Conjugate	Clone	Working Concentration	Company
rat α-mouse lipocalin-2		polyclonal	4 µg/ml	R&D systems, # 842440
rat α-mouse lipocalin-2	biotin	polyclonal	500 ng/ml	R&D systems, # 842441

2.1.8.2 Antibodies for FACS

Antibody	Conjugate	Clone	Dilution	Company
rat α-mouse CD45	Brilliant Violet 510™	30-F11	1:800	BioLegend, # 103138
rat α-mouse CD4	V450	RM4-5	1:500	BD, # 560468
rat α-mouse CD4	FITC	GK1.5	1:300	eBioscience, # 11-0041-82
mouse α-mouse RORγt	Alexa Fluor® 647	Q31-378	1:200	BD, # 562682
rat α-mouse FOXP3	PE	FJK-16s	1:200	eBioscience, # 12-5773-82
rat α-mouse IL-17A	APC	eBio17B7	1:400	eBioscience, # 17-7177-81
rat α-mouse IFN-γ	PerCP-Cy5.5	XMG1.2	1:400	BioLegend, # 505822
rat α-mouse IL-4	PE	11B11	1:300	eBioscience, # 12-7041-41

2.1.9 Primer and probes

2.1.9.1 Primer for SYBR® green-based RT-qPCR

Primer		Sequence (5'-3')	Company
Gapdh	fwd	GGG AAG CTC ACT GGC ATG G	biomers, Kim et
	rev	CTT CTT GAT GTC ATC ATA CTT GGC	al. 2009, mod.
Reg3γ	fwd	CAA GAT GCT TCC CCG TAT AAC C	biomers
	rev	AGC TGC TAC GTG AAG ATG G	
TFF3	fwd	GCT AAT GCT GTT GGT GGT CC	biomers
	rev	TCC GAT GTG ACA GAG GGG TA	
Muc2	fwd	CTT CTG TGC CAC CCT CGT	biomers,
	rev	TTC GGG ATC TGG CTT	Rosenholm et al.
			2016
Muc3	fwd	AAT AGC ACC CAA GAC GAC AG	biomol
	rev	TGG ATC TTT GCT GGT ACT CC	
Cldn8	fwd	CTG GAG GAG CAC TGT TCT GT	biomol
	rev	TGG CTG GTT TGG TGA TTT AT	
Ocln	fwd	ATC CAC CTA TCA CTT CAG A	biomers, Pearce
	rev	TAA TCT CCC ACC ATC CTC	et al. 2018
Tjp1	fwd	CCA CCT CTG TCC AGC TCT TC	biomol
	rev	CAC CGG AGT GAT GGT TTT CT	
Ki67	fwd	CTC CAC GAA CCT CAA AGA GA	biomol
	rev	TGT GGA TTC CTT CAC ACT TT	

2.1.9.2 Primer and probes for hydrolysis probe-based RT-qPCR

Primer		Sequence (5'-3')	Company
AF17242	fwd	GGT AAT ACG GAG GAT CCA AG	biomers
	rev	CCG CAA CTA CTC TCT AGT TC	
	probe	FAM-TGC GTA GGC GGT TTG ATA AGT TAG AGG-TAMRA	
Isol46_Exonucl.2_fwd		CGG ATC GTA AAG CTC TGT TGT AAG	biomers,
Isol46_Exonucl.3_rev		GCT ACC GTC ACT CCC ATA GCA	Brugiroux et al.
Probe3_Isol46		FAM-AAG AAC GGC TCA TAG AGG-BHQ1	2016

Primer	Sequence (5'-3')	Company
sol49_Exonucl._fwd	GCA CTG GCT CAA CTG ATT GAT G	biomers,
Isol49_Exonucl._rev	CCG CCA CTC ACT GGT GAT C	Brugiroux et al.
Probe_Isol49	HEX-CTT GCA CCT GAT TGA CGA-BHQ1	2016
YL58_Exonucl._fwd	GAAGAGCAAGTCTGATG	biomers,
	TGAAAGG	Brugiroux et al.
YL58_Exonucl._rev	CGG CAC TCT AGA AAA ACA GTT TCC	2016
Probe_YL58	FAM-TAA CCC CAG GAC TGC ATB-HQ1	
YL27_Exonucl.2_fwd	TCA AGTCAG CGG TAA AAA TTC G	biomers,
YL27_Exonucl.2_rev	CCC ACT CAA GAA CAT CAG TTT CAA	Brugiroux et al.
Probe2_YL27	HEX-CAA CCC CGT CGT GCC-BHQ1	2016
YL31_Exonucl.2_fwd	AGG CGG GAT TGC AAG TCA	biomers,
YL31_Exonucl.3_rev	CCA GCA CTC AAG AAC TAC AGT TTC A	Brugiroux et al.
Probe2_YL31	FAM-CAA CCT CCA GCC TGC-BHQ1	2016
YL32_Exonucl.2_fwd	AAT ACC GCA TAA GCG CAC AGT	biomers,
YL32_Exonucl.2_rev	CCA TCT CAC ACC ACC AAA GTT TT	Brugiroux et al.
Probe2_YL32	HEX-CGC ATG GCA GTG TGT-BHQ1	2016
KB1_Exonucl._fwd	CTT CTT TCC TCC CGA GTG CTT	biomers,
KB1_Exonucl._rev	CCC CTC TGA TGG GTA GGT TAC C	Brugiroux et al.
Probe_KB1	FAM-CAC TCA ATT GGA AAG AGG AG-BHQ1	2016
YL2_Exonucl._fwd	GGG TGA GTA ATG CGT GAC CAA	biomers,
YL2_Exonucl._rev	CGG AGC ATC CGG TAT TAC CA	Brugiroux et al.
Probe_YL2	HEX-CGG AAT AGC TCC TGG AAA-BHQ1	2016
KB18_Exonucl.2_fwd	TGG CAA GTC AGT AGT GAA ATC CA	biomers,
KB18_Exonucl.2_rev	TCA CTC AAG CTC GAC AGT TTC AA	Brugiroux et al.
Probe2_KB18	FAM-CTT AAC CCA TGA ACT GCB-HQ1	2016
YL44_Exonucl._fwd	CGG GAT AGC CCT GGG AAA	biomers,
YL44_Exonucl._rev	GCG CAT TGC TGC TTT AAT CTT T	Brugiroux et al.
Probe_YL44	HEX-TGG GAT TAA TAC CGC ATA GTA-BHQ1	2016

Primer	Sequence (5'-3')	Company
YL45_Exonucl._fwd	AGA CGG CCT TCG GGT TGT A	biomers,
YL45_Exonucl._rev	CGT CAT CGT CTA TCG GTA TTA TCA A	Brugiroux et al.
Probe_YL45	FAM-ACC ACT TTT GTA GAG AAC GA-BHQ1	2016
Isol48_Exonucl._fwd	GGC AGC ATG GGA GTT TGC T	biomers,
Isol48_Exonucl._rev	TTA TCG GCA GGT TGG ATA CGT	Brugiroux et al.
Probe_Isol48	HEX-CAA ACT TCC GAT GGC GAC-BHQ1	2016

2.1.9.3 Primer for 16S rRNA gene amplicon analysis

Probe	Sequence (5'-3')	Source
341F	CCT ACG GGN GGC WGC AG	Klindworth et al. 2013
785R	GAC TAC HVG GGT ATC TAA TCC	Klindworth et al. 2013

2.1.9.4 Probes for fluorescence in situ hybridisation (FISH)

Probe	Sequence (5'-3')	Source
AF17242	Cy5-GGC TCC TAC ACG TAA GAG CGT	biomers, Moschen et al. 2016, mod.
Eub338	FITC-GCT GCC TCC CGT AGG AGT	biomers, Amann et al. 1990

2.1.10 Plasmids

Plasmid	Backbone	Insert	Restriction site used for linearisation	Source
pSAB7	pJET 1.2	*'B. caecimuris'* I48	HindIII	Brugiroux et al. 2016
pSAB3	pJET 1.2	*'M. intestinale'* YL27	NotI	Brugiroux et al. 2016

Plasmid	Backbone	Insert	Restriction site used for linearisation	Source
pSAB9	pJET 1.2	*E. faecalis* KB1	NotI	Brugiroux et al. 2016
pSAB12	pJET 1.2	*'A. muris'* KB18	HindIII	Brugiroux et al. 2016
pSAB4	pJET 1.2	*B. coccoides* YL58	HindIII	Brugiroux et al. 2016
pSAB8	pJET 1.2	*L. reuteri* I49	HindIII	Brugiroux et al. 2016
pSAB6	pJET 1.2	*C. innocuum* I46	NotI	Brugiroux et al. 2016
pM1459-1	pCR®2.1-TOPO®	*A. muciniphila* YL44	HindIII	Brugiroux et al. 2016
pM1460-1	pCR®2.1-TOPO®	*'T. muris'* YL45	NcoI	Brugiroux et al. 2016
pM1452	pCR®2.1-TOPO®	*B. longum* YL2*	HindIII	Brugiroux et al. 2016
pM1457-1	pCR®2.1-TOPO®	*C. clostridioforme* YL32	HindIII	Brugiroux et al. 2016
pM1456-1	pCR®2.1-TOPO®	*F. plautii* YL31	HindIII	Brugiroux et al. 2016
p17242	pJET 1.2	*A. finegoldii* 17242	HindIII	this study

2.1.11 Software

Software	Source
Adobe Illustrator CS5	Adobe Inc.
EDGAR	Blom et al. 2009
EggNOG 4.5.1.	Huerta-Cepas et al. 2016
FlowJo 10	Becton Dickinson GmbH
GraphPad Prism 8	Graphpad Software, Inc.

Software	Source
ImageJ	National Institutes of Health
imngs	Lagkouvardos et al. 2016
KofamKoala	Aramaki et al. 2019
Legendplex™ Data Analysis Software	BioLegend
MS Office 2016	Microsoft
R, RStudio	RStudio Inc.
StepOne	Thermo Fisher

2.2 Methods

2.2.1 Mice maintenance and breeding

C57BL/6 wild type breeding pairs were ordered from Charles River Laboratory and kept at the animal facility of the Biomedical Research Centre and the Centre for Tumour Biology and Immunology of the Philipps-University Marburg. Animals were kept under specific-pathogen free conditions with 12 hours light cycle, rodent purified diets (sniff Spezialdiäten GmbH) and water *ad libitum*.

Mice harbouring the OMM^{12} (Oligo-Mouse-Microbiota 12) consortium were kindly provided by Dr. M. Basic (Hannover Medical School). Germ-free and gnotobiotic C57BL/6 mice were bred in sterile plastic isolators at the animal facility of the Biomedical Research Centre and the Centre for Tumour Biology and Immunology of the Philipps-University Marburg. They were kept under sterile conditions with 12 hours light cycle, autoclaved standard rodent diet LASQCdiet® Rod16-R (LASvendi) and water *ad libitum*. For some experiments, germ-free mice received rodent purified diets (sniff Spezialdiäten GmbH) for four weeks prior to analysis.

All experiments were performed in accordance with the animal ethics approved by Regierungspräsidium Gießen (Nr. G 1/2018 and G 72/2019).

2.2.2 DSS-induced acute colitis model

The chemical colitogenic dextran sulphate sodium (DSS; MP Biomedicals) was used to induce an acute colitis. DSS is a sulphated polysaccharide, which acts as anticoagulant and disrupts the intestinal epithelial barrier leading to inflammation (Okayasu et al. 1990; Chassaing et al. 2014).

Mice were exposed to 1.5 % to 3.5 % DSS in drinking water for five days. After five days DSS was replaced by unsupplemented drinking water. Analysis were performed on day five or six following colitis induction. Control mice received conventional drinking water. For experiments with gnotobiotic mice, drinking water was sterile-filtered with a 0.22 µm bottle top filter. The colitis was quantified by the loss of weight and colon length, diarrhea as well as micro- and macroscopic observations. The diarrhea score was set as follows: 0, normal stool; 1, soft stool or traces of blood; 2, very soft stool with traces of blood; 3, watery stool, rectal bleeding. Occult blood in faecal samples was confirmed by Haemoccult® test (Beckmann Coulter) according to manufacturer's instructions.

2.2.3 Intestinal transit time

The whole gut transit time was measured in accordance with the protocol of Nagakura and colleagues (Nagakura et al. 1996). One part of each diet was mixed with five parts of sterile water and 6 % [w/v] carmine as a maker. Mice were fasted for six hours prior feeding with 300 µl of the marked diet. The time between oral administration and the first red-coloured faecal pellet was measured.

2.2.4 Histology

2.2.4.1 Fixation and embedding

The water-free methacarn (methanol-Carnoy's) fixation was used to preserve the intestinal mucus layer during histological preparation (Puchtler et al. 1970).

Mice were sacrificed by cervical dislocation. The intestine was removed and 1 cm of the tissue containing a faecal pellet was transferred into 20 ml of methacarn solution and fixed over night at room temperature. The tissue was washed two times in dry methanol for 30 min, two times in ethanol for 15 min, once in ethanol/xylene (1:1, [v/v]) for 15 min and two times in xylene for 15 min prior to embedding in paraffine.

2.2.4.2 PAS staining

After sectioning in 3-5 µm thin sections dewaxing was accomplished by an initial incubation at 60°C for 10 min and subsequent incubation in xylene prewarmed at

60°C for 10 min and ethanol for 5 min. The sections were stained with periodic-acid-Schiff (PAS) as follows:

Solution	Time
Periodic acid, 0.5 % [w/v]	10 min
Running water	5-10 min
Schiff's reagent	20-30 min
Running water	20 min
Mayer's Hämalaun	1-5 min
Running water	5 min

2.2.4.3 Fluorescence in situ hybridisation (FISH)

Fluorescence in situ hybridisation means the detection of DNA or RNA sequences immediately in the tissue by using a probe which is linked to a fluorochrome. Here, we used a probe that binds specific to the 16S rRNA gene of bacteria to measure their location in different regions of the gut.

After sectioning in 3-5 µm thin sections dewaxing was accomplished by the following procedure:

Solution	Time
ROTI®histol, 60°C prewarmed	1 x 5 min
ROTI®histol	2 x 5 min
Ethanol, 100 % [v/v]	2 x 3 min
Ethanol, 80 % [v/v]	1 x 3 min
Ethanol, 60 % [v/v]	1 x 3 min
Aqua dest.	1 x 30 sec

The samples were treated with 50 µl 4 % lysozyme solution (45 min, 37°C) to demask nucleic acids. After washing in aqua dest. and FISH wash buffer, 50 µl hybridisation solution was added and incubated for 3 hours at 50°C. Slides were washed at 37°C and 120 rpm for 5 x 5 min with FISH wash buffer, preheated at 50°C for the first wash step. The slides were dried at RT and mounted with ProLong™ Gold Antifade Mountant with DAPI (Thermo Fisher Scientific) following manufacturer's

instructions and stored at 4°C over night in the dark. The samples were documented at a Leica DM 5500 wide field microscope (Leica) and analysed with ImageJ (National Institutes of Health). The protocol was established and the samples were documented and analysed with friendly assistance of Kai Binder.

2.2.5 Cell isolation techniques

2.2.5.1 Isolation of lymph node and spleen mononuclear cells

Mice were sacrificed by cervical dislocation. Peyer's Patches, lymph nodes and spleen were harvested and stored in BSS on ice. For preparation of single cell suspensions organs were pulped through a 30 µm cell strainer and washed with BSS. Cells were centrifuged (300 x g, 4°C, 10 min) prior to cell counting and following procedures.

To lyse erythrocytes in splenic cell suspensions, they were incubated with 3.0 ml ammonium chloride solution at RT for 7 min. After washing with BSS and centrifugation (300 x g, 4°C, 10 min) they were counted and used for subsequent applications.

2.2.5.2 Isolation of intestinal lamina propria mononuclear cells

Mice were sacrificed by cervical dislocation. Lamina propria mononuclear cells were isolated using the Lamina Propria Dissociation Kit (Miltenyi Biotec) according to manufacturer's instructions.

After sacrificing, the ileum (distal third of the small intestine) and colon were surgically removed. Fat and Peyer's Patches (ileum) were removed, intestines were longitudinally opened and washed with HBSS (w/o) to clear of faeces. The gut was cut into pieces of 0.5 cm length and stored in HBSS (w/o) on ice. Samples were incubated twice at 100 rpm and 37 °C for 20 min in 20 ml predigestion solution containing EDTA and DTT. Between and after these incubation steps the intestines were vigorously shaken for 10 sec and filtered on a 100 µm cell strainer. Thereafter they were washed in 20 ml HBSS (w/o) at 100 rpm and 37 °C for 20 min. The tissue was transferred into 2.35 ml 37°C-preheated digestion solution in C tubes (Miltenyi Biotec) and processed by gentleMACS Octo Dissociator (Miltenyi Biotec, program 37C_m_LPDK_1). The obtained cell suspension was filtered on a 100 µm cell strainer

and washed with PB buffer. Cells were centrifuged (300 x g, 4°C, 10 min) prior to cell counting and following procedures.

2.2.5.3 Determination of cell numbers

Trypan blue is an azo dye, which can pass the membrane of dead cells. Therefore, it is used to distinguish between dead and live cells.

To calculate absolute live and dead cell numbers, 10 µl of cell suspension was added to 10 µl trypan blue dye (Biorad). 10 µl of this mixture was transferred into a cell counting slide (Biorad) and measured with the TC20™ automated cell counter (Biorad).

2.2.6 Colon *ex vivo* explant culture

After sacrificing, the colons of the mice were removed. Approximately 1 cm of colon tissue was cleared of faeces and weighted. The tissue was washed in 1 ml RPMI-cm at 100 rpm and 37°C for 20 min. Afterwards the gut was opened longitudinally and incubated in 20-50 µl/mg RPMI-cm in a 24-well plate at 37°C and 5 % CO_2 for 24 hours. Supernatant was harvested and centrifuged with a microcentrifuge to remove debris. The aliquoted supernatant was stored at -20°C.

2.2.7 Microbiological and molecular microbiological methods

2.2.7.1 Cultivation and application of Alistipes finegoldii 17242

Culture plates and media were pre-reduced with Anaerocult® A (Merck) in an anaerobic jar for at least one day prior to usage. The anaerobic bacterial strain *Alistipes finegoldii* 17242 was cultivated on Schaedler blood agar under anaerobic conditions at 37°C for three days. Bacterial cells were harvested and stored in glycerol stocks at -80 °C. *A. finegoldii* 17242 was transferred from a Schaedler blood agar plate or glycerol stock to a flask containing BHI medium and cultivated under anaerobic conditions at 37°C for three to four days until bacterial growth was observed.

200 µl of *A. finegoldii* 17242 culture was administered orally by gavage to each mouse. Control mice received 200 µl native BHI medium. To ensure stabilisation of the intestinal microbiota, mice were allowed to sit for three to four weeks after association.

2.2.7.2 DNA isolation from faecal and caecal samples

Fresh faecal samples or caecal content were processed immediately or stored at -80 °C until processing.

For RT-qPCR approaches genomic DNA was isolated using the QIAamp DNA Stool mini Kit (Qiagen) following the manufacturer's instructions. In brief, faecal or caecal samples were homogenised in InhibitEX Buffer (200 mg/ml) using an inoculation loop and mixed vigorously for 1 min. The suspension was heated (70°C, 5 min) and centrifuged (13,000 x g, RT, 1 min). 200 µl of the supernatant was mixed with 15 µl proteinase K and 200 µl Buffer AL and samples were incubated at 70°C for 10 min. After that, 200 µl ethanol, absolute was added and the lysate was transferred onto a QIAamp spin column and centrifuged (13,000 x g, RT, 1 min). The column was washed twice with buffer 500 µl Buffer AW1 and subsequently 500 µl Buffer AW2, each wash step followed by centrifugation (13,000 x g, RT, 1 min). Finally, the column was dried by one more centrifugation (13,000 x g, RT, 3 min). The DNA was eluted by adding of 100 µl 70°C-prewarmed Buffer ATE and centrifugation (13,000 x g, RT, 1 min). The concentration and purity of the DNA were measured with the NanoDrop system (Thermo Fisher Scientific). DNA samples were stored at -20°C.

The DNA isolation for 16S rRNA gene amplicon analysis was performed in collaboration with Prof. T. Clavel (University Aachen) and Prof. K. Neuhaus (University Munich) as published previously (Lagkouvardos et al. 2015; Bazanella et al. 2017). Frozen caecal samples were thawed on ice and homogenised in 600 µl DNA stabilization buffer (Stratec Biomedical) and 400 µl phenol/chloroform/isoamyl alcohol (25:24:1, [v/v]; Sigma Aldrich). Bacterial cells were lysed by using 500 mg 0.1 mm glass beads and a bead beater (3 x 6.5 m/s for 40 s). Samples were heated (95°C, 8 min) and centrifuged (16,000 x g, 4°C, 5 min). 150 µl of the supernatant was treated with 15 µl ribonuclease (0.1 µg/ml; Amresco) at 37 °C for 30 min. After centrifugation (550 x g, 30 min) DNA was extracted with the NucleoSpin gDNA Clean-up Kit (Macherey-Nagel), according to manufacturer's instructions. In brief, the DNA solution was mixed with 450 µl Binding Buffer DB, loaded onto a NucleoSpin® gDNA Clean-up column and centrifuged (11,000 x g, RT, 30 sec). The column was washed twice with 700 µl Buffer DW, each wash step followed by centrifugation (11,000 x g, RT, 30 sec). Finally, the column was dried by one more

centrifugation (11,000 x g, RT, 1 min). After transferring the column into a fresh 1.5 ml microcentrifuge tube, 50 µl Buffer DE was added to the column and incubated for 1 min at RT. The DNA was eluted by centrifugation (11,000 x g, RT, 1 min). The concentration and purity of the DNA were measured with the NanoDrop system (Thermo Fisher Scientific). DNA samples were stored at -20°C.

2.2.7.3 16S rRNA gene amplicon analysis

The prokaryotic 16S rRNA gene consists of around 1,500 base pairs and has some hyper-variable regions, such as the V3/V4 region, between more conservative regions (Kim et al. 2011). 16S rRNA gene amplicon analysis of the variable regions is widely used to get insight into complex microbial communities, such as the intestinal microbiota. First, the whole genomic DNA is isolated from the sample. The library preparation includes the amplification of the V3/V4 region, the addition of sequencing adaptors and barcodes which are used to identify sequences derived from a certain sample. After sequencing, the data are bioinformatically processed to obtain OTUs (operational taxonomic units). An OTU is a cluster of similar, usually 97 % identical sequences.

The 16S rRNA gene amplicon analysis was performed in collaboration with Prof. T. Clavel (University Aachen) and Prof. K. Neuhaus (University Munich) (Lagkouvardos et al. 2015; Bazanella et al. 2017). 24 ng of genomic DNA was used for amplification (25 cycles) of the V3/V4 region of the 16S rRNA genes with the bacteria-specific primers 341F and 785R (Klindworth et al. 2013). Purification of amplicons was achieved using the AMPure XP system (Beckmann) and sequencing was performed in paired-end modus (PE275) with pooled samples in a MiSeq system (Illumina Inc.) according to manufacturer's instructions and a final concentration of 10 pM DNA and 25 % [v/v] PhiX standard library.

Demultiplexing and OTU (operational taxonomic unit) clustering from the raw 16S rRNA gene amplicon dataset was performed with imngs (Integrated Microbial Next Generation Sequencing) (Lagkouvardos et al. 2016). The similarity cut-off for OTU clustering in imngs is set to 97 % identity. The parameters for the imngs analysis were set as the following: two allowed mismatches in the barcode, minimum fastq quality score of three for trimming of unpaired reads, 350 to 550 base pairs length for amplicons for paired overlapping sequences, maximum of four expected errors

in paired sequences, ten base pairs length of trimming at the forward and reverse side of the sequences, 0.5 % relative abundance of OTU cut-off. The downstream analysis of the generated OTU-table, which contains information about the abundance and taxonomic classification of each OTU in each sample, was performed with the R script set Rhea (Lagkouvardos et al. 2017). Rhea allows inter alia the calculation of diversity, taxonomic composition, statistical comparisons and correlations.

2.2.7.4 Quantitative PCR for OMM^{12} consortium

Hydrolysis probe-based RT-qPCR assays enables the quantification of the increase of specific DNA sequences during PCR, which is, in theory, exponentially. The probe is composed of an oligo-nucleotide, which binds to the sequence amplified specifically by the primer, a fluorophore at the 5'-end and a quencher at the 3'-end. The quencher quenches the fluorescence emitted by the fluorophore. During amplification, the DNA polymerase, which harbours also 5'-3'-exonuclease activity, degrades the probe, thereby releases the fluorophore and the quencher. The fluorophore, which is no longer next to the quencher, emits a detectable signal. The more specific DNA sequences are in the sample, the more fluorophores are released and the higher is the fluorescent signal. An advantage of this method is the ability to detect more than one template per reaction by using probes with different fluorophores.

Genomic bacterial DNA was isolated from faecal and caecal samples as mentioned above. For absolute quantification of the OMM^{12} consortium and *A. finegoldii* 17242 within the intestinal microbiota we used the hydrolysis-probe-based RT-qPCR published by Brugiroux and colleagues (Brugiroux et al. 2016). Duplex RT-qPCRs were run using the LightCycler® 480 Probes Master (Roche) and a LightCycler® 480 Instrument II (Roche) with the following features:

Component	Volume
2 x Probes Master	10 µl
forward primer 1 (30 µM)	0.2 µl
forward primer 1 (30 µM)	0.2 µl
probe 1 (25 µM), FAM-labelled	0.2 µl
forward primer 2 (30 µM)	0.2 µl
forward primer 2 (30 µM)	0.2 µl
probe 2 (25 µM), HEX-labelled	0.2 µl
template/standard DNA (4 ng/µl)	2.5 µl
PCR grade water	ad 20 µl

Cycling Conditions	**Temperature and time**
1. polymerase activation	95°C, 2 min
2. denaturation	95°C, 2 min
3. annealing	43°C, 10 sec
4. extension	70°C, 10 sec
Repeats of steps 2-4	40 cycles

The absolute quantification of the copy number of certain sequences in an unknown sample requires standard curves of the fluorescent intensity dependent on known DNA concentrations. For standard curve preparation the concentration of sequence copy numbers was calculated for each plasmid (see chapter 2.2.7.5). Ten-fold serial dilutions (10^{8}-10^{-2} copies/µl) were prepared in water supplemented with 100 ng/µl yeast t-RNA. Standard curves measured once can be used for absolute quantification of the copy number in template DNA, for example DNA isolated from faecal samples. Just one single standard in every further run is needed to reproduce the standard curves by the software of the LightCycler® 480 Instrument (Roche).

2.2.7.5 Plasmids

The absolute quantification of a DNA template via quantitative RT-qPCR requires a standard with known concentration of the copy number. Therefore, plasmids harbouring a sequence of the bacterial 16S rRNA gene were prepared to serve as standard for RT-qPCR assays.

Genomic DNA of *A. finegoldii* 17242 was isolated from BHI cultures using the QIAamp DNA Stool mini Kit (Qiagen) following the manufacturer's instructions (see above), except for the first steps. Bacterial culture was centrifuged (2,000 x g, 4°C, 20 min) and the pellet was resuspended in 400 µl InhibitEX buffer.

After DNA isolation, a specific region of the 16S rRNA gene of *A. finegoldii* was amplified using the AF17242 primer and the KOD Hot Start Polymerase Kit (Novagen) according to manufacturer's instructions:

Component	**Volume**
10 x Buffer for KOD Hot Start DNA Polymerase	5.0 µl
$MgCl_2$ (25 mM)	3.0 µl
dNTPs (2 mM each)	5.0 µl
sense (5') primer AF17242_for (10 µM)	1.5 µl
antisense (3') primer AF17242_rev (10 µM)	1.5 µl
template DNA (20 ng/µl)	4.0 µl
KOD Hot Start DNA Polymerase (1 U/µl)	1.0 µl
PCR grade water	ad 50 µl

Cycling Conditions	**Temperature and time**
1. polymerase activation	95°C, 2 min
2. denaturation	95°C, 2 min
3. annealing	43°C, 10 sec
4. extension	70°C, 10 sec
Repeats of steps 2-4	40 cycles

The purity of the template was proofed by agarose gel electrophoresis with a 1.5 % agarose gel and ethidium bromide staining. The DNA fragment was then isolated from the gel using the NucleoSpin Gel and PCR Clean-up Kit (Macherey-Nagel) according to manufacturer's instructions. In short, the band was cut out of the agarose gel, mixed with Buffer NTI and heated to melt the agarose gel (50°C, 5-10 min). The solution was transferred to a NucleoSpin® Gel and PCR Clean-up Column. After several wash steps, the DNA was eluted with Buffer NE. The yielded DNA

concentration and quality were measured by NanoDrop system (Thermo Fisher Scientific).

To generate the plasmid, the fragment was inserted into a vector using the CloneJET PCR Cloning Kit (Thermo Scientific) following manufacturer's Sticky-End cloning protocol. In brief, the PCR product was incubated with the blunting reaction mix for 5 min at 70°C. After chilling on ice, the vector pJET1.2 and ligase were added and the ligation mix was incubated for 5 min at RT.

The prepared plasmid was transformed into *E. coli* DH5α via heat shock (42°C, 30 sec). Bacteria were cultured on LB-Agar plates containing ampicillin (100 µg/ml) at 37°C overnight. Several clones of the overnight culture were picked and cultured in 30 ml LB Medium containing ampicillin (100 µg/ml) at 37°C overnight.

The overnight cultures were centrifuged (3,000 x g, 4°C, 10 min). Plasmid DNA was isolated using the NucleoSpin Plasmid Kit (Macherey-Nagel) according to manufacturer's instructions. In short, bacterial cells were resuspended and lysed, following centrifugation (11,000 x g, RT, 10 min) to remove cell debris. The supernatant was loaded on a DNA-binding column. After a washing procedure and drying of the membrane the DNA was eluted by addition of elution buffer and centrifugation (11,000 x g, RT, 1min). To validate the cloning, plasmids were cleaved by two restriction enzymes at specific recognitions sites in the insert (MfeI) and in the vector (BamHI). Fragments were separated by agarose gel electrophoresis with a 1.5 % agarose gel and stained by ethidium bromide.

Plasmids containing the 16S rRNA gene of OMM^{12} bacteria were kindly provided by Prof. B Stecher (Max von Pettenkofer-Institute Munich). The dried plasmids were solved in 10 µl water and transformed into *E. coli* DH5α via heat shock (42°C, 30 sec). Bacteria were grown and plasmids were isolated as mentioned above.

The yielded plasmids were linearised by cleaving once by restriction enzymes (NotI, NcoI, HindIII). The DNA concentration was measured by NanoDrop system (Thermo Fisher Scientific) and the sequence was controlled by sequencing (Seqlab).

2.2.8 Flow cytometry

Flow cytometry enables the simultaneous analysis of multiple parameters of single cells, for example the expression of cell surface molecules or intracellular cytokines and transcription factors. Cell populations can be distinguished by cell size and

granularity, both measured by light foreword (FSC) and side scattering (SSC) due to a cell in the light beam. Fluorescent dyes and fluorochrome-conjugated antibodies are used to investigate certain markers as well as viability of a cell.

2.2.8.1 Cell surface staining

Isolated cells from different murine organs were washed with 1 x PBS. After each washing step cells were centrifuged (300 x g, 4°C, 10 min). Supernatant was discarded and cells were resuspended. For the staining of certain parameters 100 µl 1 x PBS containing Zombi NIR™ fixable viability dye (BioLegend, 1:2,000) and appropriate diluted antibodies were added and incubated for 20 min at 4°C. To remove unattached antibodies cells were washed with PBS/1 % FCS prior to intracellular staining or flow cytometry.

2.2.8.2 Intracellular staining of transcription factors

Prior to intracellular staining cells must be fixed and permeabilised. Therefore, following cell surface staining, cells were washed with 1 x PBS and fixed using the Foxp3 Fixation/Permeabilization Kit (Thermo Fisher Scientific) for 20 min at 4°C. Following washing with PBS/1 % FCS and saponin buffer cells were incubated in 100 µl saponin buffer containing appropriate diluted antibodies for 40 min at 4°C. After further washing steps with saponin buffer and PBS/1 % FCS cells were analysed by flow cytometry using the Attune NxT Flow Cytometer. The data were analysed by FlowJo 10 (BD) following the gating shown in Figure 3A.

2.2.8.3 Intracellular staining of cytokines

To measure the cytokine production, isolated cells were restimulated with restimulation medium containing PMA and ionomycin, which lead to polyclonal T cell activation, and brefeldin A, which inhibits the transport of proteins to the Golgi apparatus and thus the secretion of produced cytokines.

Isolated cells from different organs were washed with RPMI-cm. Afterwards 1 ml restimulation medium was added and cells were incubated for four hours at 37°C and 5 % CO_2. Following incubation, cell surface staining was performed as mentioned above. After washing with 1 x PBS, the cells were fixed in 2 % formaldehyde solution for 30 min at room temperature. Following washing with

PBS/1 % FCS and saponin buffer cells were incubated in 100 µl saponin buffer containing appropriate diluted antibodies for 20 min at 4°C. Flow cytometric analysis was performed after further washing steps with saponin buffer and PBS/1 % FCS using the Attune NxT Flow Cytometer. The data were analysed by FlowJo 10 (BD) following the gating shown in Figure 3B.

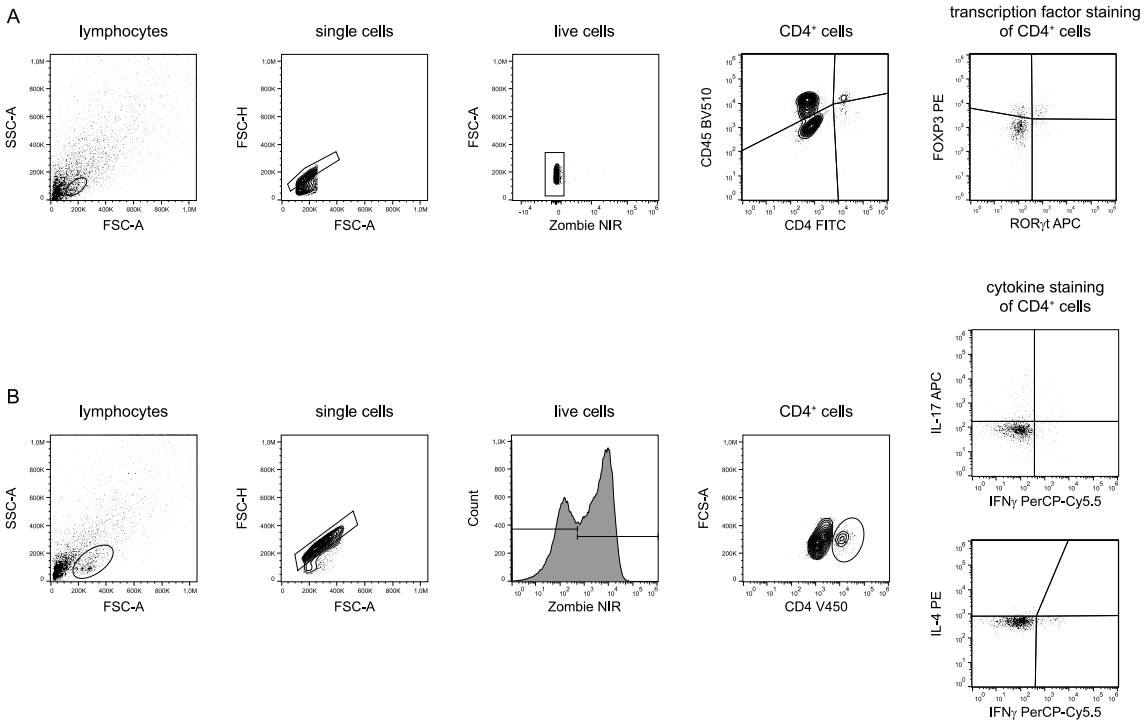

Figure 3. Gating strategy for flow cytometry analysis.

(A) FOXP3- and RORγt-expressing subsets were gated on live CD4⁺ CD45⁺ lymphocytes. (B) Subsets of IL-4-, IL-17- and IFN-γ-expressing cells were gated on live CD4⁺ lymphocytes.

2.2.9 Immunoassays

2.2.9.1 Enzyme-linked immunosorbent assay (ELISA)

ELISA is an antibody-based assay to detect and quantify proteins, such as cytokines. A coating antibody binds the analyte to a plate. Hereafter, an enzyme-conjugated primary or a combination of a primary and secondary antibody, in which the secondary antibody is conjugated, bind the analyte. For instance, the enzyme horseradish peroxidase catalyses the oxidation of the colorimetric substrate 3,3',5,5'-tetramethylbenzidine (TMB) driven by H_2O_2 and results in a blue coloration. Addition of the stop solution sulfuric acid changes the colour from blue to yellow. By using a standard of known concentration, the absorbance of this product could be used to quantify the analyte.

To quantify lipocalin-2, an innate immune-linked protein (Chassaing et al. 2012), and IL-18 in *ex vivo* colon culture supernatants the Mouse Lipocalin-2/NGAL DuoSet® ELISA (R&D Systems) and IL-18 ELISA (Sino Biologicals) were performed according to manufacturer's instruction. In short, 50 µl/well ELISA capture antibody solution was added to a polystyrene 96-well microplate, which than was incubated overnight at 4°C. Afterwards and for each following washing step, the plate was washed three times with ELISA washing buffer and dried by blotting on paper towels. Unspecific antibody binding was blocked by addition of 300 µl/well ELISA reagent diluent and incubation for at least one hour at RT. Samples were diluted 1:500 to 1:1,000 (lipocalin-2) respectively 1:10 (IL-18) in ELISA reagent diluent. The eight-point standard curve was prepared by serial 2-fold dilution of the ELISA top standard. 50 µl/well sample or standard was added to the plate and incubated for two hours at RT. Following washing, 50 µl/well ELISA detection antibody solution was added and incubated for two (lipocalin-2) respectively one hour (IL-18) at RT. Additionally for lipocalin-2 ELISA, the plate was washed and 50 µl/well ELISA enzyme solution was added and incubated for 20 min at RT in the dark. After washing, 50 µl/well ELISA substrate solution was added and incubated for 20 min at RT in the dark. After stopping the reaction by addition of 25 µl/well ELISA stop solution, the absorbance was measured by 450 nm and corrected for the absorbance of 570 nm.

ELISA was also performed to quantify secretory IgA (sIgA) in faecal protein isolates. Fresh faecal samples were collected in 2.0 ml tubes and weighted. ELISA isolation buffer was added (1 ml/100 mg) and samples were homogenised using an inoculation loop. Samples were incubated on ice for 30 min and subsequently vigorously mixed for 20 sec. After centrifugation (2,000 x g, 4°C, 30 min), the supernatant was aliquoted and stored at -20°C. 50 µl/well. ELISA capture antibody solution was added to a polystyrene 96-well microplate, which than was incubated overnight at 4°C. Afterwards and for each following washing step, the plate was washed four-times with ELISA washing buffer and dried by blotting on paper towels. Unspecific antibody binding was blocked by addition of 300 µl/well ELISA reagent diluent and incubation for at least two hours at RT. Samples were diluted 1:2 in ELISA reagent diluent. The nine-point standard curve was prepared by serial 2-fold dilution of the ELISA top standard. 50 µl/well sample or standard was added to the

plate and incubated for two hours at RT. Following washing, 50 µl/well ELISA detection antibody solution was added and incubated for two hours at RT. The plate was washed and 50 µl/well ELISA substrate solution was added and incubated for 25 min at RT in the dark. After stopping the reaction by addition of 25 µl/well ELISA stop solution, the absorbance was measured by 450 nm and corrected for the absorbance of 570 nm.

2.2.9.2 Bead-based immunoassay

The BioLegend Legendplex™ is a bead-based immunoassay, which allows the simultaneous quantification of multiple soluble analytes, such as cytokines, from culture supernatant or blood serum. The analytes were bind to antibodies on the surface of capture beads that differ in size and APC-fluorescence levels, which allows them to be differentiated. Biotinylated secondary antibodies bind specifically to the bound analytes, thereby forming capture bead-analyte-detection antibody sandwiches. Added streptavidin-phycoerythrin (SA-PE) binds to the biotinylated detection antibodies and provides a fluorescent signal proportional to the amount of bound analyte and could be detected by flow cytometry.

The mouse Th17 Cytokine Panel (8-plex) Legendplex™ assay was performed according to manufacturer's instruction. Therefore, samples were diluted 1:2 or used undiluted. The eight-point standard curve was prepared by serial 4-fold dilution of the Legendplex™ top standard. Samples respectively standards, Legendplex™ assay buffer and Legendplex™ bead mix, each 12.5 µl/well, were mixed into a polypropylene 96-well microplate and incubated overnight at 4°C while continuously shaking (800 rpm). Afterwards and for the following washing step, the plate was washed with 200 µl/well Legendplex™ washing buffer and centrifuged (800 x g, 5 min). The supernatant was discarded and the plate was dried by blotting on paper towels. 12.5 µl/well Legendplex™ detection antibody was added and the assay was incubated for one hour at RT while continuously shaking. Afterwards, 12.5 µl/well Legendplex™ SA-PE was added and incubated for 30 min further. Following washing, the beads were transferred into FACS tubes using 150 µl/well Legendplex™ washing buffer and measured at the Attune NxT Flow Cytometer. The data were analysed using the Legendplex™ Data Analysis Software.

2.2.10 Cellotetraose assay

Cellulose is large molecule and insoluble in water. Because of these physicochemical properties, cellulose is poorly suitable to study cellulolytic enzyme activities *in vitro*. Cellotetraose, which consists of four glucose molecules, is highly water-soluble, but still has the unique β-1,4-glycosidic bonds preventing cleavage by mammalian digestive enzymes. Isolated caecal proteins including cellulolytic enzymes (Lin et al. 2012) were incubated with cellotetraose and cellulolytic activity was measured by the quantification of cellotetraose cleavage products (cellotriose and cellobiose) by high-performance liquid chromatography- (HPLC-) and capillary electrophoresis- (CE-) coupled mass spectrometry.

2.2.10.1 Analysis of kinetics of caecal cellulolytic enzymes

Mice were sacrificed via cervical translocation. The caecal luminal content of three to four mice was isolated, pooled and weighted. After addition of the protein isolation buffer (300 µl/100 mg), samples were incubated on ice for 10 min. The luminal content was homogenised by using an inoculation loop and vigorously mixing for 30 sec. The samples were centrifuged twice (3,500 x g, 4°C, 20 min). The clear supernatant was 1.5-fold diluted in sterile water and used directly for subsequent applications.

The diluted supernatant which contained bacterial enzymes was mixed with cellotetraose standard in excess, resulting in a final concentration of 200 µM. Protein isolation buffer instead of cellotetraose standard was used as a negative control. For heat-inactivated controls, the enzyme solution was incubated at 95°C for 15 min prior to addition of cellotetraose standard. The samples were incubated for times indicated in the figures at 37°C. The reaction was terminated by freezing in liquid nitrogen. Samples were stored at -80°C before analysis

2.2.10.2 Quantification of cello-oligomers via HPLC- and CE-MS

The HPLC-and CE-MS analysis was performed in collaboration with Dr. U. Linne (University Marburg) and M.Sc. Filipp Bezold (University Marburg).

After thawing, the samples were heat inactivated (95°C, 15 min) to exclude further enzymatic processes. The samples were centrifuged (3,500 x g, 4°C, 20 min) and clear supernatant was 10-fold diluted.

For HPLC-MS analysis, 50 µl of this solution was transferred to an Agilent 1100 HPLC system (Agilent Technologies) and a HPLC column (NUCLEODUR 125/2 C18ec, Macherey-Nagel). The column temperature was set to 25°C. Cello-oligomers were eluted by performing a solvent system of water (eluent A) and acetonitrile (eluent B) with a gradient profile as follows:

Eluent	**Time**
starting at 2 % eluent B	5 min
increasing to 10 % eluent B	within 5 min
increasing to 85 % eluent B	within 10 min
increasing to 95 % eluent B	within 10 min, hold for 5 min

The LTQ-FT-Ultra mass spectrometer (Thermo Fisher Scientific) equipped with an electrospray ion source in positive ionisation mode was used for mass spectrometry. The CE-MS analysis was performed as previously described (Klampfl and Buchberger 2001). 25 µl sample solution was transferred to an Agilent 1600A capillary electrophoresis system (Agilent Technologies) and a 100 cm fused CE silica capillary (ID 50µM) (Agilent Technologies). 300 mM triethylamine was used as background analyte and 80 % isopropanol supplemented with 0.25 % triethylamine was provided at a flow rate of 4 µl/min as sheath liquid. The sample was injected by pressure (50 mbar, 9 s) and separated by the application of 20 kV separation voltage. The Agilent 6120 single quadrupole mass spectrometer (Agilent Technologies) in negative ionisation mode was used for mass spectrometry.

2.2.11 Quantification of SCFAs and bile acids

2.2.11.1 Isolation of caecal bile acids and short chain fatty acids

The isolation of bile acids and short chain fatty acids was performed in collaboration with Dr. A. Walker (Helmholtz Centre Munich) as published previously (Kespohl et al. 2017; Sillner et al. 2018). Mice were sacrificed via cervical translocation. Caecal luminal content was isolated, frozen in liquid nitrogen and stored at -80°C. To avoid bacterial metabolism, further steps were performed on dry ice, including cutting for weighting.

For bile acid isolation, 1 ml cold methanol containing 0.2 mg/l deuterated bile acids (Sigma Aldrich) as internal standard was added to 2 mg wet caecal content. For isolation of SCFAs, 1 ml cold methanol containing 10 ppm butyric acid-4,4,4-d3 (Sigma Aldrich) as internal standard was added to 20 mg wet caecal content to extract SCFA. The samples were homogenised in sterile ceramic bead tubes (NucleoSpin® Bead Tubes, Macherey-Nagel) using the Precellys® Evolution Homogenisator (Bertin Corp.; 4500 rpm, 40×3 sec, 2 sec pause time) and centrifuged (21,000 x g, 4°C, 10 min). The supernatants were stored at -80°C.

2.2.11.2 Quantification of bile acids via UHPLC-MS

The analysis of bile acids was performed in collaboration with Dr. A. Walker (Helmholtz Centre Munich) via mass spectrometry-coupled ultra-high-performance liquid chromatography (UHPLC-MS) as published previously (Sillner et al. 2018).
5 µl of the sample was transferred to an Acquity UHPLC system (Waters) and a UHPLC column (Acquity™ UPLC BEH™ C8, Waters). The column temperature was set to 60°C. Bile acids were eluted by performing a solvent system of 5 mM ammonium acetate and 0.1 % acetic acid in water (eluent A) and pure acetonitrile (eluent B) with a gradient profile as follows:

Eluent	**Time**
starting at 10 % eluent B	1 min
increasing to 22 % eluent B	within 2 min
increasing to 27 % eluent B	within 4 min
increasing to 95 % eluent B	within 13 min, hold for 2.5 min
returning to initial 10 % eluent B	within 2.5 min

The amaZon ETD Ion Trap (Bruker Daltonics GmbH) in negative ionisation mode was used for mass spectrometry.

2.2.11.3 Quantification of short chain fatty acids via UHPLC-MS

The analysis of short chain fatty was performed in collaboration with Dr. A. Walker (Helmholtz Centre Munich) via UHPLC-MS as published previously (Kespohl et al. 2017).

SCFA standards (Sigma Aldrich) together with butyric acid-4,4,4-d3 (Sigma Aldrich) were prepared in methanol to a final concentration of 100 ppm and used for the preparation of a calibration curve. Derivatisation of samples and standards was performed using the AMP + Mass Spectrometry Kit (Cayman Chemical) according to manufacturer's instructions. Samples were diluted 100-fold in water.

5 µl of the sample was transferred to an Acquity UHPLC system (Waters) and a UHPLC column (Acquity™ UPLC BEH™ C8, Waters). The column temperature was set to 30°C. SCFA were eluted by performing a solvent system of 5 mM ammonium acetate and 0.1 % acetic acid in water (eluent A) and pure acetonitrile (eluent B) with a gradient profile as follows:

Eluent	**Time**
starting at 1 % eluent B	1 min
increasing to 25 % eluent B	within 10 min
increasing to 95 % eluent B	within 7 min, hold for 2 min
returning to initial 1 % eluent B	within 0.2 min, hold for 2 min

The maXis (Bruker Daltonics GmbH) in positive electrospray ionisation mode was used for mass spectrometry.

2.2.12 Molecular biology methods

2.2.12.1 Total-RNA extraction from tissue

A guanidine isothiocyanate-phenol-chloroform-extraction is used to isolate RNA from homogenises tissue. Guanidine isothiocyanate, a chaotropic salt, leads to protein denaturation and inactivation. Phenol solves the proteins and partially DNA fragments. After phase separation, proteins accumulate in the organic phase, DNA in the organic and interphase whereas RNA is left in the aqueous layer. By addition of isopropanol to the aqueous part, the RNA precipitates and can be used for further applications.

After sacrificing, the large intestine of the mice was removed. Approximately 1 cm of the colon was cleared of faeces and opened longitudinally. The tissue was added to 1.0 ml Extrazol (Biolab Innovative Research Technologies) and stored at -80°C or used directly for homogenisation with the Ultra-Turrax (IKA) homogeniser. The fat

and cell debris were removed by centrifugation at (12,000 x g, 4°C, 10 min). The clear supernatant was transferred into a Biosphere® plus tube and incubated for 10 min at RT. After addition of 200 µl chloroform, the solution was mixed vigorously for 15 sec and incubated for 5 min at RT. The phases were separated by centrifugation (12,000 x g, 4°C, 15 min). The upper aqueous phase containing RNA was transferred into a fresh Biosphere® plus tube. RNA was precipitated by addition of 500 µl isopropanol and slowly inverting. After an incubation for 20 min at RT and centrifugation (12,000 x g, 4°C, 10 min), the supernatant was discarded and 800 µl 75 % Ethanol was added. The RNA was stored overnight at -20°C. Afterward, the samples were centrifuged (10,000 x g, 4°C, 10 min) and the supernatant was discarded. The RNA pellet was air dried for 5-10 min. For resuspension, 30 µl PCR-grade water was added and samples were incubated for 15 min at 58°C. The solved RNA was stored at -80°C.

2.2.12.2 Complementary DNA (cDNA) synthesis for quantitative PCR

To perform RT-qPCR the RNA transcripts must be translated into complementary DNA (cDNA). As the purity and integrity of the RNA is crucial for the following RT-qPCR, the RNA was treated with a DNase prior to cDNA synthesis to remove possible DNA contamination.

Therefore, the TURBO DNA-free™ Kit (invitrogen, Thermo Fisher Scientific) was used following the manufacturer's routine DNase treatment protocol. In short, 0.1 volume 10X TURBO DNase™ Buffer and 1.0 µl TURBO DNase™ were added to the ample and gently mixed. After incubation for 20 min at 37°C, 0.1 volume DNase Inactivation Reagent was added and mixed. Following incubation for 5 min at RT, samples were centrifuged (10,000 x g, 4°C, 1.5 min). The supernatant containing the treated RNA was transferred into a Biosphere® plus tube. The RNA concentration and quality were measured using NanoDrop system (Thermo Fisher Scientific).

The cDNA was synthesised from 500 ng RNA using the RevertAid First Strand cDNA Synthesis Kit (Thermo Fisher Scientific) following the manufacturer's instructions:

Component	Volume
template	500 ng
Oligo $(dt)^{18}$ primer	1.0 µl
5 x Reaction Buffer	4.0 µl
RiboLock RNase Inhibitor (20 U/µl)	1.0 µl
10 mM dNTP mix	2.0 µl
RevertAid M-MuLV RT (200 U/µL)	1.0 µl
PCR grade water	ad 20 µl

Reaction mix without RevertAid M-MuLV RT was used as a control for genomic DNA contamination. For cDNA synthesis, the reaction mix was incubated at 42°C for 60 min. The reaction was terminated by heating at 70°C for 5 min. For the following application the cDNA was 20-fold diluted in PCR-grade water.

2.2.12.3 Quantitative PCR of murine transcripts

As mentioned above, every PCR amplification cycle doubles the number of amplificated DNA molecules. After each cycle, the DNA amount can be detected by an intercalating fluorescent dye. The yield fluorescent signal increases directly proportional to the number of amplicons, meaning the more target DNA is in the sample, the earlier a fluorescent signal can be detected. To quantify the relative expression, the gene of interest is normalised to the housekeeping gene (ΔCt) and to the control condition (ΔΔCt).

The SYBR green-RT-qPCRs were run using the qPCR Core kit for SYBR® Green I (Eurogentec) with the following features:

Component	Volume
template	5.0 µl
10 x reaction buffer	5.0 µl
$MgCl_2$, 50 mM	3.5 µl
dNTP mix, 5 mM	2.0 µl
sense (5') primer, 10 pmol/µl	1.25 µl
antisense (3') primer, 10 pmol/µl	1.25 µl
SYBR green	1.5 µl
HotGoldStar PCR enzyme, 5 U/µl	0.25 µl
PCR grade water	ad 20 µl

Cycling Conditions	Temperature and time
1. polymerase activation	95°C, 10 min
2. denaturation	95°C, 15 sec
3. annealing, extension	60°C, 1 min
Repeats of steps 2-3	40 cycles

Samples were run in duplicates. Prior to measuring, the plate was centrifuged (1,000 rpm, RT, 1 min). The specificity of the amplicon was confirmed by melting curve analysis. To test for contamination, the amplification of controls for genomic DNA was evaluated and non-template control (PCR-grade water) was included in every run. Via ΔΔCt method the relative quantity of target DNA was quantified using glycerinaldehyd-3-phosphat-dehydrogenase (GapDH) as housekeeping gene.

2.2.13 Statistics

The data were analysed with GraphPad Prism 8 and are presented as mean ± standard deviation (SD). Significance was calculated by statistical tests indicated in the figure legends. P values less than 0.05 were considered as statistically significant.

3.1 *Lack of dietary cellulose does not affect physiological development*

'Westernised nutrition' is characterised by high fat and low dietary fibre intake. Both factors correlate with each other and promote certain diseases (Statovci et al. 2017). Cellulose is one of the most abundant fibres in grains, vegetables and fruit (Stephen et al. 2017). As it is assumed that dietary cellulose is an inert polymer, there is limited knowledge about its impact on cellular and molecular mechanisms.

To specifically investigate the physiological effects of cellulose, mice received purified diets which were identical except the ingredient cellulose. Control diet (CD) contained 7.0 % cellulose as the only source of dietary fibre, whereas the fibre free diet (FFD) was completely devoid of fibre. Mice kept on these diets showed no differences in weight development (Figure 4A) and food intake (Figure 4B) as well as litter size or fitness (data not shown). Although the intestinal transit time was significantly reduced in the FFD group (Figure 4C), no visible signs of diarrhea or constipation were observable in either group. Thus, both diets seem to be appropriate to study intervention with dietary cellulose.

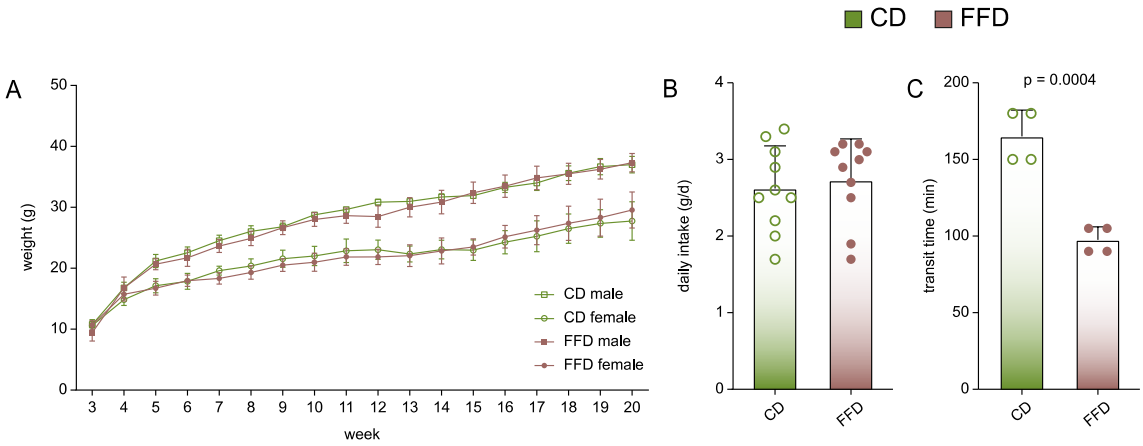

Figure 4. Influence of dietary cellulose on physiological parameters.

B6 mice received CD or FFD from birth. (A) Weight gain of mice after weaning (n = 5). (B) Repeated measurements of the food intake shown as gram per mouse and day (n = 6). (C) Intestinal transit time of fasted mice (n = 4). Statistical analysis: (A) two-way ANOVA and (B, C) unpaired, two-tailed Student's t test. Shown are individual values respectively means + SD. CD, control diet; FFD, fibre free diet.

3.2 Dietary cellulose is a potential substrate for microbial metabolism

The microbiome encompasses more than three million genes, thereby exceeding the human genome by 150-fold (Qin et al. 2010). It seems evident, that the intestinal microbiota has an enormous potential to metabolise substances, such as carbohydrates (El Kaoutari et al. 2013). To investigate whether cellulose serves as potential microbial substrate, we established an assay to determine cellulolytic enzyme activity. As cellulose is due to its physicochemical properties not suitable for enzymatic assays *in vitro*, we used the water-soluble subunit cellotetraose which consists of four glucose molecules. This cello-oligosaccharide was incubated with caecal supernatants containing bacterial enzymes and its cleavage products (cellotriose and cellobiose) were quantified by capillary electrophoresis- (CE-) and high-performance liquid chromatography-linked mass spectrometry (HPLC-MS).
As expected, increase of the degradation products cellotriose and cellobiose was found in native but not heat-inactivated supernatants of CD and FFD mice, suggesting that both dietary groups harboured cellulolytic enzymes (Figure 5A, B). Of note, cellotriose and cellobiose signals prior to incubation (0 hours) might be caused by traces of these metabolites in the cellotetraose standard.

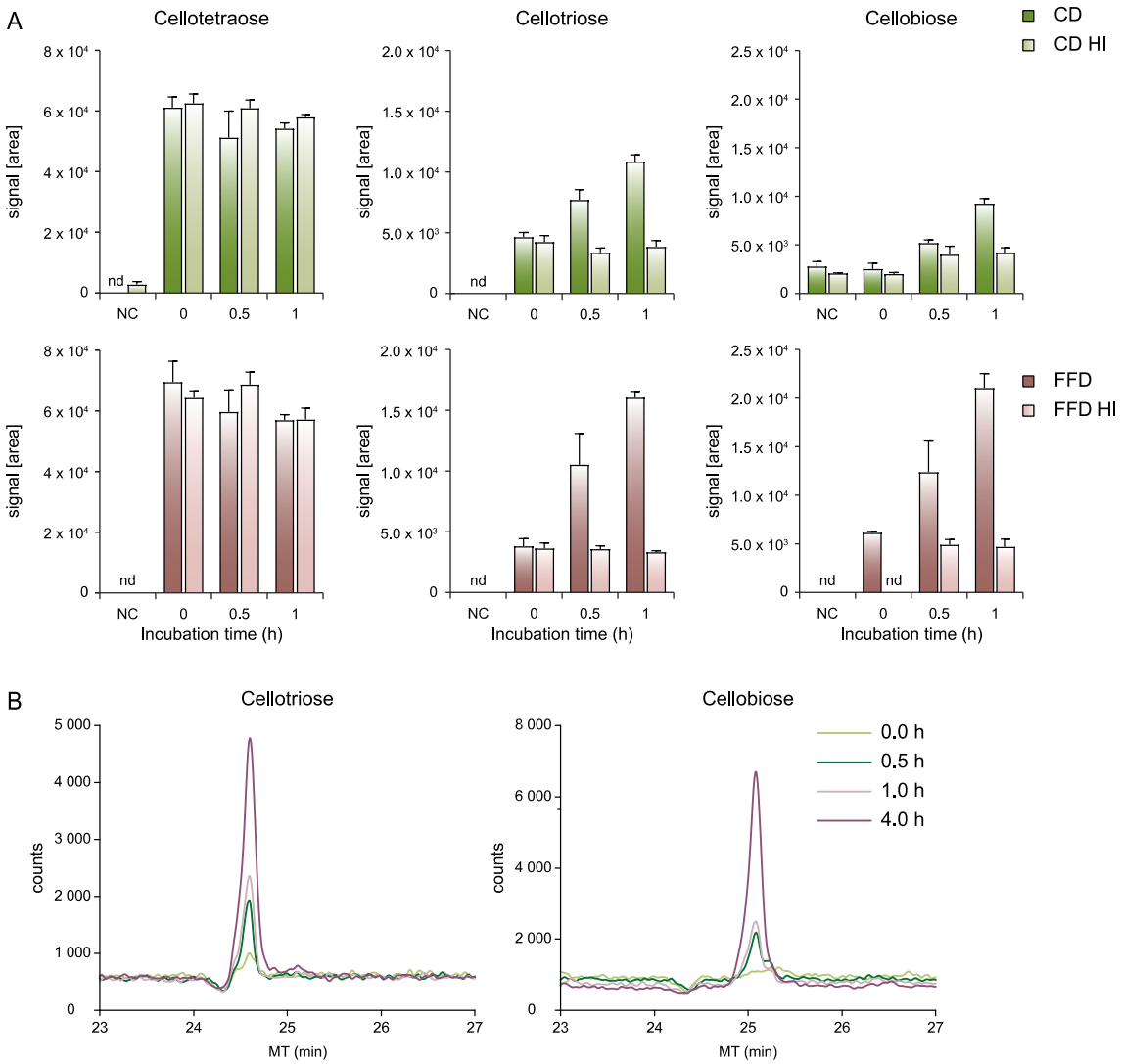

Figure 5. Cellulose as substrate for intestinal microbes.

Caecal supernatants were isolated from B6 mice receiving CD or FFD. (A) Native and heat-inactivated pooled supernatants from CD and FFD mice were incubated with cellotetraose for 30 and 60 min and analysed for degradation products via HPLC-MS in triplicates (n = 1). (B) Representative CE-MS electropherograms of cellotriose and cellobiose signals of supernatants from CD mice over time. Shown are means + SD. CD, control diet; FFD, fibre free diet; HI, heat inactivation.

3.3 Microbial maturation in early adulthood depends on dietary cellulose

Nutrient availability has a crucial impact on ecosystems, such as the intestinal microbiota (Maslowski and Mackay 2011). Since dietary cellulose was shown to be a potential substrate for intestinal bacteria, we asked for consequential effects on the microbial community. Therefore, a 16S rRNA gene amplicon analysis of the caecal microbiota of CD and FFD mice during early (week eight to twelve) and in advanced adulthood (week twenty-five) was performed.

Beta diversity analysis was performed by generalised UniFrac and is visualised by a multi-dimensional scaling (MDS) in which samples of similar microbial composition cluster together. In eight- and twelve-week old mice, diet as well as age significantly changed the caecal microbiota, as both factors led to a distinct clustering of the samples (Figure 6A). While diet-dependent differences persisted also beyond the age of twelve weeks, the clustering was less distinct with respect to age (Figure 6B) indicating that microbial diversity was rather completed at week twelve.

The diversity of the intestinal microbiota expands very fast in the first weeks and months of life and continued to increase until adulthood (Pantoja-Feliciano et al. 2013; Odamaki et al. 2016). In our model, a physiological microbial diversification occurred exclusively in the presence of dietary cellulose (Figure 6C, D). Additionally, the Firmicutes/Bacteroidetes ratio indicating microbiota maturation (Mariat et al. 2009) did not increase in the absence of cellulose (Figure 6E). This differences in microbial composition between CD and FFD mice were visible even later in life (Figure 6F). In summary, these data suggest that dietary cellulose drives the maturation of the intestinal microbiota.

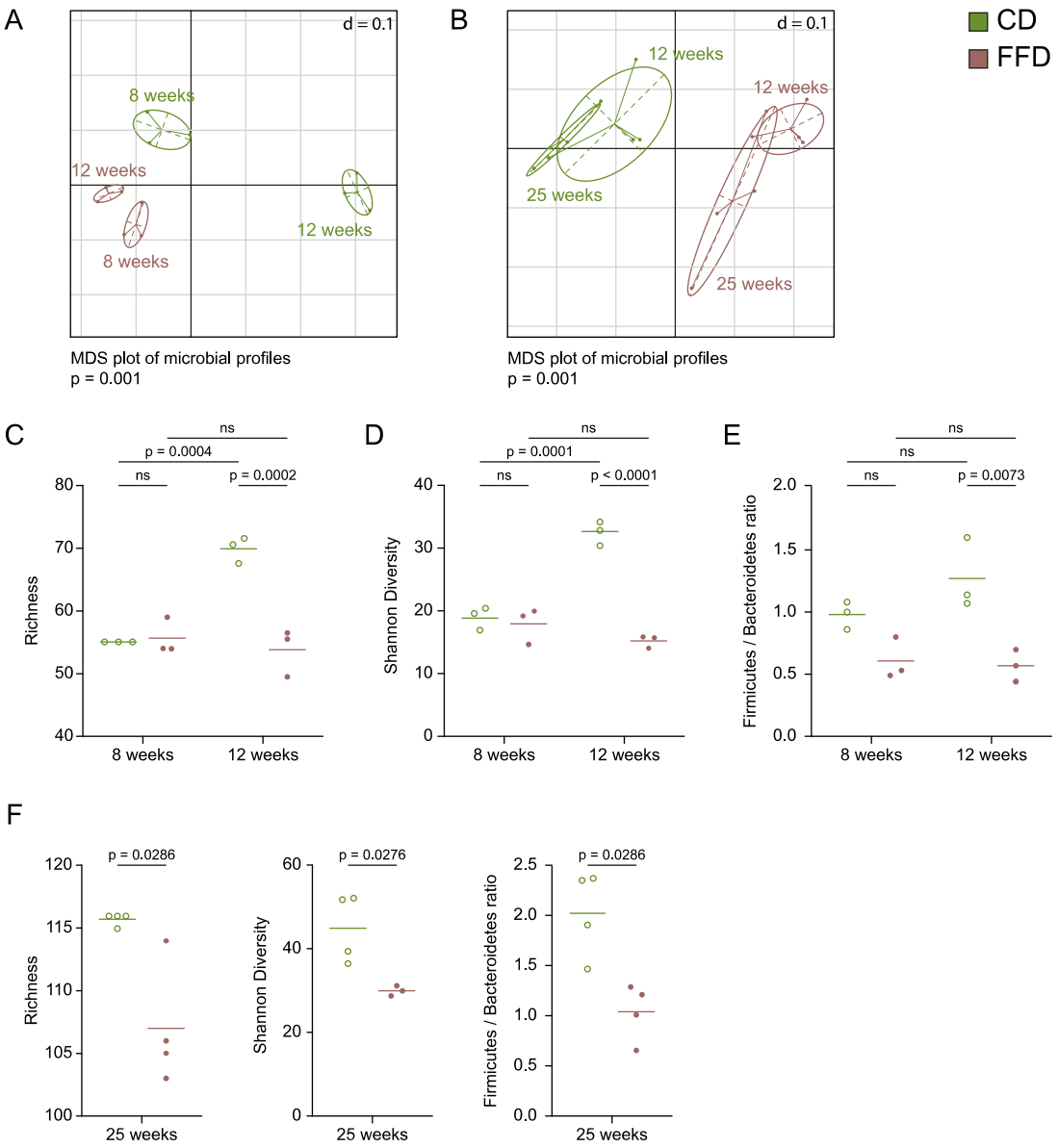

Figure 6. The influence of dietary cellulose on the intestinal microbial development.

Caecal samples isolated from B6 mice at the age of eight- and twelve-weeks (young adulthood) as well as twenty-five-weeks (advanced adulthood) receiving CD or FFD from birth were analysed via 16S rRNA gene amplicon analysis. (A, B) Multi-dimensional scaling (MDS) plot based on generalised UniFrac (n = 3-4). (C, D) Richness and Shannon diversity as well as (E) Firmicutes/Bacteroidetes ratio of the microbiota of young adult mice (n = 3). (F) Richness, Shannon diversity and Firmicutes/Bacteroidetes ratio of the microbiota in advanced adulthood (n = 4). Statistical analysis: (A, B) non-parametric, multivariate analysis of variance (Rhea), (C-E) one-way ANOVA (corrected for multiple comparison by Sidak method) and (F) unpaired, two-tailed Student's t test. Shown are individual values and means representing one of two similar experiments. CD, control diet; FFD, fibre free diet; ns, non-significant.

We further addressed the taxonomic changes in CD and FFD mice during early adulthood. Yet, 16S rRNA sequencing revealed that the abundance profiles of bacterial communities were altered at the level of phyla (Figure 7A). In eight-week-old CD mice, Bacteroidetes, Firmicutes and Verrucomicrobia contributed quite equal to the microbiota, whereas the microbiota of FFD mice was dominated by Bacteroidetes. In aged CD mice, the abundance of Verrucomicrobia decreased and Firmicutes and Bacteroidetes increased. The opposite was seen in the twelve-week-old FFD group, where Firmicutes decreased and Verrucomicrobia increased.

The analysis of relative abundances at lower taxonomic levels demonstrated that many bacterial families and genera were significantly affected by dietary cellulose. We found a higher abundance of the families *Verrucomicrobiacaea*, *Porphyromonadaceae* and *Bacteroidacea* and a lower abundance of *Lachnospiraceae*, *Ruminococcaceae* and *Desulfovibrionaceae* in the FFD group at week twelve of age in comparison to mice that received cellulose (Figure 7B). Especially *Rikenellaceae* were substantially reduced in the absence of cellulose, which resulted from the deterioration of the genus *Alistipes* (Figure 7C).

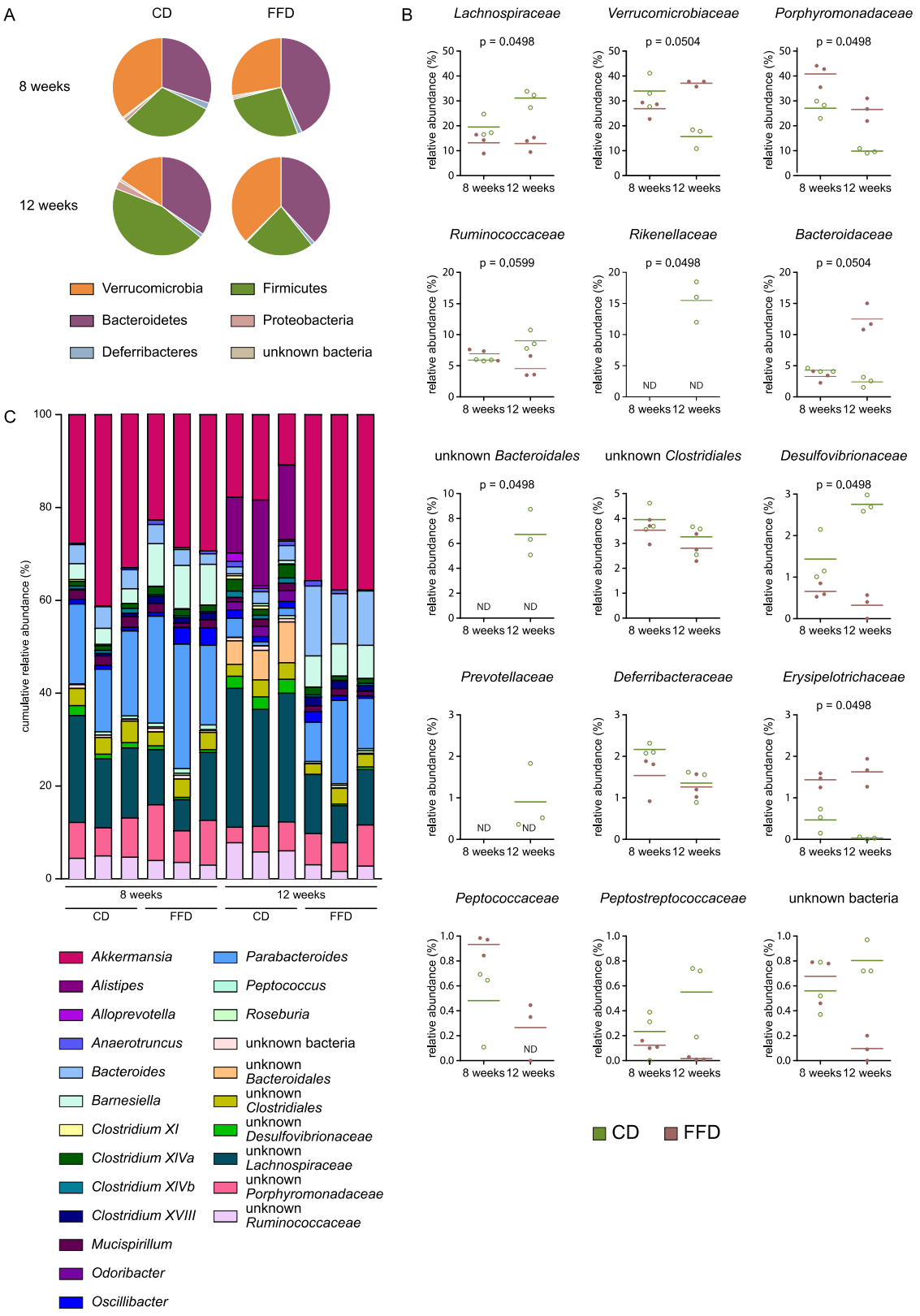

Figure 7. Cellulose-dependent alterations of the intestinal microbial composition.

Caecal samples isolated from eight- and twelve-week old B6 mice receiving CD or FFD from birth were analysed via 16S rRNA gene amplicon analysis. The composition of the entire intestinal microbiota is plotted at (A) phyla, (B) family and (C) genera level (n = 3). Statistical analysis: (B) Kruskal-Wallis Rank Sum test for all groups (corrected for multiple comparison by Benjamini-Hochberg method, Rhea). Shown are individual values and means representing one of two similar experiments. CD, control diet; FFD, fibre free diet.

3.4 Dietary cellulose shapes the intestinal metabolome

The intestinal microbiota not only utilises various substrates, but also produces a broad range of metabolites, including SCFAs and bile acids (Nicholson et al. 2012). Since we found a significant shift of the intestinal microbial community in the absence of dietary cellulose, we wondered whether this is reflected by an altered metabolome.

Although many dietary fibres are known to promote SCFA production Peng et al. (2013), we found no differences between CD and FFD mice (Figure 8A). Further, SCFAs were not detectable in germ-free mice independent of CD or FFD.

By contrast, bile acids were highly affected. The amounts of primary bile acids were elevated in germ-free mice kept on FFD as compared to those kept on CD. However, they did not differ in specific pathogen free (SPF) animals (Figure 8B), indicating a bacteria-independent mechanism. Comparing bile acids which derive from bacterial conversion, the primary unconjugated bile acid UDCA and the secondary bile acids DCA and 3-dehydroCDCA were significantly increased in SPF FFD mice (Figure 8C, D). Overall, these findings suggest, that cellulose influences the metabolism of primary and secondary bile acids directly as well as in a microbiota-dependent manner.

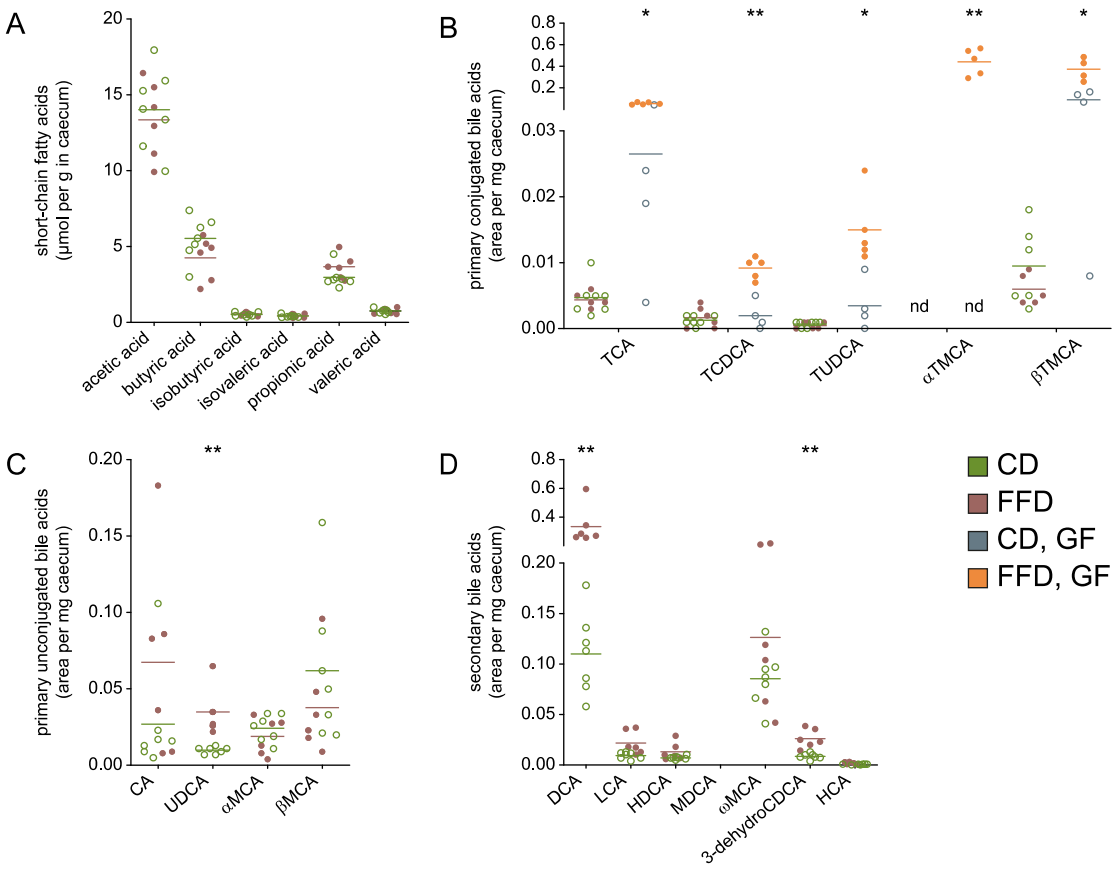

Figure 8. The influence of dietary cellulose on the bacterial metabolome.

Caecal samples were isolated from SPF and germ-free B6 mice receiving either CD or FFD from birth (SPF) or four weeks prior to analysis (germ-free). (A) Short chain fatty acids, (B) primary conjugated, (C) unconjugated and (D) secondary bile acids were measured via UHPLC-MS (n = 4-6). Statistical analysis: (A-D) non-parametric, unpaired, two-tailed Student's t test (corrected for multiple comparison by Sidak-Holm method). Shown are individual values and means representing one of two similar experiments. *p < 0.05, **p < 0.01 and ***p < 0.001. CD, control diet; FFD, fibre free diet; GF, germ-free; TCA, taurocholic acid; TCDCA, taurochenodeoxycholic acid; TUDCA, tauroursodeoxycholic acid; αTMCA, α-tauromuricholic acid; βTMCA, β-tauromuricholic acid; CA, cholic acid; UDCA, ursodeoxycholic acid; αMCA, α-muricholic acid; βMCA, β-muricholic acid; DCA, deoxycholic acid; LCA, lithocholic acid; HDCA, hyodeoxycholic acid; MDCA, murideoxycholic acid; ωMCA, ω-muricholic acid; 3-dehydroCA, 3-dehydrocholic acid; HCA, hyocholic acid.

3.5 Cellulose deprivation alters the intestinal immune status

The interaction between the microbiota and the host organism is constantly monitored by the immune system, i.e. alterations of the microbiota can influence the host's immune system and *vice versa* (Wang et al. 2019a). Since the data shown above revealed multiple cellulose-dependent alterations of the intestinal microbiota, we speculated that this has also an impact on the intestinal immune system. To investigate this, lymphocytes isolated from the intestinal lamina propria (ileum and colon) as well as peripheral lymphoid organs (mesenteric lymph nodes and spleen) were analysed for their cytokine production and transcription factors via flow cytometry.

The absolute number of lymphocytes isolated from the ileum and colon was comparable between CD and FFD mice (Figure 9A). However, the frequency of ileal $CD4^+$ T cells was significantly increased in the absence of cellulose (Figure 9B). As $CD4^+$ T cells are guardians of intestinal homeostasis, their phenotype was investigated. While no alteration of IFN-γ- and IL-4-producing $CD4^+$ T cells were observed, frequencies of IL-17-producing $CD4^+$ T cells were significantly enhanced in the ileum of FFD mice (Figure 9C, D). The same tendency was seen in the colon, but no alterations were found in secondary lymphoid organs. IL-17-producing $CD4^+$ T cells express the transcription factors RORγt and a smaller fraction also expresses the transcription factor FOXP3. Hence, we asked, which of these $CD4^+$ T cell subsets account for the observed enrichment of IL-17-producing cells. Indeed, the frequencies of both $ROR\gamma t^+$ $FOXP3^-$ (TH17 cells) and $ROR\gamma t^+$ $FOXP3^+$ $CD4^+$ T cells ($TH17_{reg}$ cells) were significantly increased during fibre deprivation (Figure 9E, F). Interestingly, the frequency of $ROR\gamma t^-$ $FOXP3^+$ $CD4^+$ T cell, which are conventional regulatory T cells (T_{reg} cells), and the amount of sIgA were not affected by cellulose (Figure 9E-G).

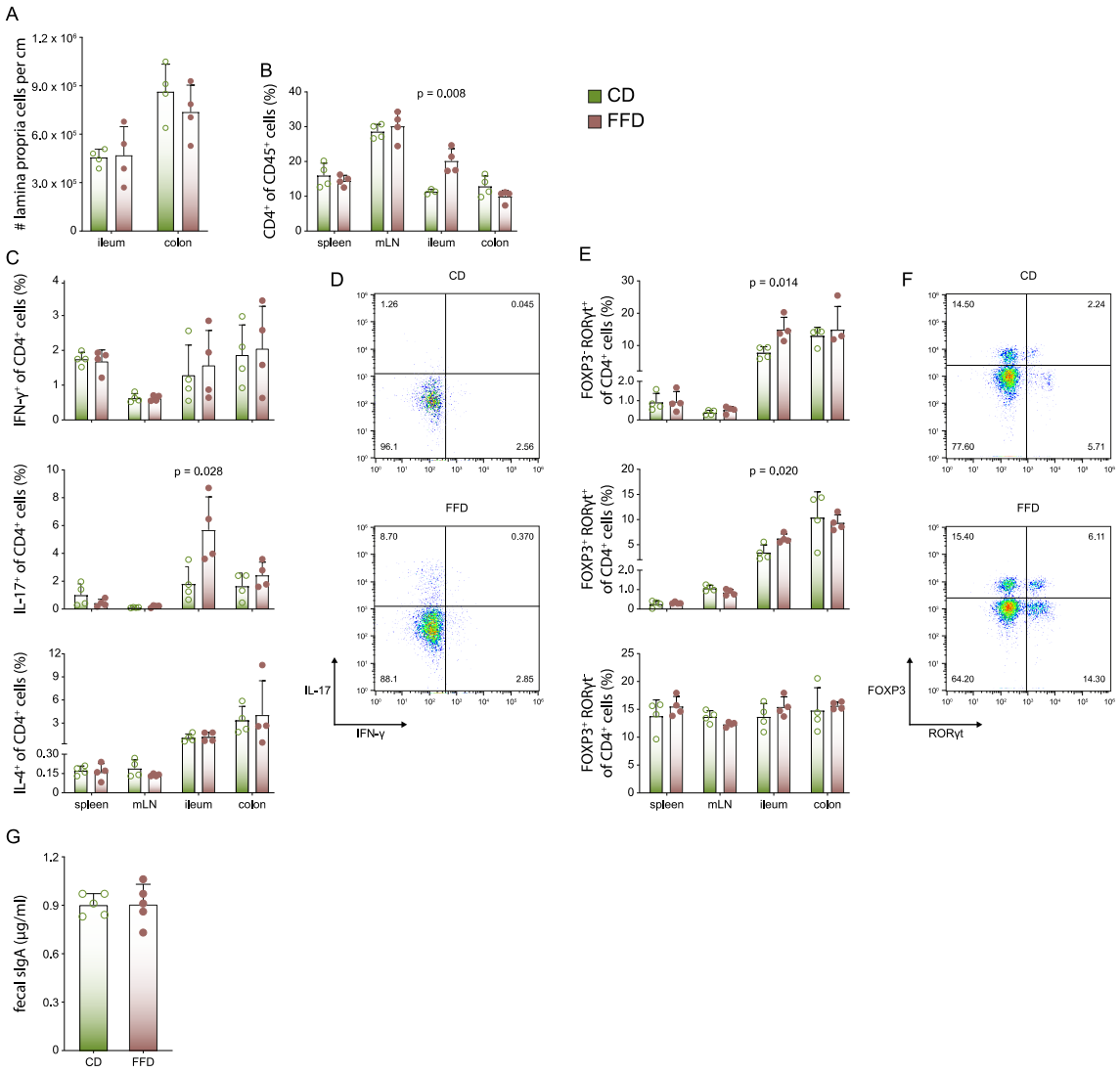

Figure 9. The intestinal immune system in fibre deprivation.

Lymphocytes from indicated organs as well as faecal samples were isolated from B6 mice receiving CD or FFD from birth. (A) The absolute cell number of lymphocytes. (B) The frequency of CD4+ T cells in lymphoid organs and the intestine. (C) IFN-γ-, IL-4- and IL-17-production of CD4+ T cells was measured after restimulation with PMA and ionomycin via FACS (n = 4). (D) A representative FACS plot shows the IFN-γ- and IL-17-expression of ileal CD4+ T cells. (E) CD4+ T cells were analysed for the transcription factors RORγt and FOXP3 via FACS (n = 4). (F) The FACS plot shows a representative staining for RORγt and FOXP3 of ileal CD4+ T cells. (G) Faecal sIgA levels were measured by ELISA (n = 5). Statistical analysis: non-parametric, unpaired, two-tailed Student's t test. Shown are individual values respectively means + SD representing one of two similar experiments. CD, control diet; FFD, fibre free diet; mLN, mesenteric lymph node; sIgA, secretory IgA.

3.6 Epithelial gene expression is affected by dietary cellulose

The intestinal epithelium is more than a passive barrier composed of absorptive enterocytes. It harbours rather various specialised cell types, which produce factors that promote the segregation between host and microbes, including mucins and antimicrobial peptides (Allaire et al. 2018). To investigate the influence of cellulose on the colonic expression of epithelial genes involved in the intestinal homeostasis, we performed RT-qPCR of colonic tissue samples from FFD and CD mice.

We found that cellulose has no influence on the expression of trefoil factor 3 (TFF3), mucins, tight junction proteins and the proliferation marker Ki76. However, the expression of the antimicrobial C-type lectin Reg3γ was massively decreased in the absence of fibre (Figure 10) demonstrating that cellulose deprivation has a selective but clear influence on gene expression of IECs.

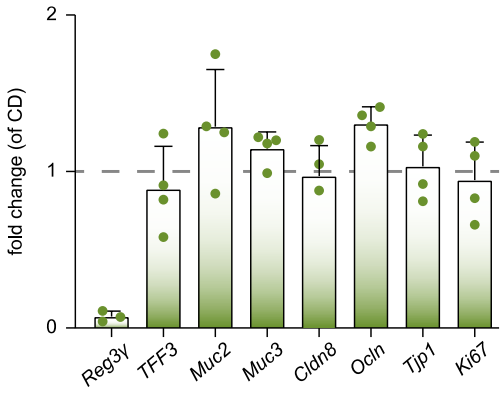

Figure 10. Influence of cellulose on epithelial gene expression related to intestinal homeostasis.

B6 mice received CD or FFD from birth. The expression of genes involved in intestinal homeostasis in the total colonic tissue of FFD mice was measured by RT-qPCR and normalised to CD mice (n = 3-4). Shown are individual values respectively means + SD representing one of two similar experiments. CD, control diet; FFD, fibre free diet; Reg3γ, regenerating islet-derived protein 3γ; TFF3, trefoil factor 3; Muc, mucin; Cldn8, claudin 8; Ocln, occludin; Tjp1, tight junction protein 1; Ki67, proliferation marker protein Ki-67.

3.7 Dietary cellulose ameliorates DSS-induced colitis

The interaction of the gut microbiota with intestinal epithelium and the mucosal immune system is required for the maintenance of the gut barrier integrity by defending against pathogens while tolerating commensal microbes. Disturbance of this homeostasis often leads to infection or inflammation (Belkaid and Harrison 2017). As we found an altered immune status and signs of dysbiosis in FFD mice, we wondered whether cellulose deprivation disrupts the intestinal homeostasis and examined functional consequences in the DSS-induced model of acute colitis, which is based on a chemical disruption of the intestinal epithelium. Subsequently, microbes and luminal antigens enter the host tissue and induce an inflammatory immune response in the lamina propria (Wirtz et al. 2007; Eichele and Kharbanda 2017).

CD and FFD mice were treated with 1.5 % or 2.5 % DSS for five days. A low concentration of DSS (1.5 %) was sufficient to induce significant weight loss, decrease of colon length, diarrhea as well as increased amounts of TNFα and lipocalin-2 in *ex vivo* colon cultures of FFD mice (Figure 11A-D). Treatment with 2.5 % DSS led to even more severe colitis in FFD mice. PAS staining of colonic tissue from these mice revealed the loss of the crypt structure, epithelial damage, excessive production of mucus and infiltration of immune cells (Figure 11E). At the macroscopic level, the intestines of DSS-treated FFD mice were reduced in length and thinner in comparison to CD mice (Figure 11F). In summary, these data suggest that dietary cellulose protects mice from DSS-induced acute colitis.

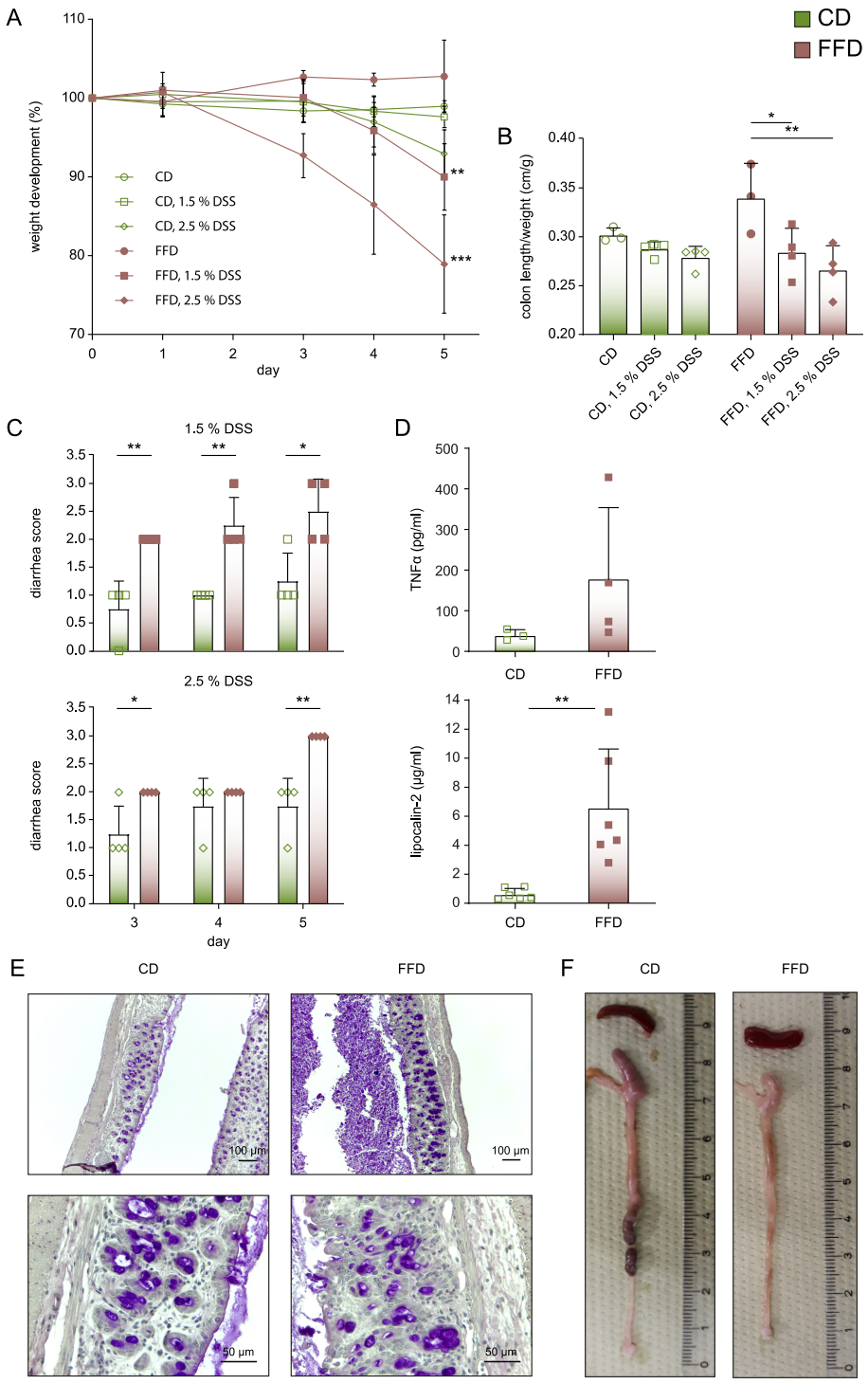

Figure 11. Dietary cellulose ameliorates DSS-induced colitis.

B6 mice received CD or FFD from birth and were treated with 1.5 % or 2.5 % DSS for five days. (A) Weight loss, (B) colon length and (C) diarrhea score were measured to quantify inflammation (n = 3-4). (D) The expression of TNFα and lipocalin-2 in *ex vivo* colon cultures were measured by ELISA (n = 3-6). The colitis induced by 2.5 % DSS was further confirmed by (E) histological (PAS staining) analysis of the colon and (F) macroscopic assessment of the colon and spleen (n = 3-4). Statistical analysis: (A) one-way ANOVA of weight loss at day five in comparison to untreated group and (B) one-way ANOVA in comparison to untreated group (corrected for multiple comparison by Sidak method), (C) non-parametric, unpaired, two-tailed Student's t test (corrected for multiple comparison by Sidak-Holm method) and (D) Mann-Whitney test. Shown are individual values respectively means + SD representing one of two similar experiments. *$p < 0.05$, **$p < 0.01$ and ***$p < 0.001$. CD, control diet; FFD, fibre free diet; DSS, dextran sulphate sodium.

3.8 *Alistipes finegoldii 17242 has a unique cellulose metabolism*

As shown above, fibre deprivation affected the gut microbiota and immune system leading to enhanced colitis susceptibility. With respect to the microbiota, the massive reduction of the genus *Alistipes* was prominent in FFD mice. Thus, we wondered whether a representative member of this genus, *Alistipes finegoldii* 17242 (*A. finegoldii*), is able to trigger beneficial effects if transferred to a recipient animal. To trace a single bacterium in immune-competent mice, the gnotobiotic OMM^{12} mouse model, which harbours a microbiota consisting of twelve predominant members of the murine intestinal microbiota, was used (Brugiroux et al. 2016). A single association of *A. finegoldii* was sufficient to stably colonise these animals without disrupting the former microbial composition, as revealed by FISH- (Figure 12A) and RT-qPCR analysis (Figure 12B). Furthermore, *A. finegoldii* was exclusively detectable in the caecum and colon, but not in the ileum of the mice which might be due to its anaerobic nature.

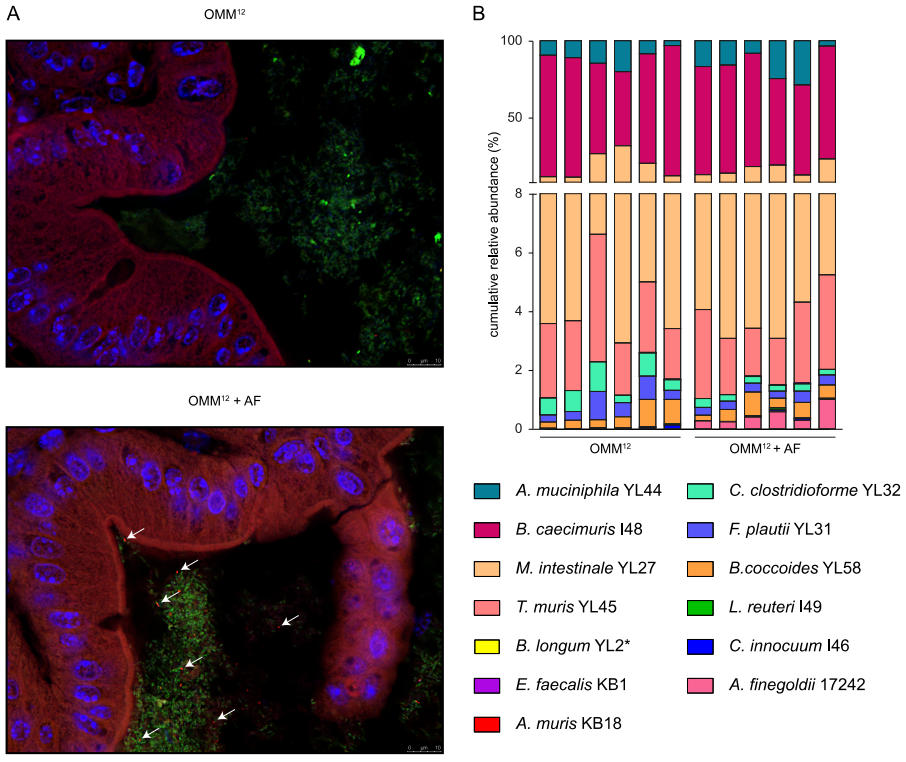

Figure 12. *A. finegoldii* 17242 stably colonises the OMM^{12} microbiota.

OMM^{12} B6 mice were associated with *A. finegoldii* 17242 three weeks prior to analysis. (A) The presence of *A. finegoldii* 17242 (white arrows) in the caecum was analysed by FISH. Blue, DAPI; green, all bacteria; red, *A. finegoldii* 17242 (n = 3-4). (B) The relative abundance of the OMM^{12} bacteria and *A. finegoldii* 17242 in the caecum was measured by RT-qPCR (n = 6). OMM^{12}, Oligo-Mouse-Microbiota 12; AF, *Alistipes finegoldii* 17242.

A comparative genome analysis with EDGAR (Blom et al. 2009) was performed to investigate the molecular characteristics of *A. finegoldii* within this model microbiota. The analysis showed that *B. caecimuris* I48 and *M. intestinale* YL27, which also belong to the phyla Bacteroidetes, are the evolutionarily closest relatives of *A. finegoldii* within the consortium (Figure 13A). Furthermore, of the 30,800 genes forming the metagenome of OMM^{12} and *A. finegoldii*, 1,653 genes were exclusively found in *A. finegoldii* and further named as singletons.

By using the EggNOG 4.5.1. software (Huerta-Cepas et al. 2016) 862 singletons were classified into clusters of orthologous genes (COGs). 376 of them were of unknown function (cluster S). The classification of the remaining 486 genes is shown in Figure 13B. We found that *A. finegoldii* harbours unique metabolic properties according to the metabolism of the cell wall and membrane (M), genetic information processing (K, L) and carbohydrate metabolism (G).

A KofamKoala analysis (Aramaki et al. 2019) was performed to investigate the potential to degrade complex carbohydrates. Hereby, singletons were assigned to K numbers (KEGG orthology identifiers) which link sequences to KEGG pathways and enzymes. Interestingly, two genes (ALFI_RS05325, ALFI_RS07785) were assigned as K01179, an endoglucanase (3.2.1.4), and two genes (ALFI_RS05270, ALFI_RS07880) were assigned to K05349, a beta-glucosidase (3.2.1.21). Both identifiers are linked to cellulose degradation, suggesting an exclusive pathway of *A. finegoldii* within the OMM^{12} consortium to deal with cellulose (Figure 13C).

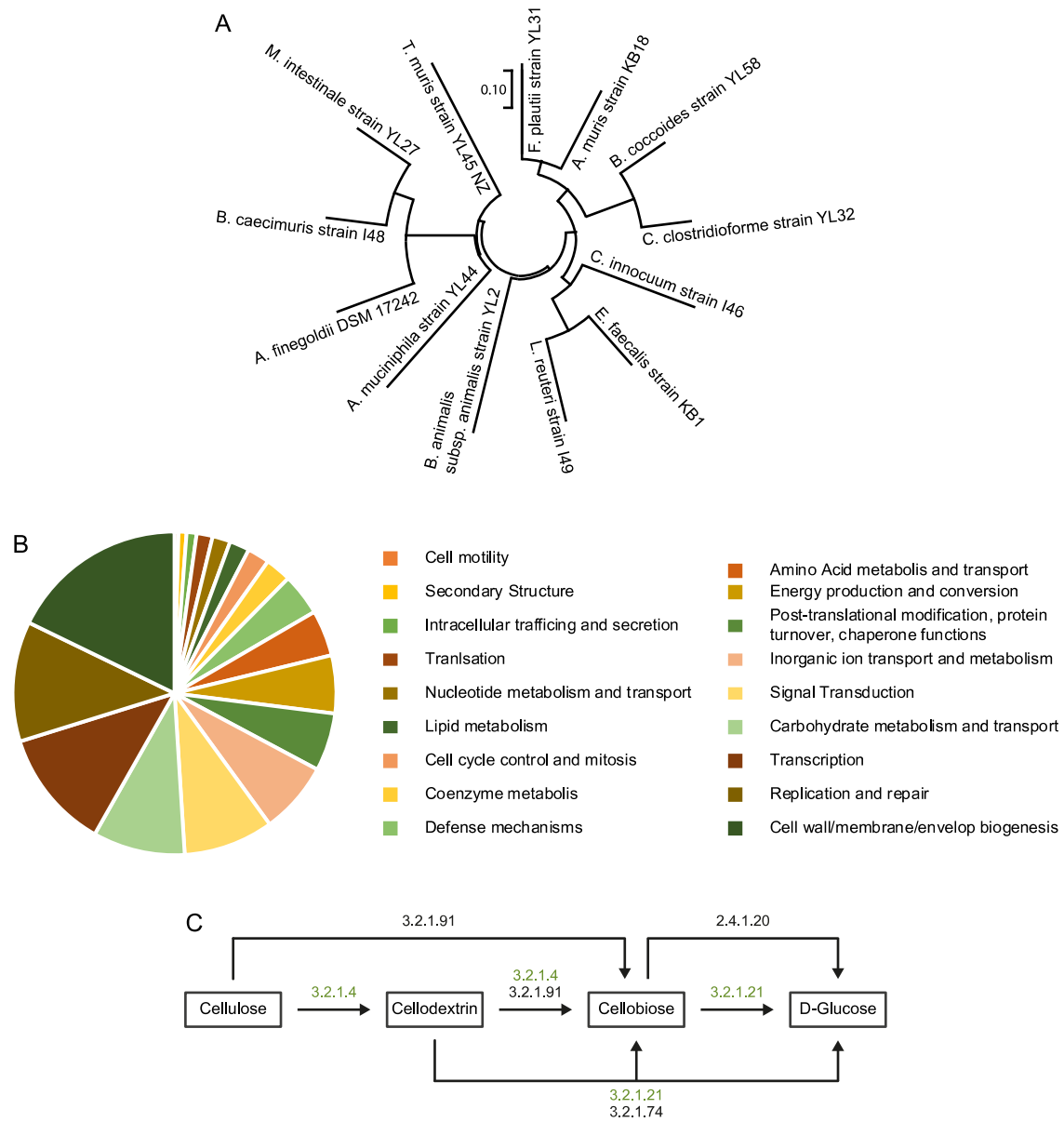

Figure 13. *A. finegoldii* 17242 has a unique cellulose metabolism.

The comparative genome analysis of *A. finegoldii* and the OMM[12] bacteria was performed using EDGAR. (A) The phylogenetic tree shows the relation of *A. finegoldii* within the OMM[12] consortium. (B) CAS classification of singletons exclusively found in *A. finegoldii.* (C) Selected singletons assigned to KEGG orthology identifiers of the cellulose-degrading pathway are highlighted in green.

In order to test the cellulose-degrading potential *in vitro*, the cellotetraose assay was performed using caecal supernatants of *A. finegoldii*-associated and control OMM[12] mice. The data showed a significant decrease of cellotetraose and an increase of cellotriose in both groups (Figure 14). This suggests that both microbiota harbour enzymes to degrade cellulose, however, *A. finegoldii* might be endowed with a unique pathway in comparison to the OMM[12] consortium.

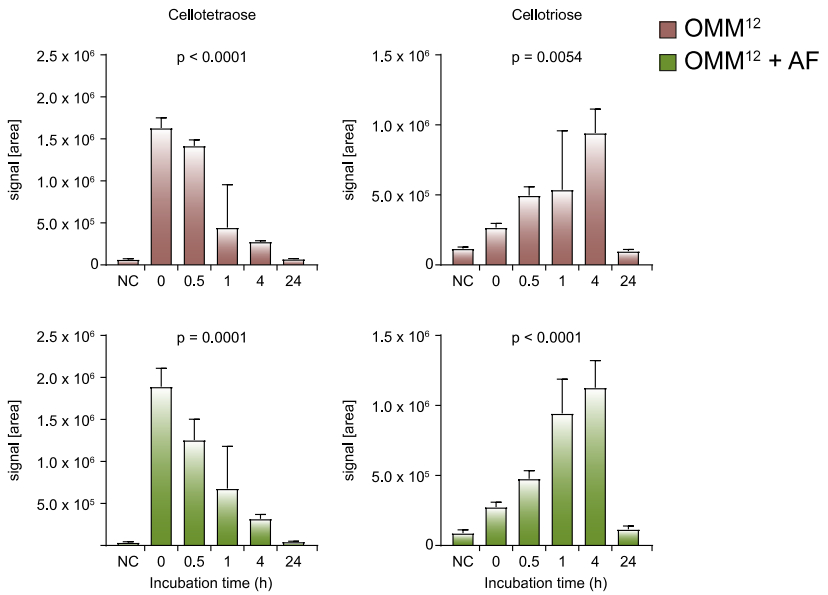

Figure 14. The OMM[12] consortium harbours enzymes to degrade cellulose.

OMM[12] B6 mice were associated with *A. finegoldii* 17242 three weeks prior to analysis. Pooled supernatants were incubated with cellotetraose for 0.5, 1, 4 and 24 hours and measured in triplicates via HPLC-MS (n = 3-4). Statistical analysis: one-way ANOVA. Shown are means + SD. OMM[12], Oligo-Mouse-Microbiota 12; AF, *Alistipes finegoldii* 17242.

3.9 Alistipes finegoldii 17242 induces an immune response

Individual bacteria are able to influence physiological processes of the host, including immune functions (Ivanov et al. 2009; Nakamoto et al. 2017). Thus, the possibility that cellulose-dependent *A. finegoldii* exerts immunomodulatory actions and mimics the effects of dietary cellulose was examined.

Lymphocytes isolated from the intestinal lamina propria (ileum and colon) and peripheral lymphoid organs (mesenteric lymph nodes and spleen) of *A. finegoldii*-associated and control OMM[12] mice were analysed for cytokines and transcription factors via FACS. No differences were found in the overall number of lymphocytes in the intestinal lamina propria and the frequencies of $CD4^+$ T cells in the analysed organs (Figure 15A, B). However, *A. finegoldii* induced IL-17^+-producing $CD4^+$ T cells in lymphatic organs, the ileum and to some degree also in the colon (Figure 15C, D). This was confirmed by elevated frequencies of TH17 cells ($ROR\gamma^+$ $FOXP3^-$ $CD4^+$ T cells) in these organs, except for the ileum (Figure 15E, F). The frequencies of IL-17^+ IFN-γ^+ and IL-17^- IFN-γ^+-producing $CD4^+$ T cells, $TH17_{reg}$ cells ($ROR\gamma^+$ $FOXP3^+$ $CD4^+$ T cells) and T_{reg} cells ($ROR\gamma^-$ $FOXP3^+$ $CD4^+$ T cells) were not affected (Figure 15C-F). In summary, *A. finegoldii* affected the immune system in several ways, which only partially overlapped with the effects caused by cellulose.

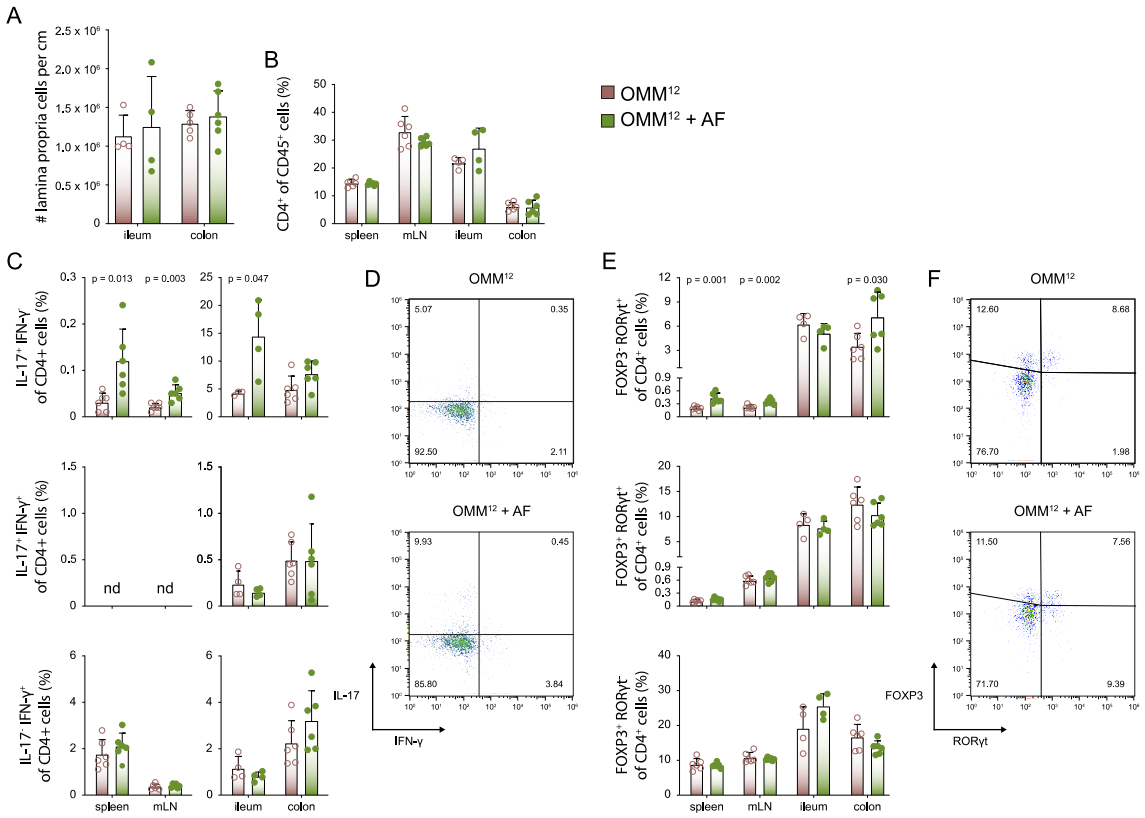

Figure 15. *A. finegoldii* 17242 impacts the intestinal immune system.

Lymphocytes from indicated organs were isolated from OMM^{12} B6 mice and OMM^{12} B6 mice associated with *A. finegoldii* 17242 three weeks prior to analysis. (A) The absolute cell number of lymphocytes. (B) The frequency of CD4$^+$ T cells in lymphoid organs and the intestine (n = 4-6). (B) The frequency of CD4$^+$ T cells (n = 4-6). (C) IL-17- and IFN-γ production of CD4$^+$ T cells was measured after restimulation with PMA and ionomycin via FACS (n = 4-6). (D) A representative FACS plot shows the IFN-γ- and IL-17-expression of colonic CD4$^+$ T cells. (E) CD4$^+$ T cells were analysed for the transcription factors RORγt and FOXP3 (n = 4-6). (F) The FACS plot shows a representative staining for RORγt and FOXP3 of colonic CD4$^+$ T cells. Statistical analysis: non-parametric, unpaired, two-tailed Student's t test. Shown are individual values respectively means + SD representing one of two similar experiments. OMM^{12}, Oligo-Mouse-Microbiota 12; AF, *Alistipes finegoldii* 17242; mLN, mesenteric lymph node; RORγt, retinoic acid receptor-related orphan receptor γt; FOXP3, forkhead-box-protein 3.

As *A. finegoldii* induced a systemic and local TH17 immune response, the secretion of cytokines as markers for inflammation was examined in *ex vivo* colon cultures of *A. finegoldii*-associated and control OMM^{12} mice via multiplex immunoassay and ELISA. TH17 cytokine concentrations were not significantly altered, except for IL-22, which was strongly increased in the presence of *A. finegoldii* (Figure 16A). In addition, lipocalin-2 showed no differences between both groups which indicated that *A. finegoldii* did not cause inflammatory immune responses in the colon (Figure 16B).

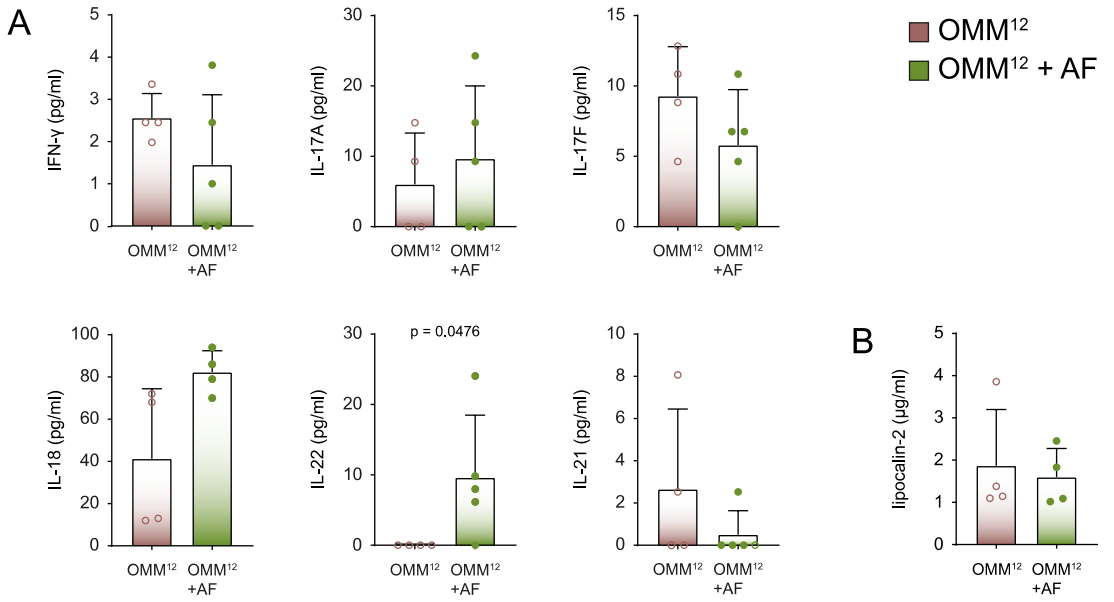

Figure 16. *A. finegoldii* 17242 impacts the intestinal cytokine profile.

OMM12 B6 mice were associated with *A. finegoldii* three weeks prior to analysis. The secretion of cytokines and lipocalin-2 in *ex vivo* colon cultures were measured by ELISA and Legendplex™ (n = 3-6). Statistical analysis: Mann-Whitney test. Shown are individual values respectively means + SD representing one of two similar experiments. OMM12, Oligo-Mouse-Microbiota 12; AF, *Alistipes finegoldii* 17242.

3.10 Alistipes finegoldii 17242 promotes Reg3γ expression

Since the intestinal epithelium represents an interphase between the host and the microbiota which is able to sense soluble as well structural components of bacteria, we wondered whether *A. finegoldii* influences the expression of epithelial genes. We compared the expression of selected genes involved in homeostasis in OMM12 mice in the presence or absence of *A. finegoldii* by RT-qPCR.

We found no substantial influence on TFF3, mucins, tight junction proteins and proliferation markers. However, the colonic expression of the antimicrobial protein Reg3γ was particularly elevated in the presence of *A. finegoldii* 17242 (Figure 17).

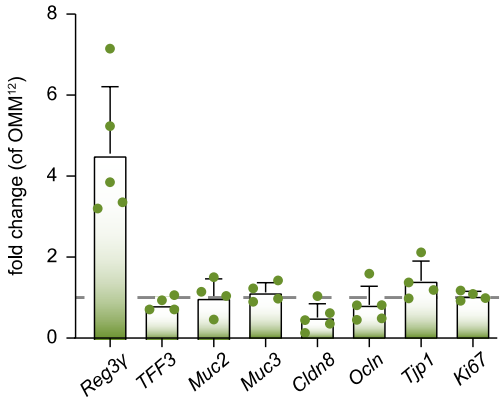

Figure 17. Influence of *A. finegoldii* 17242 on colonic gene expression.

OMM^{12} B6 mice were associated with *A. finegoldii* three weeks prior to analysis. The expression of genes involved in the intestinal homeostasis in the total colonic tissue of *A. finegoldii*-associated OMM^{12} mice was measured by RT-qPCR and normalised to OMM^{12} mice (n = 4-5). Shown are individual values respectively means + SD representing one of two similar experiments. OMM^{12}, Oligo-Mouse-Microbiota 12; Reg3γ, regenerating islet-derived protein 3γ; TFF3, trefoil factor 3; Muc2/3, mucin 2/3; Cldn8, claudin 8; Ocln, occludin; Tjp1, tight junction protein 1; Ki67, proliferation marker protein Ki-67.

3.11 Alistipes finegoldii 17242 ameliorates DSS-induced colitis

From the results presented above, we assumed that *A. finegoldii* 17242 might improve the intestinal homeostasis. To test potential anti-colitogenic effects of this bacterium, we exposed *A. finegoldii*-associated and control OMM^{12} mice to 3.5 % DSS.

Mice associated with *A. finegoldii* showed significantly lower weight loss, decrease of the colon length, lipocalin-2 and TNFα levels in *ex vivo* colon cultures (Figure 18A-C). Further, PAS staining of colonic tissue evidenced just mild signs of colitis in this group, including a slightly lower mucus production, less epithelial damage and tissue thickening (Figure 18D). These findings revealed that *A. finegoldii* ameliorates DSS-induced acute colitis in gnotobiotic OMM^{12} mice.

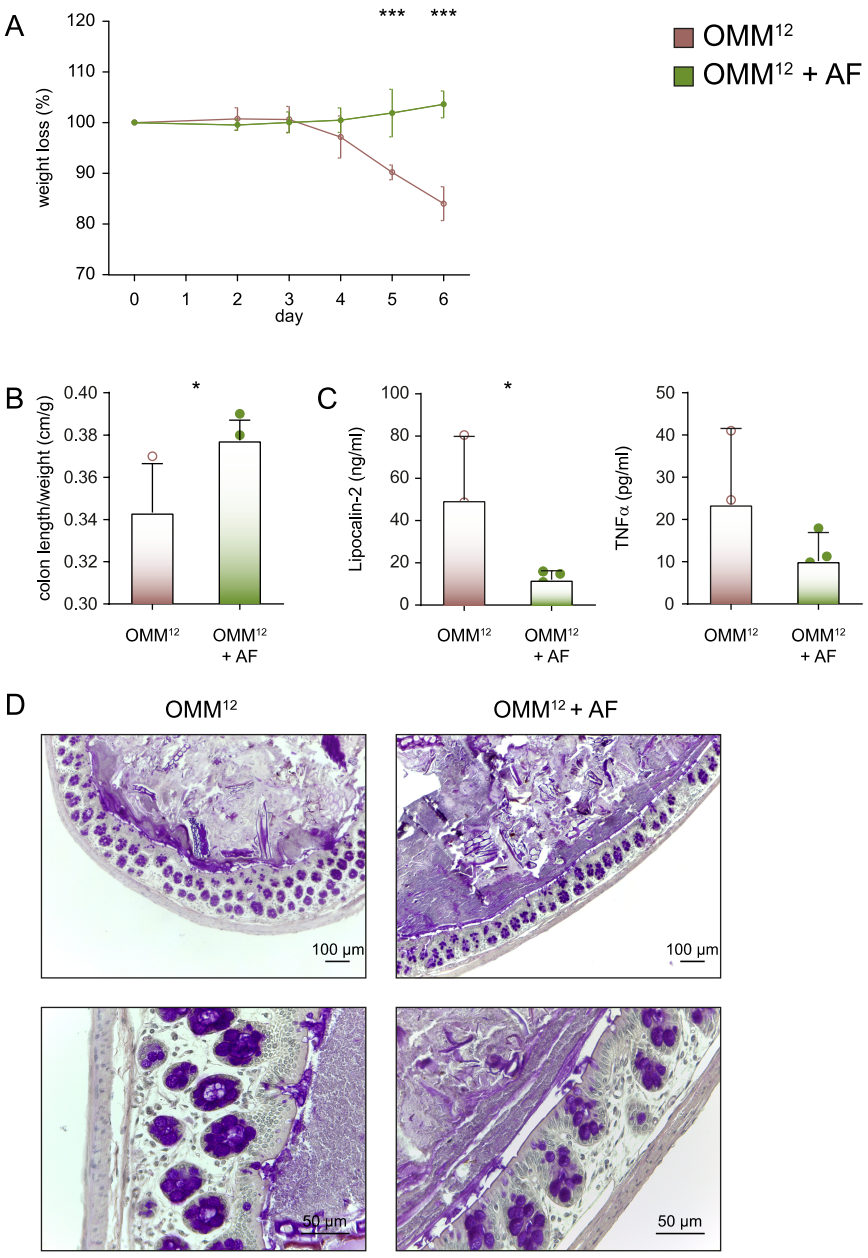

Figure 18. *A. finegoldii* 17242 ameliorates DSS-induced colitis.

OMM[12] B6 mice were associated with *A. finegoldii* 17242 and after three weeks treated with 3.5 % DSS for five days. Analysis were performed at day six after initiation of DSS-treatment. (A) Weight loss and (B) colon length were measured to quantify inflammation. (C) The secretion of lipocalin-2 and TNFα in *ex vivo* colon cultures were measured by ELISA (n = 3-4). The colitis was further confirmed by (E) histological (PAS staining) analysis of the colon (n = 3-4). Statistical analysis: (A) two-way ANOVA (corrected for multiple comparison by Bonferroni method) (B) unpaired, two-tailed Student's t test and (C) Mann-Whitney test. Shown are individual values respectively means + SD representing one of two similar experiments. *p < 0.05, **p < 0.01 and ***p < 0.001. OMM[12], Oligo-Mouse-Microbiota 12; AF, *Alistipes finegoldii* 17242; DSS, dextran sulphate sodium.

4 Discussion

4.1 Dietary cellulose promotes intestinal homeostasis

4.1.1 Investigating nutritional interventions

Conventional chow is a mixture of different native plant- and animal-derived ingredients, mainly grains. The precise composition of such crude diets is not known and varies according to the company and the batch due to the variability of natural ingredients. However, a precise knowledge of the components is required to perform or evaluate nutritional studies. Consequently, conventional chow is not suitable to investigate the impact of defined dietary factors on health and disease (Pellizzon and Ricci 2019).

With respect to fibre, chow harbours different soluble and insoluble fibres in an unknown composition and concentration. Our aim was to specifically focus on dietary cellulose as the only source of fibres. We therefore chose purified diets which were identical except that one contained cellulose with similar amounts as conventional chow (7 %; control diet, CD) and the other diet was devoid of any fibre (fibre free diet, FFD). Mice received these diets from birth and both, CD and FFD, were well tolerated since there was no influence on growth development or food intake. Dietary fibres are known regulators of the intestinal transit, thus preventing both diarrhea and constipation. Due to the lack of bulking material in the diet, the transit time in FFD mice was decreased, but no sign of diarrhea was observed. In conclusion, both purified diets seemed to be appropriate to investigate the effects of dietary cellulose on intestinal homeostasis.

4.1.2 Maturation of the intestinal microbiota is dependent on dietary cellulose

The growing knowledge of host-microbe interactions in human health and disease of man propelled trials to alter or even exchange the microbiota in order to improve health conditions. Alimentary carbohydrates and particularly prebiotics, known to have a strong influence on the intestinal microbiota, can be used as dietary intervention (David et al. 2014; Sonnenburg et al. 2016; Gibson et al. 2017). However, would you think of cellulose when talking about prebiotics? Probably, most

people have in mind that cellulose is a rather low-quality plant material, which is hardly suitable for human nutrition. Probably, people think of ruminants or even termites that are able to metabolise cellulose due to their specific microbiota (Hungate 1966; Brune 2014). Cellulose is not considered as a classic prebiotic because of controversial opinions about its fermentability (Slavin et al. 1981; Boulahrouf 1990; Robert and Bernalier-Donadille 2003; Chassard et al. 2010; Chassard et al. 2012). Although studies revealed ^{14}C excretion in breath after administration of ^{14}C-labeled cellulose, the extent and physiological role of degradation remains unclear (Cummings 1984). Yet, the data of the present study demonstrate that cellulose is more than an inert bulking material and might serve as considerable microbial substrate. Moreover, even the murine microbiota that has never seen cellulose was equipped with cellulases. This points to a conserved function of these enzymes in the gut environment (Stephen et al. 2017; Hon 1994). Cellulose might be capable of fuelling the gut microbiota by the final degradation product glucose.

However, previous studies which claimed that dietary cellulose has effects on the intestinal microbiota were partially contradictory as they reported an increase or decrease of microbial diversity (Nagy-Szakal et al. 2013; Berer et al. 2018; Morowitz et al. 2017; Riva et al. 2019). For example, a study using a crude fibre rich diet showed decreased diversity in comparison to a crude control diet (Berer et al. 2018), whereas a synthetic high versus a low fibre diet was reported to enrich the diversity (Nagy-Szakal et al. 2013). These opposing findings might be explained by differences in the study designs, especially with respect to the period of intervention, composition of the experimental diet, including origin of fibre, but also by the high variation of the indigenous intestinal microbiota of mice in different animal facilities (Rausch et al. 2016; Ericsson et al. 2018; as discussed in detail below). All these factors hinder the reproducibility of nutritional and microbiome studies.

Recent work of Riva et al. revealed that even short-term (one week) deprivation of cellulose narrows the diversity of the intestinal microbiota in comparison to a diet containing cellulose as the only source of fibre (Riva et al. 2019). The aim of the present study was to disclose long-term effects of dietary cellulose during early (eight to twelve weeks) and advanced adulthood (twelve to twenty-five weeks). The increase of diversity and the ratio of the phyla Firmicutes to Bacteroidetes are

known indicators for the maturation of the intestinal microbiota (Mariat et al. 2009; Flemer et al. 2017). In the absence of dietary cellulose, both were significantly decreased in the early (12 weeks) and a little less pronounced even in the advanced adulthood (25 weeks), indicating that microbial maturation, particularly in early adulthood, depends on dietary cellulose if other fibres are lacking.

Looking closer to the composition of the gut microbiota during early adulthood, we observed that alterations caused by cellulose deprivation were even evident at the level of phyla. Beside the increase of Bacteroidetes and the decrease of Firmicutes, we found a high abundance of Verrucomicrobia in 12-week-old FFD mice. This might be due to the ability of *Akkermansia muciniphila* - the only cultivated representative of this phylum in the gut - to feed on host-derived polysaccharides, especially if dietary fibre are lacking (Desai et al. 2016; Zhang et al. 2019). At lower taxonomic levels, we found a substantial decrease of *Ruminococcaceae* and *Lachnospiraceae*, which belong to Firmicutes and are known to be involved in fibre degradation and SCFA production, in FFD mice (Walker et al. 2011; Kasahara et al. 2018; La Rosa et al. 2019). In particular, *Ruminococcaceae* has been shown to exert cellulolytic activity in the human intestine and colonise the gut lumen while being attached to solid material (Robert and Bernalier-Donadille 2003; Walker et al. 2008; Chassard et al. 2012). This might explain their high abundance in the presence of cellulose. Moreover, the genus *Alistipes*, which belongs to the family of *Rikenellaceae* and usually expands during lifespan in the human and murine microbiota, was largely absent in FFD mice (Langille et al. 2014; Claesson et al. 2011). Collectively, these findings emphasise a crucial role of dietary cellulose for the physiological maturation of the intestinal microbiota during early adulthood.

Since alterations of the composition of the microbiota are often reflected by its metabolome, we focussed further on major microbial products in the caecum of mice feeding either CD or FFD. In accordance with prior studies, we found that cellulose does not or only marginally contribute to SCFAs production (Le Leu et al. 2002; Peng et al. 2013; Lewis et al. 2019). By contrast, our data revealed a strong impact of diet and microbiota on the intestinal pool of bile acids. In several studies it has been shown that caecal amounts of conjugated primary bile acids are much higher in germ-free than in SPF mice (Madsen et al. 1976; Sayin et al. 2013). Consistently, the concentrations of all tested conjugated primary bile acids were higher in germ-free

than in SPF mice, irrespective of diet. This is best explained by increased reabsorption in the ileum, but also by the lack of microbiota-dependent regulation of the hepatic metabolism of primary bile acid (Wostmann 1973; Sayin et al. 2013). Furthermore, differences in the amount of conjugated primary bile acids between CD and FFD mice become exclusively evident in germ-free, but not in SPF mice, which supports a mechanism that is independent of the microbiota. Despite a relatively low bile acid-binding capacity of cellulose, interactions between both molecules might limit the bioavailability of bile acids as compared to a fibre-free situation (Dubey et al. 2018; Kim et al. 2020). Regarding bile acids derived from microbial conversion, we found increased levels of the unconjugated primary bile acid UDCA and the secondary bile acids DC and 3-dehydro-CDCA in FFD mice. These effects in SPF mice, which were more specific because only a few bile acids were elevated, suggest that cellulose also interferes with the bile acid metabolism via the intestinal microbiota. However, the microbiota not only shapes the bile acid metabolism, as it has been shown for a microbiota rich in *Clostridia* which promotes bile acid excretion (Zhao et al. 2020). The resistance to bile acids also exerts a high selective pressure on intestinal microbes (Kurdi et al. 2006). Recently it was reported that UDCA administration significantly alters the microbiota as well as the bile acid pool (Kim et al. 2018; Winston et al. 2019). Taken together, this demonstrates the high complexity and multi-directionality of the bile acid metabolism and discloses that further research is needed to figure out whether the microbiota alters the bile acid pool or *vice versa* in the context of cellulose.

4.1.3 Dietary cellulose modulates intestinal immune and epithelial cell functions

'Good fences make good neighbours': although mucosal immune and epithelial cells efficiently control encounters between host and microbiota, the intestinal barrier function also depends on the contact with bacteria (Moens and Veldhoen 2012). Diet is a major environmental factor that affects this mutual interaction (Maslowski and Mackay 2011). Therefore, we were interested in analysing direct or indirect effects of cellulose on adaptive immune responses and epithelial cell functions in the gut.

Consistently with the unaffected levels of SCFAs in CD and FFD mice, we found no influence of cellulose on sIgA and T_{reg} cells known to be induced by these

metabolites (Smith et al. 2013; Kim et al. 2016). Furthermore, we have seen no influence on TH1 and TH2 immune responses which contrasts with recent findings from two groups. Both showed that a cellulose-rich diet decreases TH1 immune responses, while Berer et al. additionally described a shift towards TH2 immunity and no influence on TH17 immune responses (Berer et al. 2018; Kim et al. 2020). Since both studies differ from the present work even with respect to the diets used and the reported effects on the microbiota, it was not surprising that we found divergent immune responses as well.

In our model, where cellulose was the only source of dietary fibre, we observed that lack of this fibre caused increased frequencies of the RORγt-expressing $CD4^+$ T cell subsets, i.e. TH17 and $T_{reg}17$ cells. As cellulose is neither digested nor absorbed by the host, we consider two possibilities of how cellulose might have an impact on the intestinal immune system. First, fibre deprivation alters the intestinal microbial composition which in turn might cause TH17/$T_{reg}17$ immune responses, as some members of the microbiota, especially SFB bacteria, have already been shown to induce the differentiation of TH17 as well as $T_{reg}17$ (Ivanov et al. 2009; López et al. 2011; Sefik et al. 2015; Ohnmacht et al. 2015; Tan et al. 2016). Moreover, microbial metabolites might act on the generation of these gut-associated lymphocytes. Recent studies described that the differentiation of RORγt-dependent TH17 and $T_{reg}17$ cells is modulated by bile acids (Hang et al. 2019; Song et al. 2020; Campbell et al. 2020). Song et al. found that specific mixtures of bile acids increased $T_{reg}17$ cells in the colon. However, they did not find an influence on $T_{reg}17$ cells in other organs or TH17 cells (Song et al. 2020). By contrast, other studies revealed that even a single bile acid may induce an increase of $T_{reg}17$ in the colon and a decrease of TH17 cells in the ileum of mice (Hang et al. 2019; Campbell et al. 2020). Thus, we speculate that the increase in ileal RORγt-dependent $CD4^+$ cells in FFD mice might at least partially result from an altered bile acid metabolism. Further studies may be performed to address this issue in detail.

One of the central functions of the gut epithelium is segregation of the immune system from luminal microbes (Okumura and Takeda 2017). IECs possess many ways to accomplish this task, such as production of mucus, antimicrobial peptides and transepithelial IgA transport (Rojas and Apodaca 2002; Allaire et al. 2018). In order to test whether cellulose or cellulose-dependent microbial alterations have an

influence on intestinal homeostasis, we measured the expression of selected genes coding for antimicrobial-, tight junction- and mucin proteins as well as genes involved in proliferation and restitution. In contrast to a recent study, we found no impact of cellulose on expression of tight junctions protein-related genes, such as Ocln, Tjp1 and Cldn8 (Di Caro et al. 2019). Furthermore, cellulose did not affect proliferation and the expression of mucins and restitution factor TFF3 in IECs. Interestingly, the transcription of Reg3γ was markedly decreased in the absence of fibre. The C-type lectin inhibits bacteria and thus promotes spatial segregation between the epithelium and intestinal microbes (Cash 2006; Vaishnava et al. 2011; Loonen et al. 2014). Transcriptional studies revealed that microbes and microbial products specifically alter the gene expression profile of IECs (Camp et al. 2014; Richards et al. 2016). In particular, the transcription of antimicrobial REG3γ was shown to be induced by direct activation of TLRs or by receptors for SCFA (Vaishnava et al. 2008; Zhao et al. 2018). Moreover, the microbiota may induce REG3γ by IECs via an immune-mediated IL-22/STAT3 (signal transducer and activator of transcription 3) signalling pathway (Zheng et al. 2008; Pickert et al. 2009). IL-22 belongs to the IL-10 family and is produced by various cell types, including TH17, TH1; TH22 cells, γδ T cells and ILC3 cells (Parks et al. 2015). Depending on the milieu, IL-22 exerts pro-inflammatory or homeostatic functions (Sonnenberg et al. 2010). The latter includes the induction of genes involved in host antimicrobial defence, thereby IL-22 was shown to prevent dysbiosis (Hammer et al. 2017). Interestingly, a recent study of Zou et al. (2018) examining metabolic syndrome revealed that the soluble fibre inulin induces REG3γ via ILC3-derived IL-22 in a microbiota-dependent manner. However, when feeding mice with a high fat diet in their study, cellulose was not able to rescue the pathology and induce IL-22 (Zou et al. 2018).

Collectively, our study shows that dietary cellulose is not an inert fibrous food component, but influences host physiology at cellular and molecular levels, i.e. TH cell function and gene transcription of IECs. Further studies may disclose causal relationships between cellulose, the alterations of the microbiota, immune and epithelial cell functions.

4.1.4 Dietary cellulose deprivation increases the susceptibility to DSS-induced colitis

Dysbiosis and disturbance of the mucosal barrier might lead to gut inflammation (Maloy and Powrie 2011). The present study revealed that the insoluble fibre cellulose strengthened the gut barrier function and ameliorated DSS-induced acute colitis. Potential mechanisms may include the prevention of dysbiosis, an altered TH17/T_{reg}17 immune response and strengthening of the anti-microbial defence.

In general, dysbiosis refers to any change of the microbiota commonly found in healthy subjects and is often discussed in relation to disease and inflammation (Petersen and Round 2014). Alterations seen in FFD mice, such as the decline of overall diversity and certain bacterial families (*Ruminococcaceae*, *Lachnospiraceae* and *Rikenellaceae*) have also been discussed in murine colitis models and IBD patients (Ott et al. 2004; Munyaka et al. 2016; Hart et al. 2017; Lo Presti et al. 2019). Despite some functional redundancy within an ecosystem, a restriction of the diversity might cause the loss of specific health-promoting host-microbe-interactions (Allison and Martiny 2008; Petersen and Round 2014). This was shown, for example, for a defined set of *Clostridium* strains which induced expansion of T_{reg} cells in the colon, whereas single strains or just a few of them were not sufficient to mediate this effect (Atarashi et al. 2013). On the other side, also the expansion of pathobionts may have harmful consequences. As mentioned above, we found an increased abundance of *A. muciniphila* in the absence of dietary fibre. The expansion of this mucin-degrading bacterium in a fibre-deprived situation has been shown to damage the mucus barrier and to increase the susceptibility for intestinal infections (Desai et al. 2016).

Moreover, dysbiosis was shown to favour IL-17-producing $CD4^+$ T cells, leading to an pro-inflammatory milieu (Maeda et al. 2016; Dutzan et al. 2018). In the present study, both TH17 and T_{reg}17 cells known to secrete IL-17 were elevated in the ileum of FFD mice. IL-17 acts on various cellular targets, including macrophages and IECs, and induces the production of pro-inflammatory mediators (Kempski et al. 2017). An increase in TH17 cells has been implicated in several autoimmune and inflammatory diseases, including IBD (Fujino et al. 2003; Kleinschek et al. 2009; Wu et al. 2010; Lee et al. 2011). Thus, elevated TH17 frequencies as seen in FFD mice indicate a shift of the intestinal immune system towards inflammation. On the other

hand, $T_{reg}17$ cells have a regulatory phenotype that is able to attenuate colitis (Yang et al. 2016). They have been shown to differentiate in response to inflammatory stimuli, which might consequently explain their high abundance in the absence of cellulose (Yang et al. 2018). Further studies might clarify, which $CD4^+$ T cell subset contributes to the increase in ileal IL-17 in production and whether these cells are functionally linked to the increased susceptibility to DSS in FFD mice. However, following decreased REG3γ expression in FFD mice, the observed TH17/$T_{reg}17$ response might indeed have a rather pro-inflammatory than homeostatic nature. REG3γ-deficiency has also been shown to prone mice to intestinal infection and bacterial translocation into host tissue (Loonen et al. 2014; Hendrikx et al. 2019). Thus, it is difficult to evaluate whether increased TH17 responses or the reduced expression of REG3γ in FFD mice contributes to the observed phenotype.

In summary, our data expand prior observations that cellulose has anti-colitogenic properties via several potential mechanisms (Nagy-Szakal et al. 2013; Kim et al. 2020). Further investigation might clarify which of these factors is causally involved in the strengthening of the barrier by cellulose.

4.2 Alistipes finegoldii 17242 protects mice from colitis

4.2.1 Gnotobiotic mice as a tool to study host-microbe-interactions

The microbiota composition of laboratory mice is highly susceptible to environmental factors, including diet or husbandry (Ericsson et al. 2018). Thus, the microbiota within the same and different animal facilities might differ profoundly (Rausch et al. 2016; Ericsson et al. 2018). In addition, also intrinsic factors such as the host's immune system and genetic background impact the microbiota, leading to difficulties to differentiate whether a certain microbial alteration is cause or consequence of a disease (Rogala et al. 2020).

With that knowledge, studies dealing with the host-microbe-interaction need to be carefully controlled (Rogala et al. 2020). One straightforward strategy to investigate the host's response to a defined bacterial strain or consortium and *vice versa* is the association of germ-free-born mice. However, these animals differ in many ways from conventional mice, particularly with respect to the intestinal immune system, including a thinner mucus layer and reduced T_{reg} as well as TH17 cell numbers

(Ivanov et al. 2008; Atarashi et al. 2013; Johansson et al. 2015). Recently it was shown that the microbiota induces a specific immune reaction during a defined time window during early development. This so-called 'weaning reaction' was absent in germ-free mice with the consequence of increased susceptibility to colitis and cancer later in life (Al Nabhani et al. 2019). Furthermore, not only the susceptibility, but also the course of certain diseases is different in germ-free and conventional mice. For example, even though DSS-induced colitis is accompanied with severe weight loss, diarrhea and higher mortality in germ-free mice, the typical inflammatory response (elevated amounts of TNFα and IL-17, colonic thickening) does not take place (Hernández-Chirlaque et al. 2016). Thus, mono-associated germ-free-born mice have several immunological deficits, which may limit their suitability for some applications.

These limitations can be overcome by using gnotobiotic mice associated with a defined microbiota. These models facilitate to address host-microbe interactions and to trace a single bacterium in the presence of a functional immune system. In this study, we used OMM12 mice which harbour a microbiota that is composed of twelve strains representing the major bacterial phyla of the murine intestinal microbiota. The OMM^{12} was shown to mimic the functional properties of a natural complex microbiota, such as providing colonization resistance to an enteric pathogen (Brugiroux et al. 2016).

4.2.2 The cellulose-dependent commensal *Alistipes finegoldii* 17242 ameliorates DSS-induced colitis

A. finegoldii 17242 is a gram-negative, strictly anaerobic rod of the family *Rikenellaceae* (Rautio et al. 2003) and a common member of the human and murine intestinal microbiota (Gu et al. 2013; Rajilić-Stojanović and Vos 2014; Xiao et al. 2015). The decline of *Alistipes spp.* was one of the most conspicuous findings in cellulose-deprived mice, which might partially be explained by starvation of the bacterium, the loss of its biological niche and the susceptibility to inflammation. A recent study showed that if cellulose is the only carbon source in the culture medium, it is utilised by *A. finegoldii* and enhances its growth *in vitro* (Maesschalck et al. 2019). In accordance with these findings, our bioinformatic analysis revealed that *A. finegoldii* is equipped with enzymes to degrade this fibre. Consequently, the

decrease of the bacterium during fibre deprivation favours the idea that *A. finegoldii* suffers from starvation. In addition, by triggering a drastic shift in the microbial composition, cellulose might also act indirectly by outcompeting certain bacterial species. Microbe-microbe mutualisms are crucial for an ecosystem, including generation and diminishing biological niches. Thus, alterations of the microbial composition can lead to both increase and decline of a certain species (Messer and Chang). Moreover, *Alistipes spp.* was assumed not to tolerate an inflammatory milieu (Borton et al. 2017). This hypothesis is further supported by the low abundance of this microbe in human colitis (Jiang et al. 2015; Mancabelli et al. 2017; Meij et al. 2018; Lo Presti et al. 2019). Given that cellulose deprivation drives a low-grade inflammation in the gut, the presented data confirm these findings. In summary, the environment in the intestine of FFD mice might be a rather inappropriate habitat for *Alistipes spp.* resulting in its growth inhibition. Additional studies have to clarify whether the influence of cellulose on *Alistipes spp.* is unique for cellulose or can also be mimicked by other dietary fibres.

To further dissect whether the decline of *Alistipes spp.* in FFD mice was a passenger or driver of the severe colitis, gnotobiotic OMM^{12} were stably colonised with *A. finegoldii* 17242 by a single application of this bacterium via gavage. Contrary to our expectations, this association did not entirely mimic the effect of cellulose, but also induced IL-17-producing CD4$^+$ T cells in lymphatic organs (spleen, mLN) and the intestinal lamina propria. Staining for transcription factors revealed that these cells are TH17 and not $T_{reg}17$ cells. TH17 cells are a Janus-faced T lymphocyte subset present in mucosal tissues: Homeostatic TH17 cells induced by commensals produce IL-17A and IL-22, whereas pathogen-driven inflammatory TH17 cells additionally secrete IFN-γ (Omenetti et al. 2019). In contrast to the immune reactions induced by cellulose deprivation, the *A. finegoldii*-elicited TH17 response was rather more homeostatic as we could not detect an increased IFN-γ-production in the intestine or periphery. Increased amounts of IL-22 and unchanged lipocalin-2 in colon *ex vivo* cultures further suggested a commensal-induced response.

In line with increased amounts of IL-22, we found a more than four-fold induction of colonic REG3γ in *A. finegoldii*-associated OMM^{12} mice. Despite the unclear molecular mechanism, these data provide evidence that *A. finegoldii* promotes IL-22-induced upregulation of the antimicrobial lectin REG3γ, which strengthens the epithelial

barrier and finally results in a decreased susceptibility to DSS-induced colitis (Vaishnava et al. 2011; Loonen et al. 2014). Furthermore, IL-22 might also directly enhance epithelial wound healing (Pickert et al. 2009). Thus, the present study supports the recent finding that *A. finegoldii* ameliorates DSS-induced colitis (Dziarski et al. 2016) and provides rationale for a potential mechanism.

The fact that *A. finegoldii* does not exactly reflect the situation of cellulose deprivation might be best explained by the massive alterations of the microbiota in FFD mice. Yet, it is astonishing, that one representative bacterium is able to mimic the effects of cellulose. Our findings suggest that *A. finegoldii* induced upregulation of REG3γ is a central mechanism of the colitis protection of CD mice and thus, in a certain sense, support that *Alistipes* has deserved its name – the 'other rod' (lat. *alius*, the other; lat. *stipes*, rod). Further research might lead to a better functional and molecular understanding of the pathways.

Especially the mechanism of how *A. finegoldii* exerts physiological effects would be interesting. Since, our FISH analysis of *A. finegoldii*-associated OMM^{12} mice revealed little evidence of any adherence of the bacterium to the epithelium, a mechanism that is induced by bacterial metabolites seems more likely than a direct interaction with the host. Potential bioactive substances produced by *A. finegoldii* are succinate, sulphonolipids and indoles (Rautio et al. 2003; Walker et al. 2017). Especially the latter might be a reasonable link to enhanced REG3γ expression since indoles are known ligands of the aryl hydrocarbon receptor which induces IL-22 secretion following activation (Gao et al. 2018; Monteleone et al. 2011).

It has to be mentioned that *Alistipes spp.* are not always considered as commensals or 'friends' in literature. Several studies designated these species as pathobionts or 'foes' since *Alistipes spp.* were also associated with colorectal cancer (Baxter et al. 2014; Feng et al. 2015; Dai et al. 2018). However, today there are still no clear data about the causal involvement of *A. finegoldii* in the pathogenesis of this disease (Sun et al. 2017). One potential mechanistical link was shown in IL-10$^{-/-}$ and IL-10/lipocalin-2$^{-/-}$ mice by Moschen et al., showing that *A. finegoldii* promotes tumorigenesis by activating the IL-22/STAT3 pathway. Interestingly, the high abundance of *Alistipes* as seen in IL-10/lipocalin-2$^{-/-}$ mice was accompanied with increased REG3γ levels as well (Moschen et al. 2016). Thus, the mechanism discussed by Moschen and colleagues does not seem entirely contradictory to the

findings of the present study in that *A. finegoldii* induces antimicrobial host responses via IL-22 signalling. However, the outcome with respect to pathology may be controversial because host-microbe interactions are highly related to nutrition, microbiota and the genetic background of the host. In contrast to the study of Moschen and colleagues we never have observed that association of OMM^{12} mice with *A. finegoldii* led to tumorigenesis or any sign for inflammation. Instead, our data clearly showed that association of OMM^{12} mice with *A. finegoldii* protected them from acute colitis.

4.3 Final discussion and outlook

The present study demonstrate that dietary cellulose promotes intestinal homeostasis (Figure 19). Cellulose served as a potential substrate for intestinal bacteria, fuelled the microbial diversification and thus prevented dysbiosis. Moreover, cellulose also affected the intestinal metabolome, including the pool of primary and secondary bile acids. Further work might dissect the interactions between cellulose, the microbiota and bile acids, since these factors are mutually dependent on each other. Additionally, dietary cellulose suppressed pro-inflammatory TH17/T_{reg}17 immune responses, induced epithelial expression of antimicrobial REG3γ and attenuated acute intestinal inflammation. It might be interesting to examine whether cellulose, either via the microbiota or microbial metabolites, induce these alterations, which signalling pathways are involved and which of these factors lead to the decreased colitis susceptibility.

To further elucidate a specific cellulose-dependent host-microbe interaction, we focussed on *Alistipes finegoldii* as a representative of a genus which was highly affected by cellulose deprivation. We could demonstrate that this commensal, which is endowed with cellulolytic enzymes, enhanced the expression of IL-22 and REG3γ and restored the intestinal barrier function in a gnotobiotic mouse model. Additional studies might clarify the cellular and molecular mechanisms of how *A. finegoldii* exerts these effects.

In summary, this study provides a rationale for the health promoting effects of dietary cellulose. We could demonstrate that cellulose strengthens the intestinal barrier function. Further, our data strongly suggest that some of these anti-

inflammatory effects are mediated by the cellulose-dependent commensal *Alistipes finegoldii*. Thus, these findings offer the scientific basis for further research on the physiological effects of dietary cellulose and for specific recommendation on fibre consumption to improve public health nutrition.

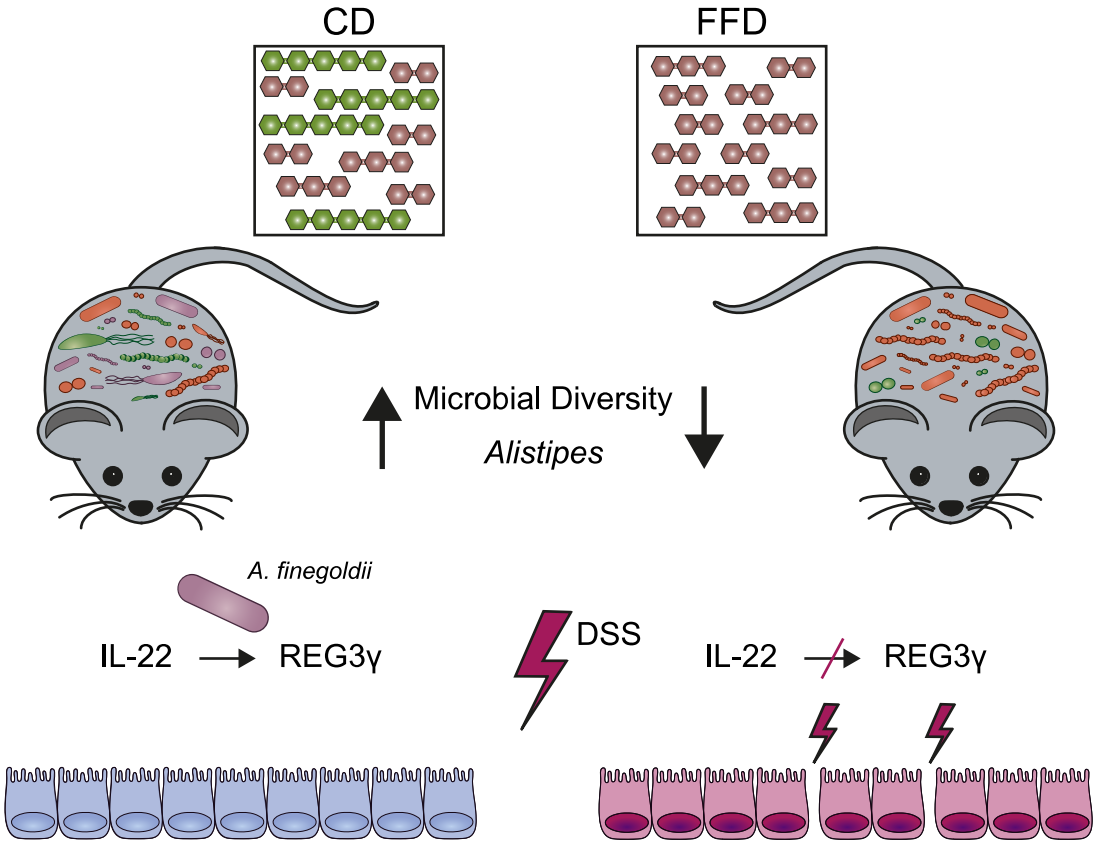

Figure 19. Impact of dietary cellulose on intestinal homeostasis.

Scheme of potential mechanisms of how cellulose impacts on the intestinal homeostasis. Mice received cellulose-containing control diet (CD) or fibre-free diet (FFD) from birth. The lack of dietary cellulose disrupted the diversification of the intestinal microbiota with *Alistipes* being one of the most affected genera. The association of gnotobiotic mice with a representative of this genus, *Alistipes finegodlii*, induced IL-22 and restored expression of REG3γ, which might contribute to the attenuation of DSS-induced acute colitis in these mice.

5 Summary

It is almost fifty years ago that dietary fibres were recognized to be health-promoting. However, the cellular and molecular mechanisms of health-promoting effects are not yet well understood, especially with respect to dietary cellulose, the most common biopolymer on earth.

In this study, the impact of dietary cellulose on the intestinal microbiota, immune and epithelial cell functions in health and disease was examined. Cellulose served as a potential substrate for intestinal microbes and promoted the maturation of the gut microbiota. Moreover, the lack of this fibre skewed immune responses towards inflammation, decreased the transcription of antimicrobial REG3γ and increased the susceptibility to acute colitis.

One of the genera most affected by cellulose deprivation was *Alistipes*. Analysis of *Alistipes finegoldii, a* dominant representative of this genus, revealed that this microbe mimics some of the molecular and cellular effects of dietary cellulose in a gnotobiotic mouse model. We found that *A. finegoldii* is equipped with cellulolytic enzymes and that intestinal colonization led to enhanced expression of IL-22 and REG3γ. Functionally, *A. finegoldii* was able to restore intestinal barrier function during acute colitis.

Collectively, this study supports epidemiological observations and gives a rationale for the health promoting effects of dietary cellulose. Since the intake of fibres in most western societies is very low, this study provides a scientific rationale to set up recommendations on fibre consumption, with special emphasis on cellulose, in order to improve public health.

6 Zusammenfassung

Die gesundheitsförderliche Bedeutung von Ballaststoffen in der Nahrung wurden bereits vor fünfzig Jahren entdeckt. Dennoch sind die Mechanismen ihrer Wirkungen auf zellulärer und molekularer Ebene bis heute noch nicht vollständig verstanden, insbesondere im Hinblick auf Nahrungszellulose, dem am weitesten verbreiteten Biopolymer der Erde.

In dieser Studie wurde der Einfluss von Zellulose auf die intestinale Mikrobiota, Immun- sowie Epithelzellen unter homöostatischen und inflammatorischen Bedingungen untersucht. Wir konnten zeigen, dass Zellulose als potenzielles Substrat für Darmbakterien dient und die physiologische Entwicklung der intestinalen Mikrobiota fördert. Der Mangel an Zellulose induzierte eine pro-inflammatorische Immunantwort, verminderte die Expression des antimikrobiellen REG3γ und erhöhte die Anfälligkeit für akute Darmentzündungen.

Eine der am stärksten von Zellulosemangel betroffenen Gattungen der Mikrobiota war *Alistipes*. Die isolierte Analyse eines dominanten Vertreters dieser Gattung, *Alistipes finegoldii*, zeigte, dass dieses Bakterium für einige der molekularen und zellulären Effekte von Zellulose verantwortlich war. *A. finegoldii*, das mit cellulolytischen Enzymen ausgestattet ist, induzierte die Expression von IL-22 und REG3γ und stellte die Funktion der Darmbarriere in einem gnotobiotischen Mausmodell wieder her.

Die Ergebnisse dieser Studie unterstützen somit epidemiologische Daten und liefern mögliche Kausalitäten für die gesundheitsförderlichen Wirkungen des Ballaststoffs Zellulose. Da der Verzehr von Ballaststoffen in vielen westlichen Gesellschaften alarmierend gering ist, liefert diese Studie auch die wissenschaftliche Grundlage für mögliche Empfehlungen zur Ballaststoffaufnahme mit dem Ziel, die Ernährungssituation in der Gesellschaft zu verbessern.

7 Publication bibliography

Abreu MT (2010) Toll-like receptor signalling in the intestinal epithelium: How bacterial recognition shapes intestinal function. Nat Rev Immunol 10:131–144

Aguiar Vallim TQ de, Tarling EJ, Edwards PA (2013) Pleiotropic roles of bile acids in metabolism. Cell Metab 17:657–669

Al Nabhani Z, Dulauroy S, Marques R, Cousu C, Al Bounny S, Déjardin F, Sparwasser T, Bérard M, Cerf-Bensussan N, Eberl G (2019) A Weaning Reaction to Microbiota Is Required for Resistance to Immunopathologies in the Adult. Immunity 50:1276-1288.e5

Al Nabhani Z, Eberl G (2020) Imprinting of the immune system by the microbiota early in life. Mucosal Immunol 13:183–189

Alexander JK (1968) Purification and specificity of cellobiose phosphorylase from Clostridium thermocellum. J Biol Chem 243:2899–2904

Allaire JM, Crowley SM, Law HT, Chang S-Y, Ko H-J, Vallance BA (2018) The Intestinal Epithelium: Central Coordinator of Mucosal Immunity. Trends Immunol 39:677–696

Allison SD, Martiny JBH (2008) Colloquium paper: Resistance, resilience, and redundancy in microbial communities. Proc Natl Acad Sci U S A 105 Suppl 1:11512–11519

Amann RI, Binder BJ, Olson RJ, Chisholm SW, Devereux R, Stahl DA (1990) Combination of 16S rRNA-targeted oligonucleotide probes with flow cytometry for analyzing mixed microbial populations. Appl Environ Microbiol 56:1919–1925

An R, Wilms E, Masclee AAM, Smidt H, Zoetendal EG, Jonkers D (2018) Age-dependent changes in GI physiology and microbiota: Time to reconsider? Gut 67:2213–2222

Ananthakrishnan AN, Khalili H, Konijeti GG, Higuchi LM, Silva P de, Korzenik JR, Fuchs CS, Willett WC, Richter JM, Chan AT (2013) A prospective study of long-term intake of dietary fiber and risk of Crohn's disease and ulcerative colitis. Gastroenterology 145:970–977

Anderson JW, Baird P, Davis RH, Ferreri S, Knudtson M, Koraym A, Waters V, Williams CL (2009) Health benefits of dietary fiber. Nutrition Reviews 67:188–205

Aramaki T, Blanc-Mathieu R, Endo H, Ohkubo K, Kanehisa M, Goto S, Ogata H (2019) KofamKOALA: KEGG ortholog assignment based on profile HMM and adaptive score threshold. Bioinformatics

Arpaia N, Campbell C, Fan X, Dikiy S, van der Veeken J, deRoos P, Liu H, Cross JR, Pfeffer K, Coffer PJ, Rudensky AY (2013) Metabolites produced by commensal bacteria promote peripheral regulatory T-cell generation. Nature 504:451–455

Atarashi K, Tanoue T, Oshima K, Suda W, Nagano Y, Nishikawa H, Fukuda S, Saito T, Narushima S, Hase K, Kim S, Fritz JV, Wilmes P, Ueha S, Matsushima K, Ohno H, Olle B, Sakaguchi S, Taniguchi T, Morita H, Hattori M, Honda K (2013) Treg induction by a rationally selected mixture of Clostridia strains from the human microbiota. Nature 500:232–236

Bach J-F (2018) The hygiene hypothesis in autoimmunity: The role of pathogens and commensals. Nat Rev Immunol 18:105–120

Barker N (2014) Adult intestinal stem cells: Critical drivers of epithelial homeostasis and regeneration. Nat Rev Mol Cell Biol 15:19–33

Barnich N, Aguirre JE, Reinecker H-C, Xavier R, Podolsky DK (2005) Membrane recruitment of NOD2 in intestinal epithelial cells is essential for nuclear factor-{kappa}B activation in muramyl dipeptide recognition. J Cell Biol 170:21–26

Barrasa JI, Olmo N, Lizarbe MA, Turnay J (2013) Bile acids in the colon, from healthy to cytotoxic molecules. Toxicol In Vitro 27:964–977

Baxter NT, Zackular JP, Chen GY, Schloss PD (2014) Structure of the gut microbiome following colonization with human feces determines colonic tumor burden. Microbiome 2:20

Bazanella M, Maier TV, Clavel T, Lagkouvardos I, Lucio M, Maldonado-Gòmez MX, Autran C, Walter J, Bode L, Schmitt-Kopplin P, Haller D (2017) Randomized controlled trial on the impact of early-life intervention with bifidobacteria on the healthy infant fecal microbiota and metabolome. Am J Clin Nutr 106:1274–1286

Belkaid Y, Harrison OJ (2017) Homeostatic Immunity and the Microbiota. Immunity 46:562–576

Berer K, Martínez I, Walker A, Kunkel B, Schmitt-Kopplin P, Walter J, Krishnamoorthy G (2018) Dietary non-fermentable fiber prevents autoimmune neurological disease by changing gut metabolic and immune status. Sci Rep 8:10431

Bevins CL, Salzman NH (2011) Paneth cells, antimicrobial peptides and maintenance of intestinal homeostasis. Nat Rev Microbiol 9:356–368

Bingham SA, Day NE, Luben R, Ferrari P, Slimani N, Norat T, Clavel-Chapelon F, Kesse E, Nieters A, Boeing H, Tjϕnneland A, Overvad K, Martinez C, Dorronsoro M, Gonzalez CA, Key TJ, Trichopoulou A, Naska A, Vineis P, Tumino R, Krogh V, Bueno-de-Mesquita HB, Peeters PHM, Berglund G, Hallmans G, Lund E, Skeie G, Kaaks R, Riboli E (2003) Dietary fibre in food and protection against colorectal cancer in the European Prospective Investigation into Cancer and Nutrition (EPIC): An observational study. The Lancet 361:1496–1501

Bischoff SC (2016) Microbiota and aging. Curr Opin Clin Nutr Metab Care 19:26–30

Blom J, Albaum SP, Doppmeier D, Pühler A, Vorhölter F-J, Zakrzewski M, Goesmann A (2009) EDGAR: A software framework for the comparative analysis of prokaryotic genomes

Borton MA, Sabag-Daigle A, Wu J, Solden LM, O'Banion BS, Daly RA, Wolfe RA, Gonzalez JF, Wysocki VH, Ahmer BMM, Wrighton KC (2017) Chemical and pathogen-induced inflammation disrupt the murine intestinal microbiome. Microbiome 5:47

Boulahrouf A (1990) Establishment of cellulolytic bacteria in the digestive tract of conventionally reared young mice: Effect of the dietary cellulose content in the adult. FEMS Microbiology Letters 69:87–90

Brandtzaeg P (2010) Function of mucosa-associated lymphoid tissue in antibody formation. Immunol Invest 39:303–355

Brotherton CS (2015) Insoluble fiber and intestinal microbiota metabolism. J Gastroenterol 50:491

Brucklacher-Waldert V, Carr EJ, Linterman MA, Veldhoen M (2014) Cellular Plasticity of CD4+ T Cells in the Intestine. Front Immunol 5:488

Brugiroux S, Beutler M, Pfann C, Garzetti D, Ruscheweyh H-J, Ring D, Diehl M, Herp S, Lötscher Y, Hussain S, Bunk B, Pukall R, Huson DH, Münch PC, McHardy AC, McCoy KD, Macpherson AJ, Loy A, Clavel T, Berry D, Stecher B (2016) Genome-guided design of a defined mouse microbiota that confers colonization resistance against Salmonella enterica serovar Typhimurium. Nat Microbiol 2:16215

Brune A (2014) Symbiotic digestion of lignocellulose in termite guts. Nat Rev Microbiol 12:168–180

Buonocore S, Ahern PP, Uhlig HH, Ivanov II, Littman DR, Maloy KJ, Powrie F (2010) Innate lymphoid cells drive interleukin-23-dependent innate intestinal pathology. Nature 464:1371–1375

Burger-van Paassen N, Loonen LMP, Witte-Bouma J, Korteland-van Male AM, Bruijn ACJM de, van der Sluis M, Lu P, van Goudoever JB, Wells JM, Dekker J, van Seuningen I, Renes IB, Bereswill S (2012) Mucin Muc2 Deficiency and Weaning Influences the Expression of the Innate Defense Genes Reg3β, Reg3γ and Angiogenin-4. PLoS ONE 7:e38798

Burkitt D (ed) (1975) Refined Carbohydrate Foods And Disease: Some Implications of Dietary Fibre. Elsevier Science, New York

Burkitt DP, Trowell HC (1977) Dietary fibre and western diseases. Ir Med J 70:272–277

Cammack KM, Austin KJ, Lamberson WR, Conant GC, Cunningham HC (2018) RUMINANT NUTRITION SYMPOSIUM: Tiny but mighty: the role of the rumen microbes in livestock production, vol 96

Camp JG, Frank CL, Lickwar CR, Guturu H, Rube T, Wenger AM, Chen J, Bejerano G, Crawford GE, Rawls JF (2014) Microbiota modulate transcription in the intestinal epithelium without remodeling the accessible chromatin landscape. Genome Res 24:1504–1516

Campbell C, McKenney PT, Konstantinovsky D, Isaeva OI, Schizas M, Verter J, Mai C, Jin W-B, Guo C-J, Violante S, Ramos RJ, Cross JR, Kadaveru K, Hambor J, Rudensky AY (2020) Bacterial metabolism of bile acids promotes generation of peripheral regulatory T cells. Nature 581:475–479

Cash HL (2006) Symbiotic Bacteria Direct Expression of an Intestinal Bactericidal Lectin. Science 313:1126–1130

Castleman MJ, Dillon SM, Purba CM, Cogswell AC, Kibbie JJ, McCarter MD, Santiago ML, Barker E, Wilson CC (2019) Commensal and Pathogenic Bacteria Indirectly Induce IL-22 but Not IFNγ Production From Human Colonic ILC3s via Multiple Mechanisms. Front Immunol 10:649

Chassaing B, Aitken JD, Malleshappa M, Vijay-Kumar M (2014) Dextran sulfate sodium (DSS)-induced colitis in mice. Curr Protoc Immunol 104:Unit 15.25

Chassaing B, Srinivasan G, Delgado MA, Young AN, Gewirtz AT, Vijay-Kumar M (2012) Fecal lipocalin 2, a sensitive and broadly dynamic non-invasive biomarker for intestinal inflammation. PLoS ONE 7:e44328

Chassard C, Delmas E, Robert C, Bernalier-Donadille A (2010) The cellulose-degrading microbial community of the human gut varies according to the presence or absence of methanogens. FEMS Microbiol Ecol 74:205–213

Chassard C, Delmas E, Robert C, Lawson PA, Bernalier-Donadille A (2012) Ruminococcus champanellensis sp. nov., a cellulose-degrading bacterium from human gut microbiota. Int J Syst Evol Microbiol 62:138–143

Cheng H, Leblond CP (1974) Origin, differentiation and renewal of the four main epithelial cell types in the mouse small intestine. I. Columnar cell. Am J Anat 141:461–479

Claesson MJ, Cusack S, O'Sullivan O, Greene-Diniz R, Weerd H de, Flannery E, Marchesi JR, Falush D, Dinan T, Fitzgerald G, Stanton C, van Sinderen D, O'Connor M, Harnedy N, O'Connor K, Henry C, O'Mahony D, Fitzgerald AP, Shanahan F, Twomey C, Hill C, Ross RP, O'Toole PW (2011) Composition, variability, and temporal stability of the intestinal microbiota of the elderly. Proc Natl Acad Sci U S A 108 Suppl 1:4586–4591

Coates M, Lee MJ, Norton D, MacLeod AS (2019) The Skin and Intestinal Microbiota and Their Specific Innate Immune Systems. Front Immunol 10:2950

Cordain L, Eaton SB, Sebastian A, Mann N, Lindeberg S, Watkins BA, O'Keefe JH, Brand-Miller J (2005) Origins and evolution of the Western diet: Health implications for the 21st century. Am J Clin Nutr 81:341–354

Cummings JH (1984) Cellulose and the human gut. Gut 25:805–810

Cummings JH, Engineer A (2018) Denis Burkitt and the origins of the dietary fibre hypothesis. Nutr. Res. Rev. 31:1–15

Curtis MM, Way SS (2009) Interleukin-17 in host defence against bacterial, mycobacterial and fungal pathogens. Immunology 126:177–185

Dai Z, Coker OO, Nakatsu G, Wu WKK, Zhao L, Chen Z, Chan FKL, Kristiansen K, Sung JJY, Wong SH, Yu J (2018) Multi-cohort analysis of colorectal cancer metagenome identified altered bacteria across populations and universal bacterial markers. Microbiome 6:70

Daly K, Shirazi-Beechey SP (2006) Microarray analysis of butyrate regulated genes in colonic epithelial cells. DNA Cell Biol 25:49–62

David LA, Maurice CF, Carmody RN, Gootenberg DB, Button JE, Wolfe BE, Ling AV, Devlin AS, Varma Y, Fischbach MA, Biddinger SB, Dutton RJ, Turnbaugh PJ (2014) Diet rapidly and reproducibly alters the human gut microbiome. Nature 505:559–563

Denning TL, Wang Y-c, Patel SR, Williams IR, Pulendran B (2007) Lamina propria macrophages and dendritic cells differentially induce regulatory and interleukin 17-producing T cell responses. Nat Immunol 8:1086–1094

Derrien M, Alvarez A-S, Vos WM de (2019) The Gut Microbiota in the First Decade of Life. Trends Microbiol 27:997–1010

Desai MS, Seekatz AM, Koropatkin NM, Kamada N, Hickey CA, Wolter M, Pudlo NA, Kitamoto S, Terrapon N, Muller A, Young VB, Henrissat B, Wilmes P, Stappenbeck TS, Núñez G, Martens EC (2016) A Dietary Fiber-Deprived Gut Microbiota Degrades the Colonic Mucus Barrier and Enhances Pathogen Susceptibility. Cell 167:1339-1353.e21

DGE, ÖGE, SGE (ed) (2019) D-A-C-H-Referenzwerte für die Nährstoffzufuhr, 2. Auflage, revidierte Ausgabe, bearbeitete Ausgabe. Deutsche Ges. f. Ernährung, Bonn

Di Caro V, Alcamo AM, Cummings JL, Clark RSB, Novak EA, Mollen KP, Morowitz MJ, Aneja RK (2019) Effect of dietary cellulose supplementation on gut barrier function and apoptosis in a murine model of endotoxemia. PLoS ONE 14:e0224838

Dominguez-Bello MG, Costello EK, Contreras M, Magris M, Hidalgo G, Fierer N, Knight R (2010) Delivery mode shapes the acquisition and structure of the initial

microbiota across multiple body habitats in newborns. Proc Natl Acad Sci U S A 107:11971–11975

Dong Y, Chen L, Gutin B, Zhu H (2019) Total, insoluble, and soluble dietary fiber intake and insulin resistance and blood pressure in adolescents. Eur J Clin Nutr 73:1172–1178

Dubey R, Toh Y-R, Yeh A-I (2018) Enhancing cellulose functionalities by size reduction using media-mill. Sci Rep 8:11343

Dutzan N, Kajikawa T, Abusleme L, Greenwell-Wild T, Zuazo CE, Ikeuchi T, Brenchley L, Abe T, Hurabielle C, Martin D, Morell RJ, Freeman AF, Lazarevic V, Trinchieri G, Diaz PI, Holland SM, Belkaid Y, Hajishengallis G, Moutsopoulos NM (2018) A dysbiotic microbiome triggers TH17 cells to mediate oral mucosal immunopathology in mice and humans. Sci Transl Med 10

Dziarski R, Park SY, Des Kashyap R, Dowd SE, Gupta D (2016) Pglyrp-Regulated Gut Microflora Prevotella falsenii, Parabacteroides distasonis and Bacteroides eggerthii Enhance and Alistipes finegoldii Attenuates Colitis in Mice. PLoS ONE 11:e0146162

Eberl G, Colonna M, Di Santo JP, McKenzie ANJ (2015) Innate lymphoid cells. Innate lymphoid cells: A new paradigm in immunology. Science 348:aaa6566

Eichele DD, Kharbanda KK (2017) Dextran sodium sulfate colitis murine model: An indispensable tool for advancing our understanding of inflammatory bowel diseases pathogenesis. World J Gastroenterol 23:6016–6029

El Kaoutari A, Armougom F, Gordon JI, Raoult D, Henrissat B (2013) The abundance and variety of carbohydrate-active enzymes in the human gut microbiota. Nat Rev Microbiol 11:497–504

Ericsson AC, Gagliardi J, Bouhan D, Spollen WG, Givan SA, Franklin CL (2018) The influence of caging, bedding, and diet on the composition of the microbiota in different regions of the mouse gut. Sci Rep 8:4065

European Food Safety Authority (2010) Scientific Opinion on Dietary Reference Values for carbohydrates and dietary fibre: Question number: EFSA‐Q‐2008‐467. EFSA Journal 8:605

Eyerich K, Dimartino V, Cavani A (2017) IL-17 and IL-22 in immunity: Driving protection and pathology. Eur J Immunol 47:607–614

Ezeilo UR, Zakaria II, Huyop F, Wahab RA (2017) Enzymatic breakdown of lignocellulosic biomass: The role of glycosyl hydrolases and lytic polysaccharide monooxygenases. Biotechnology & Biotechnological Equipment 7:1–16

Faith JJ, Guruge JL, Charbonneau M, Subramanian S, Seedorf H, Goodman AL, Clemente JC, Knight R, Heath AC, Leibel RL, Rosenbaum M, Gordon JI (2013) The long-term stability of the human gut microbiota. Science 341:1237439

FAO/WHO (1998) Carbohydrates in human nutrition: Report of a joint FAO/WHO expert consultation, Rome, 14-18 April 1997. FAO food and nutrition paper, vol 66. World Health Organization, Rome

FAO/WHO codex alimentarius commission (2009) Report of the 30th session of the Codex Committee on Nutrition and Foods for Special Dietary Uses: ALINORM 02/32/26

Feng Q, Liang S, Jia H, Stadlmayr A, Tang L, Lan Z, Zhang D, Xia H, Xu X, Jie Z, Su L, Li X, Li X, Li J, Xiao L, Huber-Schönauer U, Niederseer D, Xu X, Al-Aama JY, Yang H, Wang J, Kristiansen K, Arumugam M, Tilg H, Datz C, Wang J (2015) Gut microbiome development along the colorectal adenoma-carcinoma sequence. Nat Commun 6:6528

Filippo C de, Di Paola M, Ramazzotti M, Albanese D, Pieraccini G, Banci E, Miglietta F, Cavalieri D, Lionetti P (2017) Diet, Environments, and Gut Microbiota. A Preliminary Investigation in Children Living in Rural and Urban Burkina Faso and Italy. Front Microbiol 8:1979

Flemer B, Gaci N, Borrel G, Sanderson IR, Chaudhary PP, Tottey W, O'Toole PW, Brugère J-F (2017) Fecal microbiota variation across the lifespan of the healthy laboratory rat. Gut Microbes 8:428–439

Fransen F, van Beek AA, Borghuis T, Aidy SE, Hugenholtz F, van der Gaast-de Jongh C, Savelkoul HFJ, Jonge MI de, Boekschoten MV, Smidt H, Faas MM, Vos P de (2017) Aged Gut Microbiota Contributes to Systemical Inflammaging after Transfer to Germ-Free Mice. Front Immunol 8:1385

Friedman ES, Bittinger K, Esipova TV, Hou L, Chau L, Jiang J, Mesaros C, Lund PJ, Liang X, FitzGerald GA, Goulian M, Lee D, Garcia BA, Blair IA, Vinogradov SA, Wu GD (2018) Microbes vs. chemistry in the origin of the anaerobic gut lumen. Proc Natl Acad Sci U S A 115:4170–4175

Fujino S, Andoh A, Bamba S, Ogawa A, Hata K, Araki Y, Bamba T, Fujiyama Y (2003) Increased expression of interleukin 17 in inflammatory bowel disease. Gut 52:65–70

Furusawa Y, Obata Y, Fukuda S, Endo TA, Nakato G, Takahashi D, Nakanishi Y, Uetake C, Kato K, Kato T, Takahashi M, Fukuda NN, Murakami S, Miyauchi E, Hino S, Atarashi K, Onawa S, Fujimura Y, Lockett T, Clarke JM, Topping DL, Tomita M, Hori S, Ohara O, Morita T, Koseki H, Kikuchi J, Honda K, Hase K, Ohno H (2013) Commensal microbe-derived butyrate induces the differentiation of colonic regulatory T cells. Nature 504:446–450

Furuse M, Fujita K, Hiiragi T, Fujimoto K, Tsukita S (1998) Claudin-1 and -2: Novel integral membrane proteins localizing at tight junctions with no sequence similarity to occludin. J Cell Biol 141:1539–1550

Furuse M, Hirase T, Itoh M, Nagafuchi A, Yonemura S, Tsukita S (1993) Occludin: A novel integral membrane protein localizing at tight junctions. J Cell Biol 123:1777–1788

Gao J, Xu K, Liu H, Liu G, Bai M, Peng C, Li T, Yin Y (2018) Impact of the Gut Microbiota on Intestinal Immunity Mediated by Tryptophan Metabolism. Front Cell Infect Microbiol 8:13

Gerbe F, Legraverend C, Jay P (2012) The intestinal epithelium tuft cells: Specification and function. Cell Mol Life Sci 69:2907–2917

Gewirtz AT, Navas TA, Lyons S, Godowski PJ, Madara JL (2001) Cutting edge: Bacterial flagellin activates basolaterally expressed TLR5 to induce epithelial proinflammatory gene expression. J Immunol 167:1882–1885

Gibson GR, Hutkins R, Sanders ME, Prescott SL, Reimer RA, Salminen SJ, Scott K, Stanton C, Swanson KS, Cani PD, Verbeke K, Reid G (2017) Expert consensus document: The International Scientific Association for Probiotics and Prebiotics (ISAPP) consensus statement on the definition and scope of prebiotics. Nat Rev Gastroenterol Hepatol 14:491–502

Gibson GR, Roberfroid MB (1995) Dietary modulation of the human colonic microbiota: Introducing the concept of prebiotics. J Nutr 125:1401–1412

Glocker E-O, Kotlarz D, Boztug K, Gertz EM, Schäffer AA, Noyan F, Perro M, Diestelhorst J, Allroth A, Murugan D, Hätscher N, Pfeifer D, Sykora K-W, Sauer M, Kreipe H, Lacher M, Nustede R, Woellner C, Baumann U, Salzer U, Koletzko S, Shah N, Segal AW, Sauerbrey A, Buderus S, Snapper SB, Grimbacher B, Klein C (2009) Inflammatory bowel disease and mutations affecting the interleukin-10 receptor. N Engl J Med 361:2033–2045

Gonzalez CA, Riboli E (2010) Diet and cancer prevention: Contributions from the European Prospective Investigation into Cancer and Nutrition (EPIC) study. Eur J Cancer 46:2555–2562

Gu S, Chen D, Zhang J-N, Lv X, Wang K, Duan L-P, Nie Y, Wu X-L (2013) Bacterial community mapping of the mouse gastrointestinal tract. PLoS ONE 8:e74957

Guan Q (2019) A Comprehensive Review and Update on the Pathogenesis of Inflammatory Bowel Disease. J Immunol Res 2019:7247238

Guillon F, Champ M (2000) Structural and physical properties of dietary fibres, and consequences of processing on human physiology. Food Research International 33:233–245

Haber AL, Biton M, Rogel N, Herbst RH, Shekhar K, Smillie C, Burgin G, Delorey TM, Howitt MR, Katz Y, Tirosh I, Beyaz S, Dionne D, Zhang M, Raychowdhury R, Garrett WS, Rozenblatt-Rosen O, Shi HN, Yilmaz O, Xavier RJ, Regev A (2017) A single-cell survey of the small intestinal epithelium. Nature 551:333–339

Hammer AM, Morris NL, Cannon AR, Khan OM, Gagnon RC, Movtchan NV, van Langeveld I, Li X, Gao B, Choudhry MA (2017) Interleukin-22 Prevents Microbial Dysbiosis and Promotes Intestinal Barrier Regeneration Following Acute Injury. Shock 48:657–665

Hang S, Paik D, Yao L, Kim E, Jamma T, Lu J, Ha S, Nelson BN, Kelly SP, Wu L, Zheng Y, Longman RS, Rastinejad F, Devlin AS, Krout MR, Fischbach MA, Littman DR, Huh JR (2019) Bile acid metabolites control TH17 and Treg cell differentiation. Nature 576:143–148

Hart ML, Ericsson AC, Franklin CL (2017) Differing Complex Microbiota Alter Disease Severity of the IL-10-/- Mouse Model of Inflammatory Bowel Disease. Front Microbiol 8:792

Helander HF, Fändriks L (2014) Surface area of the digestive tract - revisited. Scand J Gastroenterol 49:681–689

Hendrikx T, Duan Y, Wang Y, Oh J-H, Alexander LM, Huang W, Stärkel P, Ho SB, Gao B, Fiehn O, Emond P, Sokol H, van Pijkeren J-P, Schnabl B (2019) Bacteria engineered to produce IL-22 in intestine induce expression of REG3G to reduce ethanol-induced liver disease in mice. Gut 68:1504–1515

Hernández-Chirlaque C, Aranda CJ, Ocón B, Capitán-Cañadas F, Ortega-González M, Carrero JJ, Suárez MD, Zarzuelo A, Sánchez de Medina F, Martínez-Augustin O (2016) Germ-free and Antibiotic-treated Mice are Highly Susceptible to Epithelial Injury in DSS Colitis. J Crohns Colitis 10:1324–1335

Höfte H, Voxeur A (2017) Plant cell walls. Curr Biol 27:R865-R870

Hollister EB, Riehle K, Luna RA, Weidler EM, Rubio-Gonzales M, Mistretta T-A, Raza S, Doddapaneni HV, Metcalf GA, Muzny DM, Gibbs RA, Petrosino JF, Shulman RJ, Versalovic J (2015) Structure and function of the healthy pre-adolescent pediatric gut microbiome. Microbiome 3:36

Hon DN-S (1994) Cellulose: A random walk along its historical path. Cellulose 1:1–25

Hou JK, Abraham B, El-Serag H (2011) Dietary intake and risk of developing inflammatory bowel disease: A systematic review of the literature. Am J Gastroenterol 106:563–573

Huerta-Cepas J, Szklarczyk D, Forslund K, Cook H, Heller D, Walter MC, Rattei T, Mende DR, Sunagawa S, Kuhn M, Jensen LJ, Mering C von, Bork P (2016) eggNOG 4.5: A hierarchical orthology framework with improved functional annotations for eukaryotic, prokaryotic and viral sequences

Human Microbiome Project Consortium (2012) Structure, function and diversity of the healthy human microbiome. Nature 486:207–214

Hungate RE (1966) Rumen and Its Microbes. Elsevier Science, s.l.

Isomäki AM (1973) A new cell type (tuft cell) in the gastrointestinal mucosa of the rat. A transmission and scanning electron microscopic study. Acta Pathol Microbiol Scand A:Suppl 240:1-35

Ivanov II, Atarashi K, Manel N, Brodie EL, Shima T, Karaoz U, Wei D, Goldfarb KC, Santee CA, Lynch SV, Tanoue T, Imaoka A, Itoh K, Takeda K, Umesaki Y, Honda K, Littman DR (2009) Induction of intestinal Th17 cells by segmented filamentous bacteria. Cell 139:485–498

Ivanov II, Frutos RdL, Manel N, Yoshinaga K, Rifkin DB, Sartor RB, Finlay BB, Littman DR (2008) Specific microbiota direct the differentiation of IL-17-producing T-helper cells in the mucosa of the small intestine. Cell Host Microbe 4:337–349

Ivanov II, McKenzie BS, Zhou L, Tadokoro CE, Lepelley A, Lafaille JJ, Cua DJ, Littman DR (2006) The orphan nuclear receptor RORgammat directs the differentiation program of proinflammatory IL-17+ T helper cells. Cell 126:1121–1133

Jiang W, Wu N, Wang X, Chi Y, Zhang Y, Qiu X, Hu Y, Li J, Liu Y (2015) Dysbiosis gut microbiota associated with inflammation and impaired mucosal immune function in intestine of humans with non-alcoholic fatty liver disease. Sci Rep 5:8096

Johansson MEV, Hansson GC (2016) Immunological aspects of intestinal mucus and mucins. Nat Rev Immunol 16:639–649

Johansson MEV, Jakobsson HE, Holmén-Larsson J, Schütte A, Ermund A, Rodríguez-Piñeiro AM, Arike L, Wising C, Svensson F, Bäckhed F, Hansson GC (2015) Normalization of Host Intestinal Mucus Layers Requires Long-Term Microbial Colonization. Cell Host Microbe 18:582–592

Johansson MEV, Phillipson M, Petersson J, Velcich A, Holm L, Hansson GC (2008) The inner of the two Muc2 mucin-dependent mucus layers in colon is devoid of bacteria. Proc Natl Acad Sci U S A 105:15064–15069

Jones JM (2014) CODEX-aligned dietary fiber definitions help to bridge the 'fiber gap'. Nutr J 13:34

Kasahara K, Krautkramer KA, Org E, Romano KA, Kerby RL, Vivas EI, Mehrabian M, Denu JM, Bäckhed F, Lusis AJ, Rey FE (2018) Interactions between Roseburia intestinalis and diet modulate atherogenesis in a murine model. Nat Microbiol 3:1461–1471

Kayama H, Takeda K (2012) Regulation of intestinal homeostasis by innate and adaptive immunity. Int Immunol 24:673–680

Kayama H, Takeda K (2020) Manipulation of epithelial integrity and mucosal immunity by host and microbiota-derived metabolites. Eur J Immunol

Kelleher J, Walters MP, Srinivasan TR, Hart G, Findlay JM, Losowsky MS (1984) Degradation of cellulose within the gastrointestinal tract in man. Gut 25:811–815

Kellock B (1985) The fiber man: The life story of Dr Denis Burkitt, 1st ed. Lion paperback. Lion Pub. Co, Tring, Belleville, Mich.

Kempski J, Brockmann L, Gagliani N, Huber S (2017) TH17 Cell and Epithelial Cell Crosstalk during Inflammatory Bowel Disease and Carcinogenesis. Front Immunol 8:1373

Kespohl M, Vachharajani N, Luu M, Harb H, Pautz S, Wolff S, Sillner N, Walker A, Schmitt-Kopplin P, Boettger T, Renz H, Offermanns S, Steinhoff U, Visekruna A (2017) The Microbial Metabolite Butyrate Induces Expression of Th1-Associated Factors in CD4+ T Cells. Front Immunol 8:1036

Khatri IA, Ho C, Specian RD, Forstner JF (2001) Characteristics of rodent intestinal mucin Muc3 and alterations in a mouse model of human cystic fibrosis. Am J Physiol Gastrointest Liver Physiol 280:G1321-30

Kim DJ, Yoon S, Ji SC, Yang J, Kim Y-K, Lee S, Yu K-S, Jang I-J, Chung J-Y, Cho J-Y (2018) Ursodeoxycholic acid improves liver function via phenylalanine/tyrosine pathway and microbiome remodelling in patients with liver dysfunction. Sci Rep 8:11874

Kim M, Morrison M, Yu Z (2011) Evaluation of different partial 16S rRNA gene sequence regions for phylogenetic analysis of microbiomes. J Microbiol Methods 84:81–87

Kim M, Qie Y, Park J, Kim CH (2016) Gut Microbial Metabolites Fuel Host Antibody Responses. Cell Host Microbe 20:202–214

Kim SK, Kim YM, Yeum CE, Jin S-H, Chae GT, Lee S-B (2009) Rifampicin Inhibits the LPS-induced Expression of Toll-like Receptor 2 via the Suppression of NF-κB DNA-binding Activity in RAW 264.7 Cells. Korean J Physiol Pharmacol 13:475

Kim Y, Hwang SW, Kim S, Lee Y-S, Kim T-Y, Lee S-H, Kim SJ, Yoo HJ, Kim EN, Kweon M-N (2020) Dietary cellulose prevents gut inflammation by modulating lipid metabolism and gut microbiota. Gut Microbes:1–18

Klampfl CW, Buchberger W (2001) Determination of carbohydrates by capillary electrophoresis with electrospray-mass spectrometric detection

Kleinschek MA, Boniface K, Sadekova S, Grein J, Murphy EE, Turner SP, Raskin L, Desai B, Faubion WA, Waal Malefyt R de, Pierce RH, McClanahan T, Kastelein RA (2009) Circulating and gut-resident human Th17 cells express CD161 and promote intestinal inflammation. J Exp Med 206:525–534

Klindworth A, Pruesse E, Schweer T, Peplies J, Quast C, Horn M, Glöckner FO (2013) Evaluation of general 16S ribosomal RNA gene PCR primers for classical and next-generation sequencing-based diversity studies. Nucleic Acids Res 41:e1

Klose CSN, Artis D (2016) Innate lymphoid cells as regulators of immunity, inflammation and tissue homeostasis. Nat Immunol 17:765–774

Koenig JE, Spor A, Scalfone N, Fricker AD, Stombaugh J, Knight R, Angenent LT, Ley RE (2011) Succession of microbial consortia in the developing infant gut microbiome. Proc Natl Acad Sci U S A 108 Suppl 1:4578–4585

Koh A, Vadder F de, Kovatcheva-Datchary P, Bäckhed F (2016) From Dietary Fiber to Host Physiology: Short-Chain Fatty Acids as Key Bacterial Metabolites. Cell 165:1332–1345

Kronman MP, Zaoutis TE, Haynes K, Feng R, Coffin SE (2012) Antibiotic exposure and IBD development among children: A population-based cohort study. Pediatrics 130:e794-803

Kühn R, Löhler J, Rennick D, Rajewsky K, Müller W (1993) Interleukin-10-deficient mice develop chronic enterocolitis. Cell 75:263–274

Kurdi P, Kawanishi K, Mizutani K, Yokota A (2006) Mechanism of growth inhibition by free bile acids in lactobacilli and bifidobacteria. J Bacteriol 188:1979–1986

La Rosa SL, Leth ML, Michalak L, Hansen ME, Pudlo NA, Glowacki R, Pereira G, Workman CT, Arntzen MØ, Pope PB, Martens EC, Hachem MA, Westereng B (2019) The human gut Firmicute Roseburia intestinalis is a primary degrader of dietary β-mannans. Nat Commun 10:905

Lagkouvardos I, Fischer S, Kumar N, Clavel T (2017) Rhea: A transparent and modular R pipeline for microbial profiling based on 16S rRNA gene amplicons. PeerJ 5:e2836

Lagkouvardos I, Joseph D, Kapfhammer M, Giritli S, Horn M, Haller D, Clavel T (2016) IMNGS: A comprehensive open resource of processed 16S rRNA microbial profiles for ecology and diversity studies. Sci Rep 6:33721

Lagkouvardos I, Kläring K, Heinzmann SS, Platz S, Scholz B, Engel K-H, Schmitt-Kopplin P, Haller D, Rohn S, Skurk T, Clavel T (2015) Gut metabolites and bacterial community networks during a pilot intervention study with flaxseeds in healthy adult men. Mol Nutr Food Res 59:1614–1628

Lairon D, Arnault N, Bertrais S, Planells R, Clero E, Hercberg S, Boutron-Ruault M-C (2005) Dietary fiber intake and risk factors for cardiovascular disease in French adults. Am J Clin Nutr 82:1185–1194

Lange KM de, Moutsianas L, Lee JC, Lamb CA, Luo Y, Kennedy NA, Jostins L, Rice DL, Gutierrez-Achury J, Ji S-G, Heap G, Nimmo ER, Edwards C, Henderson P, Mowat C, Sanderson J, Satsangi J, Simmons A, Wilson DC, Tremelling M, Hart A, Mathew

CG, Newman WG, Parkes M, Lees CW, Uhlig H, Hawkey C, Prescott NJ, Ahmad T, Mansfield JC, Anderson CA, Barrett JC (2017) Genome-wide association study implicates immune activation of multiple integrin genes in inflammatory bowel disease. Nat Genet 49:256–261

Langille MG, Meehan CJ, Koenig JE, Dhanani AS, Rose RA, Howlett SE, Beiko RG (2014) Microbial shifts in the aging mouse gut. Microbiome 2:50

Le Leu RK, Hu Y, Young GP (2002) Effects of resistant starch and nonstarch polysaccharides on colonic luminal environment and genotoxin-induced apoptosis in the rat. Carcinogenesis 23:713–719

Lee J, Gonzales-Navajas JM, Raz E (2008) The "polarizing-tolerizing" mechanism of intestinal epithelium: Its relevance to colonic homeostasis. Semin Immunopathol 30:3–9

Lee J, Mo J-H, Katakura K, Alkalay I, Rucker AN, Liu Y-T, Lee H-K, Shen C, Cojocaru G, Shenouda S, Kagnoff M, Eckmann L, Ben-Neriah Y, Raz E (2006) Maintenance of colonic homeostasis by distinctive apical TLR9 signalling in intestinal epithelial cells. Nat Cell Biol 8:1327–1336

Lee YK, Menezes JS, Umesaki Y, Mazmanian SK (2011) Proinflammatory T-cell responses to gut microbiota promote experimental autoimmune encephalomyelitis. Proc Natl Acad Sci U S A 108 Suppl 1:4615–4622

Levi Mortera S, Soggiu A, Vernocchi P, Del Chierico F, Piras C, Carsetti R, Marzano V, Britti D, Urbani A, Roncada P, Putignani L (2019) Metaproteomic investigation to assess gut microbiota shaping in newborn mice: A combined taxonomic, functional and quantitative approach. J Proteomics 203:103378

Lewis G, Wang B, Shafiei Jahani P, Hurrell BP, Banie H, Aleman Muench GR, Maazi H, Helou DG, Howard E, Galle-Treger L, Lo R, Santosh S, Baltus A, Bongers G, San-Mateo L, Gilliland FD, Rehan VK, Soroosh P, Akbari O (2019) Dietary Fiber-Induced Microbial Short Chain Fatty Acids Suppress ILC2-Dependent Airway Inflammation. Front Immunol 10:2051

Li D, Chen H, Mao B, Yang Q, Zhao J, Gu Z, Zhang H, Chen YQ, Chen W (2017) Microbial Biogeography and Core Microbiota of the Rat Digestive Tract. Sci Rep 8:45840

Liang SC, Tan X-Y, Luxenberg DP, Karim R, Dunussi-Joannopoulos K, Collins M, Fouser LA (2006) Interleukin (IL)-22 and IL-17 are coexpressed by Th17 cells and cooperatively enhance expression of antimicrobial peptides. J Exp Med 203:2271–2279

Lin L, Kan X, Yan H, Wang D (2012) Characterization of extracellular cellulose-degrading enzymes from Bacillus thuringiensis strains. Electron. J. Biotechnol. 15

Lloyd-Price J, Arze C, Ananthakrishnan AN, Schirmer M, Avila-Pacheco J, Poon TW, Andrews E, Ajami NJ, Bonham KS, Brislawn CJ, Casero D, Courtney H, Gonzalez

A, Graeber TG, Hall AB, Lake K, Landers CJ, Mallick H, Plichta DR, Prasad M, Rahnavard G, Sauk J, Shungin D, Vázquez-Baeza Y, White RA, Braun J, Denson LA, Jansson JK, Knight R, Kugathasan S, McGovern DPB, Petrosino JF, Stappenbeck TS, Winter HS, Clish CB, Franzosa EA, Vlamakis H, Xavier RJ, Huttenhower C (2019) Multi-omics of the gut microbial ecosystem in inflammatory bowel diseases. Nature 569:655–662

Lo Presti A, Zorzi F, Del Chierico F, Altomare A, Cocca S, Avola A, Biasio F de, Russo A, Cella E, Reddel S, Calabrese E, Biancone L, Monteleone G, Cicala M, Angeletti S, Ciccozzi M, Putignani L, Guarino MPL (2019) Fecal and Mucosal Microbiota Profiling in Irritable Bowel Syndrome and Inflammatory Bowel Disease. Front Microbiol 10:1655

Loonen LMP, Stolte EH, Jaklofsky MTJ, Meijerink M, Dekker J, van Baarlen P, Wells JM (2014) REG3γ-deficient mice have altered mucus distribution and increased mucosal inflammatory responses to the microbiota and enteric pathogens in the ileum. Mucosal Immunol 7:939–947

López P, González-Rodríguez I, Gueimonde M, Margolles A, Suárez A (2011) Immune response to Bifidobacterium bifidum strains support Treg/Th17 plasticity. PLoS ONE 6:e24776

Mabbott NA, Donaldson DS, Ohno H, Williams IR, Mahajan A (2013) Microfold (M) cells: Important immunosurveillance posts in the intestinal epithelium. Mucosal Immunol 6:666–677

Madsen D, Beaver M, Chang L, Bruckner-Kardoss E, Wostmann B (1976) Analysis of bile acids in conventional and germfree rats. J Lipid Res 17:107–111

Maeda Y, Kurakawa T, Umemoto E, Motooka D, Ito Y, Gotoh K, Hirota K, Matsushita M, Furuta Y, Narazaki M, Sakaguchi N, Kayama H, Nakamura S, Iida T, Saeki Y, Kumanogoh A, Sakaguchi S, Takeda K (2016) Dysbiosis Contributes to Arthritis Development via Activation of Autoreactive T Cells in the Intestine. Arthritis & rheumatology (Hoboken, N.J.) 68:2646–2661

Maesschalck C de, Eeckhaut V, Maertens L, Lange L de, Marchal L, Daube G, Dewulf J, Haesebrouck F, Ducatelle R, Taminau B, van Immerseel F (2019) Amorphous cellulose feed supplement alters the broiler caecal microbiome. Poult Sci 98:3811–3817

Maloy KJ, Powrie F (2011) Intestinal homeostasis and its breakdown in inflammatory bowel disease. Nature 474:298–306

Mancabelli L, Milani C, Lugli GA, Turroni F, Cocconi D, van Sinderen D, Ventura M (2017) Identification of universal gut microbial biomarkers of common human intestinal diseases by meta-analysis. FEMS Microbiol Ecol 93

Mantis NJ, Rol N, Corthésy B (2011) Secretory IgA's complex roles in immunity and mucosal homeostasis in the gut. Mucosal Immunol 4:603–611

Mariat D, Firmesse O, Levenez F, Guimarães V, Sokol H, Doré J, Corthier G, Furet J-P (2009) The Firmicutes/Bacteroidetes ratio of the human microbiota changes with age. BMC Microbiol 9:123

Martinez-Guryn K, Leone V, Chang EB (2019) Regional Diversity of the Gastrointestinal Microbiome. Cell Host Microbe 26:314–324

Mashimo H, Wu DC, Podolsky DK, Fishman MC (1996) Impaired defense of intestinal mucosa in mice lacking intestinal trefoil factor. Science 274:262–265

Maslowski KM, Mackay CR (2011) Diet, gut microbiota and immune responses. Nat Immunol 12:5–9

Max Rubner-Institut & Bundesinstitut für Ernährung und Lebensmittel (2008) Nationale Verzehrsstudie II: Ergebnisbericht Teil 2

Maynard CL, Weaver CT (2009) Intestinal effector T cells in health and disease. Immunity 31:389–400

McDermott AJ, Huffnagle GB (2014) The microbiome and regulation of mucosal immunity. Immunology 142:24–31

Meij TGJ de, Groot EFJ de, Peeters CFW, Boer NKH de, Kneepkens CMF, Eck A, Benninga MA, Savelkoul PHM, van Bodegraven AA, Budding AE (2018) Variability of core microbiota in newly diagnosed treatment-naïve paediatric inflammatory bowel disease patients. PLoS ONE 13:e0197649

Mesa MD, Loureiro B, Iglesia I, Fernandez Gonzalez S, Llurba Olivé E, García Algar O, Solana MJ, Cabero Perez MJ, Sainz T, Martinez L, Escuder-Vieco D, Parra-Llorca A, Sánchez-Campillo M, Rodriguez Martinez G, Gómez Roig D, Perez Gruz M, Andreu-Fernández V, Clotet J, Sailer S, Iglesias-Platas I, López-Herce J, Aras R, Pallás-Alonso C, Pipaon MS de, Vento M, Gormaz M, Larqué Daza E, Calvo C, Cabañas F (2020) The Evolving Microbiome from Pregnancy to Early Infancy: A Comprehensive Review. Nutrients 12

Messer JS, Chang EB (eds) Microbial Physiology of the Digestive Tract and Its Role in Inflammatory Bowel Diseases

Metzler S, Frei R, Schmaußer-Hechfellner E, Mutius E von, Pekkanen J, Karvonen AM, Kirjavainen PV, Dalphin J-C, Divaret-Chauveau A, Riedler J, Lauener R, Roduit C (2019) Association between antibiotic treatment during pregnancy and infancy and the development of allergic diseases. Pediatr Allergy Immunol 30:423–433

Moens E, Veldhoen M (2012) Epithelial barrier biology: Good fences make good neighbours. Immunology 135:1–8

Monteleone I, Rizzo A, Sarra M, Sica G, Sileri P, Biancone L, MacDonald TT, Pallone F, Monteleone G (2011) Aryl hydrocarbon receptor-induced signals up-regulate IL-22 production and inhibit inflammation in the gastrointestinal tract. Gastroenterology 141:237-48, 248.e1

Morowitz MJ, Di Caro V, Pang D, Cummings J, Firek B, Rogers MB, Ranganathan S, Clark RSB, Aneja RK (2017) Dietary Supplementation With Nonfermentable Fiber Alters the Gut Microbiota and Confers Protection in Murine Models of Sepsis. Crit Care Med 45:e516-e523

Moschen AR, Gerner RR, Wang J, Klepsch V, Adolph TE, Reider SJ, Hackl H, Pfister A, Schilling J, Moser PL, Kempster SL, Swidsinski A, Orth Höller D, Weiss G, Baines JF, Kaser A, Tilg H (2016) Lipocalin 2 Protects from Inflammation and Tumorigenesis Associated with Gut Microbiota Alterations. Cell Host Microbe 19:455–469

Mowat AM (2003) Anatomical basis of tolerance and immunity to intestinal antigens. Nature Reviews Immunology 3:331–341

Mowat AM, Agace WW (2014) Regional specialization within the intestinal immune system. Nat Rev Immunol 14:667–685

Munyaka PM, Rabbi MF, Khafipour E, Ghia J-E (2016) Acute dextran sulfate sodium (DSS)-induced colitis promotes gut microbial dysbiosis in mice. J Basic Microbiol 56:986–998

Nagakura Y, Naitoh Y, Kamato T, Yamano M, Miyata K (1996) Compounds possessing 5-HT3 receptor antagonistic activity inhibit intestinal propulsion in mice. European Journal of Pharmacology 311:67–72

Nagy-Szakal D, Hollister EB, Luna RA, Szigeti R, Tatevian N, Smith CW, Versalovic J, Kellermayer R (2013) Cellulose supplementation early in life ameliorates colitis in adult mice. PLoS ONE 8:e56685

Nakamoto N, Amiya T, Aoki R, Taniki N, Koda Y, Miyamoto K, Teratani T, Suzuki T, Chiba S, Chu P-S, Hayashi A, Yamaguchi A, Shiba S, Miyake R, Katayama T, Suda W, Mikami Y, Kamada N, Ebinuma H, Saito H, Hattori M, Kanai T (2017) Commensal Lactobacillus Controls Immune Tolerance during Acute Liver Injury in Mice. Cell Rep 21:1215–1226

Nava GM, Friedrichsen HJ, Stappenbeck TS (2011) Spatial organization of intestinal microbiota in the mouse ascending colon. ISME J 5:627–638

Ng SC, Shi HY, Hamidi N, Underwood FE, Tang W, Benchimol EI, Panaccione R, Ghosh S, Wu JCY, Chan FKL, Sung JJY, Kaplan GG (2017) Worldwide incidence and prevalence of inflammatory bowel disease in the 21st century: A systematic review of population-based studies. The Lancet 390:2769–2778

Ni J, Wu GD, Albenberg L, Tomov VT (2017) Gut microbiota and IBD: Causation or correlation? Nat Rev Gastroenterol Hepatol 14:573–584

Nicholson JK, Holmes E, Kinross J, Burcelin R, Gibson G, Jia W, Pettersson S (2012) Host-gut microbiota metabolic interactions. Science 336:1262–1267

Odamaki T, Kato K, Sugahara H, Hashikura N, Takahashi S, Xiao J-Z, Abe F, Osawa R (2016) Age-related changes in gut microbiota composition from newborn to centenarian: A cross-sectional study. BMC Microbiol 16:90

O'Hara AM, Shanahan F (2006) The gut flora as a forgotten organ. EMBO Rep 7:688–693

Ohnmacht C, Park J-H, Cording S, Wing JB, Atarashi K, Obata Y, Gaboriau-Routhiau V, Marques R, Dulauroy S, Fedoseeva M, Busslinger M, Cerf-Bensussan N, Boneca IG, Voehringer D, Hase K, Honda K, Sakaguchi S, Eberl G (2015) MUCOSAL IMMUNOLOGY. The microbiota regulates type 2 immunity through RORγt^{+} T cells. Science 349:989–993

Okayasu I, Hatakeyama S, Yamada M, Ohkusa T, Inagaki Y, Nakaya R (1990) A novel method in the induction of reliable experimental acute and chronic ulcerative colitis in mice. Gastroenterology 98:694–702

O'Keefe SJ (2019) The association between dietary fibre deficiency and high-income lifestyle-associated diseases: Burkitt's hypothesis revisited. The Lancet Gastroenterology & Hepatology 4:984–996

Okumura R, Takeda K (2017) Roles of intestinal epithelial cells in the maintenance of gut homeostasis. Exp Mol Med 49:e338

Omenetti S, Bussi C, Metidji A, Iseppon A, Lee S, Tolaini M, Li Y, Kelly G, Chakravarty P, Shoaie S, Gutierrez MG, Stockinger B (2019) The Intestine Harbors Functionally Distinct Homeostatic Tissue-Resident and Inflammatory Th17 Cells. Immunity 51:77-89.e6

Omenetti S, Pizarro TT (2015) The Treg/Th17 Axis: A Dynamic Balance Regulated by the Gut Microbiome. Front Immunol 6:639

O'Sullivan A (1997) Cellulose: the structure slowly unravels. Cellulose 4:173–207

Ott SJ, Musfeldt M, Wenderoth DF, Hampe J, Brant O, Fölsch UR, Timmis KN, Schreiber S (2004) Reduction in diversity of the colonic mucosa associated bacterial microflora in patients with active inflammatory bowel disease. Gut 53:685–693

Owen RL, Jones AL (1974) Epithelial Cell Specialization within Human Peyer's Patches: An Ultrastructural Study of Intestinal Lymphoid Follicles. Gastroenterology 66:189–203

Pantoja-Feliciano IG, Clemente JC, Costello EK, Perez ME, Blaser MJ, Knight R, Dominguez-Bello MG (2013) Biphasic assembly of the murine intestinal microbiota during early development. ISME J 7:1112–1115

Park H, Li Z, Yang XO, Chang SH, Nurieva R, Wang Y-H, Wang Y, Hood L, Zhu Z, Tian Q, Dong C (2005) A distinct lineage of CD4 T cells regulates tissue inflammation by producing interleukin 17. Nat Immunol 6:1133–1141

Parks OB, Pociask DA, Hodzic Z, Kolls JK, Good M (2015) Interleukin-22 Signaling in the Regulation of Intestinal Health and Disease. Front Cell Dev Biol 3:85

Parlato M, Yeretssian G (2014) NOD-like receptors in intestinal homeostasis and epithelial tissue repair. Int J Mol Sci 15:9594–9627

Pearce SC, Al-Jawadi A, Kishida K, Yu S, Hu M, Fritzky LF, Edelblum KL, Gao N, Ferraris RP (2018) Marked differences in tight junction composition and macromolecular permeability among different intestinal cell types. BMC Biol 16:19

Pédron T, Mulet C, Dauga C, Frangeul L, Chervaux C, Grompone G (2012) A crypt-specific core microbiota resides in the mouse colon. MBio 3

Pellizzon MA, Ricci MR (2019) Nutriphenomics in Rodent Models. In: Gupta RC (ed) Biomarkers in toxicology, Second edition. Elsevier/Academic Press, London, pp 715–731

Peng X, Li S, Luo J, Wu X, Liu L (2013) Effects of dietary fibers and their mixtures on short chain fatty acids and microbiota in mice guts. Food Funct 4:932–938

Petersen C, Round JL (2014) Defining dysbiosis and its influence on host immunity and disease. Cell Microbiol 16:1024–1033

Pickard JM, Zeng MY, Caruso R, Núñez G (2017) Gut microbiota: Role in pathogen colonization, immune responses, and inflammatory disease. Immunol Rev 279:70–89

Pickert G, Neufert C, Leppkes M, Zheng Y, Wittkopf N, Warntjen M, Lehr H-A, Hirth S, Weigmann B, Wirtz S, Ouyang W, Neurath MF, Becker C (2009) STAT3 links IL-22 signaling in intestinal epithelial cells to mucosal wound healing. J Exp Med 206:1465–1472

Puchtler H, Waldrop FS, Meloan SN, Terry MS, Conner HM (1970) Methacarn (methanol-Carnoy) fixation. Practical and theoretical considerations. Histochemie 21:97–116

Qin J, Li R, Raes J, Arumugam M, Burgdorf KS, Manichanh C, Nielsen T, Pons N, Levenez F, Yamada T, Mende DR, Li J, Xu J, Li S, Li D, Cao J, Wang B, Liang H, Zheng H, Xie Y, Tap J, Lepage P, Bertalan M, Batto J-M, Hansen T, Le Paslier D, Linneberg A, Nielsen HB, Pelletier E, Renault P, Sicheritz-Ponten T, Turner K, Zhu H, Yu C, Li S, Jian M, Zhou Y, Li Y, Zhang X, Li S, Qin N, Yang H, Wang J, Brunak S, Doré J, Guarner F, Kristiansen K, Pedersen O, Parkhill J, Weissenbach J, Bork P, Ehrlich SD, Wang J (2010) A human gut microbial gene catalogue established by metagenomic sequencing. Nature 464:59–65

Rajilić-Stojanović M, Vos WM de (2014) The first 1000 cultured species of the human gastrointestinal microbiota. FEMS Microbiol Rev 38:996–1047

Rausch P, Basic M, Batra A, Bischoff SC, Blaut M, Clavel T, Gläsner J, Gopalakrishnan S, Grassl GA, Günther C, Haller D, Hirose M, Ibrahim S, Loh G, Mattner J, Nagel S, Pabst O, Schmidt F, Siegmund B, Strowig T, Volynets V, Wirtz S, Zeissig S, Zeissig Y, Bleich A, Baines JF (2016) Analysis of factors contributing to variation in the C57BL/6J fecal microbiota across German animal facilities. Int J Med Microbiol 306:343–355

Rautio M, Eerola E, Väisänen-Tunkelrott M-L, Molitoris D, Lawson P, Collins MD, Jousimies-Somer H (2003) Reclassification of Bacteroides putredinis (Weinberg et al., 1937) in a new genus Alistipes gen. nov., as Alistipes putredinis comb. nov., and description of Alistipes finegoldii sp. nov., from human sources. Syst Appl Microbiol 26:182–188

Rescigno M, Urbano M, Valzasina B, Francolini M, Rotta G, Bonasio R, Granucci F, Kraehenbuhl JP, Ricciardi-Castagnoli P (2001) Dendritic cells express tight junction proteins and penetrate gut epithelial monolayers to sample bacteria. Nat Immunol 2:361–367

Richards AL, Burns MB, Alazizi A, Barreiro LB, Pique-Regi R, Blekhman R, Luca F (2016) Genetic and transcriptional analysis of human host response to healthy gut microbiota. mSystems 1

Ridlon JM, Kang DJ, Hylemon PB, Bajaj JS (2014) Bile acids and the gut microbiome. Curr Opin Gastroenterol 30:332–338

Ridlon JM, Kang D-J, Hylemon PB (2006) Bile salt biotransformations by human intestinal bacteria. J Lipid Res 47:241–259

Riva A, Kuzyk O, Forsberg E, Siuzdak G, Pfann C, Herbold C, Daims H, Loy A, Warth B, Berry D (2019) A fiber-deprived diet disturbs the fine-scale spatial architecture of the murine colon microbiome. Nat Commun 10:4366

Robert C, Bernalier-Donadille A (2003) The cellulolytic microflora of the human colon: Evidence of microcrystalline cellulose-degrading bacteria in methane-excreting subjects. FEMS Microbiol Ecol 46:81–89

Rogala AR, Oka A, Sartor RB (2020) Strategies to Dissect Host-Microbial Immune Interactions That Determine Mucosal Homeostasis vs. Intestinal Inflammation in Gnotobiotic Mice. Front Immunol 11:1268

Rojas R, Apodaca G (2002) Immunoglobulin transport across polarized epithelial cells. Nat Rev Mol Cell Biol 3:944–955

Rosenholm J, Desai D, Prabhakar N, Mamaeva V, Sen Karaman D, Lähdeniemi I, Sahlgren C, Toivola D (2016) Targeted modulation of cell differentiation in distinct regions of the gastrointestinal tract via oral administration of differently PEG-PEI functionalized mesoporous silica nanoparticles. IJN:299

Russell JB, Muck RE, Weimer PJ (2009) Quantitative analysis of cellulose degradation and growth of cellulolytic bacteria in the rumen. FEMS Microbiol Ecol 67:183–197

Sayin SI, Wahlström A, Felin J, Jäntti S, Marschall H-U, Bamberg K, Angelin B, Hyötyläinen T, Orešič M, Bäckhed F (2013) Gut microbiota regulates bile acid metabolism by reducing the levels of tauro-beta-muricholic acid, a naturally occurring FXR antagonist. Cell Metab 17:225–235

Sefik E, Geva-Zatorsky N, Oh S, Konnikova L, Zemmour D, McGuire AM, Burzyn D, Ortiz-Lopez A, Lobera M, Yang J, Ghosh S, Earl A, Snapper SB, Jupp R, Kasper D, Mathis D, Benoist C (2015) MUCOSAL IMMUNOLOGY. Individual intestinal symbionts induce a distinct population of RORγ$^+$ regulatory T cells. Science 349:993–997

Sillner N, Walker A, Koch W, Witting M, Schmitt-Kopplin P (2018) Metformin impacts cecal bile acid profiles in mice. J Chromatogr B Analyt Technol Biomed Life Sci 1083:35–43

Sjölund K, Sandén G, Håkanson R, Sundler F (1983) Endocrine Cells in Human Intestine: An Immunocytochemical Study. Gastroenterology 85:1120–1130

Slavin JL, Brauer PM, Marlett JA (1981) Neutral detergent fiber, hemicellulose and cellulose digestibility in human subjects. J Nutr 111:287–297

Smith PM, Howitt MR, Panikov N, Michaud M, Gallini CA, Bohlooly-Y M, Glickman JN, Garrett WS (2013) The microbial metabolites, short-chain fatty acids, regulate colonic Treg cell homeostasis. Science 341:569–573

Snoeck V, Goddeeris B, Cox E (2005) The role of enterocytes in the intestinal barrier function and antigen uptake. Microbes Infect 7:997–1004

Song X, Sun X, Oh SF, Wu M, Zhang Y, Zheng W, Geva-Zatorsky N, Jupp R, Mathis D, Benoist C, Kasper DL (2020) Microbial bile acid metabolites modulate gut RORγ+ regulatory T cell homeostasis. Nature 577:410–415

Sonnenberg GF, Nair MG, Kirn TJ, Zaph C, Fouser LA, Artis D (2010) Pathological versus protective functions of IL-22 in airway inflammation are regulated by IL-17A. J Exp Med 207:1293–1305

Sonnenburg ED, Smits SA, Tikhonov M, Higginbottom SK, Wingreen NS, Sonnenburg JL (2016) Diet-induced extinctions in the gut microbiota compound over generations. Nature 529:212–215

Sonnenburg ED, Sonnenburg JL (2014) Starving our microbial self: The deleterious consequences of a diet deficient in microbiota-accessible carbohydrates. Cell Metab 20:779–786

Statovci D, Aguilera M, MacSharry J, Melgar S (2017) The Impact of Western Diet and Nutrients on the Microbiota and Immune Response at Mucosal Interfaces. Front Immunol 8:838

Stephen AM, Champ MM-J, Cloran SJ, Fleith M, van Lieshout L, Mejborn H, Burley VJ (2017) Dietary fibre in Europe: Current state of knowledge on definitions, sources, recommendations, intakes and relationships to health. Nutr Res Rev 30:149–190

Stevenson BR, Siliciano JD, Mooseker MS, Goodenough DA (1986) Identification of ZO-1: A high molecular weight polypeptide associated with the tight junction (zonula occludens) in a variety of epithelia. J Cell Biol 103:755–766

Stewart CJ, Ajami NJ, O'Brien JL, Hutchinson DS, Smith DP, Wong MC, Ross MC, Lloyd RE, Doddapaneni H, Metcalf GA, Muzny D, Gibbs RA, Vatanen T, Huttenhower C, Xavier RJ, Rewers M, Hagopian W, Toppari J, Ziegler A-G, She J-X, Akolkar B, Lernmark A, Hyoty H, Vehik K, Krischer JP, Petrosino JF (2018) Temporal development of the gut microbiome in early childhood from the TEDDY study. Nature 562:583–588

Strachan DP (1989) Hay fever, hygiene, and household size. BMJ 299:1259–1260

Suemori S, Lynch-Devaney K, Podolsky DK (1991) Identification and characterization of rat intestinal trefoil factor: Tissue- and cell-specific member of the trefoil protein family. Proc Natl Acad Sci U S A 88:11017–11021

Sun T, Liu S, Zhou Y, Yao Z, Zhang D, Cao S, Wei Z, Tan B, Li Y, Lian Z, Wang S (2017) Evolutionary biologic changes of gut microbiota in an 'adenoma-carcinoma sequence' mouse colorectal cancer model induced by 1, 2-Dimethylhydrazine. Oncotarget 8:444–457

Tan TG, Sefik E, Geva-Zatorsky N, Kua L, Naskar D, Teng F, Pasman L, Ortiz-Lopez A, Jupp R, Wu H-JJ, Kasper DL, Benoist C, Mathis D (2016) Identifying species of symbiont bacteria from the human gut that, alone, can induce intestinal Th17 cells in mice. Proc Natl Acad Sci U S A 113:E8141-E8150

Tanoue T, Atarashi K, Honda K (2016) Development and maintenance of intestinal regulatory T cells. Nat Rev Immunol 16:295–309

Ueda Y, Kayama H, Jeon SG, Kusu T, Isaka Y, Rakugi H, Yamamoto M, Takeda K (2010) Commensal microbiota induce LPS hyporesponsiveness in colonic macrophages via the production of IL-10. Int Immunol 22:953–962

Vaishnava S, Behrendt CL, Ismail AS, Eckmann L, Hooper LV (2008) Paneth cells directly sense gut commensals and maintain homeostasis at the intestinal host-microbial interface. Proc Natl Acad Sci U S A 105:20858–20863

Vaishnava S, Yamamoto M, Severson KM, Ruhn KA, Yu X, Koren O, Ley R, Wakeland EK, Hooper LV (2011) The antibacterial lectin RegIIIgamma promotes the spatial segregation of microbiota and host in the intestine. Science 334:255–258

van der Sluis M, Koning BAE de, Bruijn ACJM de, Velcich A, Meijerink JPP, van Goudoever JB, Büller HA, Dekker J, van Seuningen I, Renes IB, Einerhand AWC (2006) Muc2-deficient mice spontaneously develop colitis, indicating that MUC2 is critical for colonic protection. Gastroenterology 131:117–129

Vargas-Robles H, Castro-Ochoa KF, Citalán-Madrid AF, Schnoor M (2019) Beneficial effects of nutritional supplements on intestinal epithelial barrier functions in experimental colitis models in vivo. World J Gastroenterol 25:4181–4198

Vince AJ, McNeil NI, Wager JD, Wrong OM (1990) The effect of lactulose, pectin, arabinogalactan and cellulose on the production of organic acids and metabolism of ammonia by intestinal bacteria in a faecal incubation system. Br J Nutr 63:17–26

Wahlström A, Sayin SI, Marschall H-U, Bäckhed F (2016) Intestinal Crosstalk between Bile Acids and Microbiota and Its Impact on Host Metabolism. Cell Metab 24:41–50

Walker A, Pfitzner B, Harir M, Schaubeck M, Calasan J, Heinzmann SS, Turaev D, Rattei T, Endesfelder D, Castell WZ, Haller D, Schmid M, Hartmann A, Schmitt-Kopplin P (2017) Sulfonolipids as novel metabolite markers of Alistipes and Odoribacter affected by high-fat diets. Sci Rep 7:11047

Walker AW, Duncan SH, Harmsen HJM, Holtrop G, Welling GW, Flint HJ (2008) The species composition of the human intestinal microbiota differs between particle-associated and liquid phase communities. Environ Microbiol 10:3275–3283

Walker AW, Ince J, Duncan SH, Webster LM, Holtrop G, Ze X, Brown D, Stares MD, Scott P, Bergerat A, Louis P, McIntosh F, Johnstone AM, Lobley GE, Parkhill J, Flint HJ (2011) Dominant and diet-responsive groups of bacteria within the human colonic microbiota. ISME J 5:220–230

Wang L, Zhu L, Qin S (2019a) Gut Microbiota Modulation on Intestinal Mucosal Adaptive Immunity. J Immunol Res 2019:4735040

Wang S, Ye Q, Zeng X, Qiao S (2019b) Functions of Macrophages in the Maintenance of Intestinal Homeostasis. J Immunol Res 2019:1512969

Wedlake L, Slack N, Andreyev HJN, Whelan K (2014) Fiber in the treatment and maintenance of inflammatory bowel disease: A systematic review of randomized controlled trials. Inflamm Bowel Dis 20:576–586

Weimer PJ (1992) Cellulose Degradation by Ruminal Microorganisms. Critical Reviews in Biotechnology 12:189–223

Winston JA, Rivera A, Cai J, Patterson AD, Theriot CM (2019) Secondary bile acid ursodeoxycholic acid (UDCA) alters weight, the gut microbiota, and the bile acid pool in conventional mice. This article is a preprint and has not been certified by peer review. bioRxiv

Wirtz S, Neufert C, Weigmann B, Neurath MF (2007) Chemically induced mouse models of intestinal inflammation. Nat Protoc 2:541–546

Wolin MJ (1981) Fermentation in the rumen and human large intestine. Science 213:1463–1468

Worthington JJ, Reimann F, Gribble FM (2018) Enteroendocrine cells-sensory sentinels of the intestinal environment and orchestrators of mucosal immunity. Mucosal Immunol 11:3–20

Wostmann BS (1973) Intestinal bile acids and cholesterol absorption in the germfree rat. J Nutr 103:982–990

Wu H-J, Ivanov II, Darce J, Hattori K, Shima T, Umesaki Y, Littman DR, Benoist C, Mathis D (2010) Gut-residing segmented filamentous bacteria drive autoimmune arthritis via T helper 17 cells. Immunity 32:815–827

Xiao L, Feng Q, Liang S, Sonne SB, Xia Z, Qiu X, Li X, Long H, Zhang J, Zhang D, Liu C, Fang Z, Chou J, Glanville J, Hao Q, Kotowska D, Colding C, Licht TR, Wu D, Yu J, Sung JJY, Liang Q, Li J, Jia H, Lan Z, Tremaroli V, Dworzynski P, Nielsen HB, Bäckhed F, Doré J, Le Chatelier E, Ehrlich SD, Lin JC, Arumugam M, Wang J, Madsen L, Kristiansen K (2015) A catalog of the mouse gut metagenome. Nat Biotechnol 33:1103–1108

Yang B-H, Hagemann S, Mamareli P, Lauer U, Hoffmann U, Beckstette M, Föhse L, Prinz I, Pezoldt J, Suerbaum S, Sparwasser T, Hamann A, Floess S, Huehn J, Lochner M (2016) Foxp3(+) T cells expressing RORγt represent a stable regulatory T-cell effector lineage with enhanced suppressive capacity during intestinal inflammation. Mucosal Immunol 9:444–457

Yang J, Zou M, Pezoldt J, Zhou X, Huehn J (2018) Thymus-derived Foxp3+ regulatory T cells upregulate RORγt expression under inflammatory conditions. J Mol Med 96:1387–1394

Yassour M, Vatanen T, Siljander H, Hämäläinen A-M, Härkönen T, Ryhänen SJ, Franzosa EA, Vlamakis H, Huttenhower C, Gevers D, Lander ES, Knip M, Xavier RJ (2016) Natural history of the infant gut microbiome and impact of antibiotic treatment on bacterial strain diversity and stability. Sci Transl Med 8:343ra81

Yatsunenko T, Rey FE, Manary MJ, Trehan I, Dominguez-Bello MG, Contreras M, Magris M, Hidalgo G, Baldassano RN, Anokhin AP, Heath AC, Warner B, Reeder J, Kuczynski J, Caporaso JG, Lozupone CA, Lauber C, Clemente JC, Knights D, Knight R, Gordon JI (2012) Human gut microbiome viewed across age and geography. Nature 486:222–227

Zeng H, Umar S, Rust B, Lazarova D, Bordonaro M (2019) Secondary Bile Acids and Short Chain Fatty Acids in the Colon: A Focus on Colonic Microbiome, Cell Proliferation, Inflammation, and Cancer. Int J Mol Sci 20

Zhang T, Li Q, Cheng L, Buch H, Zhang F (2019) Akkermansia muciniphila is a promising probiotic. Microb Biotechnol 12:1109–1125

Zhao L, Yang W, Chen Y, Huang F, Lu L, Lin C, Huang T, Ning Z, Zhai L, Zhong LL, Lam W, Yang Z, Zhang X, Cheng C, Han L, Qiu Q, Shang X, Huang R, Xiao H, Ren Z, Chen D, Sun S, El-Nezami H, Cai Z, Lu A, Fang X, Jia W, Bian Z (2020) A Clostridia-rich microbiota enhances bile acid excretion in diarrhea-predominant irritable bowel syndrome. J Clin Invest 130:438–450

Zhao Y, Chen F, Wu W, Sun M, Bilotta AJ, Yao S, Xiao Y, Huang X, Eaves-Pyles TD, Golovko G, Fofanov Y, D'Souza W, Zhao Q, Liu Z, Cong Y (2018) GPR43 mediates microbiota metabolite SCFA regulation of antimicrobial peptide expression in intestinal epithelial cells via activation of mTOR and STAT3. Mucosal Immunol 11:752–762

Zheng Y, Valdez PA, Danilenko DM, Hu Y, Sa SM, Gong Q, Abbas AR, Modrusan Z, Ghilardi N, Sauvage FJ de, Ouyang W (2008) Interleukin-22 mediates early host defense against attaching and effacing bacterial pathogens. Nat Med 14:282–289

Zihni C, Mills C, Matter K, Balda MS (2016) Tight junctions: From simple barriers to multifunctional molecular gates. Nat Rev Mol Cell Biol 17:564–580

Zou J, Chassaing B, Singh V, Pellizzon M, Ricci M, Fythe MD, Kumar MV, Gewirtz AT (2018) Fiber-Mediated Nourishment of Gut Microbiota Protects against Diet-Induced Obesity by Restoring IL-22-Mediated Colonic Health. Cell Host Microbe 23:41-53.e4

8 Attachment

8.1 List of academic teachers

The following ladies and gentlemen taught me during my academic education in Gießen:

Ahlemeyer, Barbara

Becker, Katja

Bräunig, Diemar

Brunn, Hubertus

Domann, Eugen

Eder, Klaus

Erhardt, Georg

Evers, Adalbert

Frisch, Matthias

Göttlich, Richard

Herrmann, Roland

Honermeier, Bernd

Klar, Peter

Krawinkel, Michael

Kühl, Rainer

Kunz, Clemens

Linn, Thomas

Leonhäuser, Ingrid-Ute

Meier-Gräwe, Uta

Morlock, Gertrud

Neuhäuser-Berthold, Monika

Pätzold, Ralf

Rudloff, Silvia

Schachtel, Gabriel

Schindler, Siegfried

Skrandies, Wolfgang

Schlich, Elmar

Schmitz, Michael

Schnell, Sylvia

Schubert, Sven

Schulz, Sabine

Schwiertz, Andreas

Wenisch, Sabine

Wenzel, Uwe

Wissemann, Volker

Wolters, Volkmar

8.2 Danksagung

Mein Dank gilt allen voran meinem Doktorvater Herrn Prof. Ulrich Steinhoff für seine Bereitschaft, meine Promotion zu betreuen, für seine wissenschaftliche Unterstützung und die zahlreichen konstruktiven Gespräche in jeder Phase der Bearbeitung meines Themas. Lieber Uli, du hast mir die Möglichkeit gegeben, mich nicht nur fachlich als Immunologin, sondern auch persönlich in so vielerlei Hinsicht weiterzuentwickeln. Dafür danke ich dir von ganzem Herzen.

Zudem bedanke ich mich bei Prof. Michael Lohoff für die Möglichkeit am Institut für Medizinische Mikrobiologie meine Dissertation anfertigen zu können. Ein herzliches Dankeschön gebührt auch Prof. Alexander Visekruna und Prof. Magdalena Huber für ihre wissenschaftliche Unterstützung.

Ein ganz besonderer Dank gilt Anne Hellhund und Rossana Romero für ihre Hilfe bei meinen praktischen Arbeiten, für die ausgesprochen angenehme Atmosphäre im Labor und auch für die vielen freundschaftlichen Gespräche. Ich danke euch, liebe Anne und Rossana, für die unvergessliche Zeit und werde euch sehr vermissen.

Bedanken möchte ich mich ebenfalls bei Hartmann Raifer, Maik Luu, Addi Romero, Felix Picard, Daniel Staudenraus, Alekhya Porapu, Rouzbeh Mahdavi, Hanna Leister, Dennis Vogel, Manuel Gerlach, Christina Lückel, Olaf Pinkenburg, Claudia Trier, Nadine Buschmann, Bärbel Camara, Anna Guralnik, Melanie Wolf, Conny Würtz, Petra Sarck, Hosam Shams-Eldin, Guido Schemken, Waltraud Ackermann, Katrin Roth, Julia Kirch, Uwe Linne und der gesamten Arbeitsgruppe für die freundliche Hilfe und Unterstützung bei der experimentellen Durchführung meiner Arbeit. Habt Dank für die hilfreichen Anregungen und den guten Rat, den ich stets bei allen Fragen und Problemen bekam. Ich bin sehr froh, diese Erfahrungen zusammen mit euch gemacht zu haben.

Danke sagen möchte ich auch meiner Familie und meinen Freunden für ihre kraftgebenden und ermutigenden Worte und ihre Liebe, die ich jeden Tag erfahren darf. Ein ganz besonderes Dankeschön richte ich an dieser Stelle an Dane Kotas, der mir immer den Rücken gestärkt und fest an mich geglaubt hat.

Denn von ihm und durch ihn und zu ihm sind alle Dinge.
Ihm sei Ehre in Ewigkeit! Amen.

Römer 11, 36